UNIVERSITÀ DEGLI STUDI DI ROMA
"TOR VERGATA"

FACOLTA' DI INGEGNERIA

DOTTORATO DI RICERCA IN INGEGNERIA AMBIENTALE

XXV CICLO

Carbonation of minerals and industrial residues for storing CO_2 emissions from different sources

Daniela Zingaretti

A.A. 2011/2012

Tutor: Prof. Renato Baciocchi

Co-Tutor: Giulia Costa

Coordinatore: Prof. Renato Gavasci

SOMMARIO

La carbonatazione è una reazione che avviene spontaneamente in natura nella quale la CO_2 reagisce con le rocce ricche di silicati di metalli alcalino-terrosi, come calcio e magnesio, formando i rispettivi carbonati. Considerando l'ampia disponibilità di questi minerali, la reazione di carbonatazione può essere utilizzata anche come tecnica di stoccaggio della CO_2 ottenendo come prodotti dei composti innocui per l'ambiente e termodinamicamente stabili per milioni di anni. La reazione di carbonatazione, inoltre, è esotermica ed il calore prodotto può essere utilizzato per ridurre almeno in parte le penalità energetiche del processo. In natura, tuttavia, tale reazione avviene con velocità abbastanza modeste e per essere utilizzata a livello industriale, quindi, la carbonatazione deve essere condotta in specifiche condizioni operative in modo da accelerare la reazione e ottenere lo stoccaggio della CO_2 in alcune ore invece di migliaia di anni. In alternativa, al posto dei minerali presenti sulla crosta terrestre, nel processo possono essere impiegate anche alcune tipologie di residui industriali caratterizzati da elevati contenuti di ossidi o silicati di calcio e magnesio. Questi materiali, che solitamente sono disponibili in prossimità delle sorgenti puntiformi di emissioni di anidride carbonica, sono più reattivi con la CO_2 e, quindi, richiedono condizioni operative meno severe. Diversi studi hanno analizzato la possibilità di applicare la carbonatazione sia alle rocce silicatiche, come l'olivina, il serpentino e la wollastonite, sia ad alcuni residui industriali alcalini ottenendo dei risultati promettenti. Tuttavia l'applicazione della carbonatazione su scala industriale finora è stata ostacolata dalle elevate richieste di energia e materiale associate al processo.

L'obiettivo principale di questa tesi, quindi, è stato quello di testare la fattibilità di alcune opzioni di processo che permettessero di ridurre le richieste energetiche associate alla carbonatazione in vista della sua applicazione come tecnica di stoccaggio della CO_2. Nel presente lavoro è stata analizzata in particolare la possibilità di utilizzare delle fonti diluite di anidride carbonica al posto della CO_2 pura al fine di evitare la fase di cattura dell'anidride carbonica, che rappresenta uno degli step di maggior rilievo per il consumo energetico complessivo del processo. In quest'ottica sono stati condotti due studi sperimentali utilizzando un minerale e alcune tipologie di residui industriali. Nel primo studio è stata analizzata la possibilità di condurre in condizioni operative blande (ovvero basse temperature e pressioni di CO_2) un processo di carbonatazione diretta in fase slurry di un campione di serpentino attivato termicamente. Inizialmente, quindi, sono state studiate le cinetiche di dissoluzione del materiale attraverso dei test condotti utilizzando una miscela gassosa contenente il 10% di CO_2. In base a questi test è stato possibile osservare che le cinetiche di dissoluzione del magnesio e del silicio dal serpentino attivato termicamente sono abbastanza veloci. In particolare la dissoluzione del silicio dal materiale è risultata inferiore a quella del magnesio ma all'aumentare della temperatura le differenze tra la dissoluzione di Mg e Si diminuiscono. Successivamente, visti i buoni risultati ottenuti nei test di dissoluzione, è stato studiato il potenziale di carbonatazione del campione di serpentino conducendo dei test ad una pressione parziale di CO_2 di 1 bar. Questi test hanno messo in evidenza che in un processo di carbonatazione diretta in fase acquosa il potenziale del serpentino attivato termicamente non supera il 20% nelle condizioni operative analizzate, suggerendo che un processo indiretto potrebbe essere più efficiente. Il secondo studio, invece, ha riguardato la valutazione del potenziale di carbonatazione di diverse tipologie di residui industriali in un processo ad umido ($L/S<1$ l/kg) condotto utilizzando una miscela gassosa contenente il 40% di CO_2 invece di anidride carbonica pura. I tre diversi residui utilizzati in questo studio hanno mostrato un comportamento simile per le stesse pressioni parziali di CO_2 indipendentemente dall'impiego della miscela gassosa o della CO_2 pura, indicando, quindi, che la composizione del gas influenza solo parzialmente il potenziale di carbonatazione di questi residui.

In questa tesi, inoltre, è stata analizzata la possibilità di applicare la carbonatazione di residui industriali in un processo innovativo di upgrading di biogas con l'obiettivo di stoccare in forma solida la CO_2 separata. Questo processo, sviluppato all'interno del progetto europeo Life+ "UPGAS-LOWCO2", è costituito da un primo step in cui l'anidride carbonica è rimossa dal biogas attraverso un processo di assorbimento chimico con una soluzione di idrossido di potassio o sodio. Nel secondo step del processo la soluzione ottenuta in uscita dalla colonna di assorbimento viene rigenerata mettendola in contatto con le ceneri ottenute dal trattamento fumi di un impianto di incenerimento rifiuti (ceneri da APC). In questo modo oltre alla rigenerazione dell'idrossido contenuto nella soluzione alcalina è possibile ottenere anche lo stoccaggio della CO_2 separata dal biogas sotto forma di carbonato di calcio contenuto nel materiale solido finale ed il miglioramento del comportamento ambientale delle ceneri da APC. Sulla base dei risultati ottenuti dagli esperimenti condotti in laboratorio, è stata progettata e costruita un'unità di rigenerazione/carbonatazione in scala pilota al fine di valutare la fattibilità del processo. Tale unità è stata, quindi, installata in una discarica in Toscana ed è stata utilizzata per condurre alcuni test integrati di assorbimento-rigenerazione per valutare le rese di processo in termini di recupero del reagente alcalino per lo step di assorbimento, di stoccaggio della CO_2 e miglioramento del comportamento ambientale dei residui.

In questa tesi, infine, sono state valutate le richieste di materiale ed energia in un processo di carbonatazione diretta applicato a diverse tipologie di minerali e residui industriali, considerando sia la route slurry che quella ad umido. Questo studio ha permesso di identificare le operazioni unitarie che maggiormente influenzano i requisiti energetici del processo e di chiarire anche le differenze tra le stime energetiche già disponibili in letteratura. I risultati ottenuti hanno messo in evidenza che la fattibilità del processo è fortemente legata alla possibilità di recuperare almeno in parte il calore del materiale in uscita dal reattore di carbonatazione. Lo studio ha permesso di osservare, inoltre, che i requisiti energetici del processo di carbonatazione applicato ad alcune tipologie di residui non variano notevolmente utilizzando fonti diluite di CO_2 (ad es. una miscela contenente il 40 % di CO_2) invece di anidride carbonica pura, portando quindi ad una notevole riduzione della penalità energetica dell'intero processo di cattura e stoccaggio della CO_2.

ABSTRACT

Mineral carbonation is a naturally occurring reaction by which CO_2 reacts with rocks rich in alkaline earth silicates forming Mg and Ca carbonates. Given the abundance of these minerals this reaction can be exploited as a method to permanently store large amounts of CO_2 since the products are thermodynamically stable over geological time periods (millions of years) and environmentally benign. Furthermore, the reaction is exothermic and the heat of reaction could be at least partially recovered to reduce the energy requirements of the process. However as the reaction rate is quite low under ambient conditions, in order to accelerate the process and to make it viable for industrial applications it must be performed at specific operating conditions. As an alternative feedstock, several types of industrial residues characterized by significant content of Ca and Mg oxides or silicates could be used instead of minerals. These materials, in fact, are more reactive and thus less energy intensive operating conditions may be generally applied; in addition industrial residues are also usually available at CO_2 point-source emission locations.

Several studies have investigated the feasibility of applying carbonation to both natural silicate rocks (i.e. olivine, serpentine and wollastonite) and alkaline industrial residues, obtaining promising results. However, one of the main issues that has hindered so far the application of carbonation at industrial scale is represented by the energy and material requirements associated to the process.

The main goal of this thesis was to investigate the feasibility of process options that could allow to reduce the energy requirements associated to the carbonation process in view of its application as a CO_2 storage option. Specifically, one aspect investigated in this thesis was the possibility of using diluted carbon dioxide sources instead of pure CO_2, thus avoiding the capture step. With this aim two preliminary experimental studies were carried out to test the performances achievable using activated serpentine and industrial residues. In the first study the feasibility of carbonation of thermally activated serpentine via the direct aqueous route applying mild operating conditions was investigated initially analysing the dissolution kinetics of the material using a gas mixture containing 10% CO_2 and, then, testing the carbonation extent achievable with a CO_2 partial pressure of 1 bar. The results of dissolution experiments indicated that the release of Mg and Si from activated serpentine was quite fast. However, the dissolution rate of silicon was under-stoichiometric with respect to magnesium although this ratio became less under-stoichiometric with increasing temperature. Regarding the carbonation performances, the results showed that at the tested mild conditions (i.e. p_{CO2}=1 bar) the extent of direct carbonation of the activated serpentine was lower than 20%, suggesting that an indirect process could be more effective. The second study was performed in order to test the performances of different types of industrial residues in a wet direct carbonation process using a gas mixture containing 40 % of CO_2 instead of pure carbon dioxide. The three types of tested industrial residues (i.e. APC residues, BOF and AOD slags) presented a similar carbonation behaviour using either the gas mixture or pure carbon dioxide at the same partial pressure of CO_2, thus indicating that the gas composition exerts only a limited effect on the carbonation extent of these materials.

Furthermore, in this thesis the possibility of applying carbonation of industrial residues within an innovative biogas upgrading process that allows also to store the separated CO_2 was investigated in the framework of the European Life+ project UPGAS-LOWCO2. This process consists in a first stage in which CO_2 is removed from the biogas by chemical absorption with KOH or NaOH solutions followed by a second stage in which the spent absorption solution is contacted with waste incineration Air Pollution Control (APC) residues. The latter reaction leads to the regeneration of the alkali reagent in the solution and to the precipitation of calcium carbonate and, hence, allows to reuse the regenerated solution in the absorption process and to permanently store the separated CO_2 in the final solid product, characterized by an improved environmental behaviour compared to the untreated residues. To evaluate the feasibility of this process, a pilot-scale regeneration unit was designed, built and installed in a landfill site and several tests were carried out in order to evaluate the performance of the process in terms of the recovery of the alkali reagent for the absorption step, CO_2 storage and improvement of the environmental behaviour of the residues.

Finally, the material and energy requirements of direct aqueous carbonation of different types of minerals and industrial residues, considering either the slurry phase or the wet route were assessed. This study allowed also to identify the critical operations that mostly affect the energy requirements associated to the process and also to clarify the difference between the estimates already available in the literature. Based on the results of this study, the feasibility of the process proved to be strictly related to the possibility of recovering, even partially, the heat of the outlet stream from the carbonation reactor. Furthermore the energy requirements associated to the carbonation of selected types of industrial residues did not prove to vary significantly using a diluted CO_2 source (e.g. a gas mixture with 40% CO_2) instead of pure carbon dioxide, suggesting that a noteworthy reduction in the overall energy penalty of the CCS chain could be achieved.

Acknowledgments

First of all, I would like to thank prof. Renato Gavasci for giving me the possibility to work in his group of Environmental and Sanitary Engineering. He, together with prof. Baciocchi and prof. Lombardi, put all the Ph.D students of his group in the condition to work at a high scientific level also giving the opportunity of working abroad.

I wish to thank my tutor, prof. Renato Baciocchi, who first sparked my interest in the experimental work. His guidance, assistance, and expertise have been of great help in overcoming many of the difficulties which arose throughout my doctoral program.

I also want to thank Dr. Giulia Costa, her continuous support and the fruitful discussions with her were important for my progress.

I am grateful to Prof. Marco Mazzotti for giving me the possibility of spending a period in his group at the Separation Processes Laboratory of the Swiss Federal Institute of Technology (ETH-Zürich). It was an interesting experience to work with him, Mischa and Hari that allowed me to learn a lot.

I would like to acknowledge also Lidia Lombardi, Tommaso Olivieri, Alessandro Paradisi and Laura Zanchi from the University of Florence with whom I have collaborated within the LIFE project.

I would like to thank all the members of the ISA group, each one of them influenced my work and my stay in the laboratory in a different way. However a special thank goes to my colleagues (but moreover friends) Stefania and Iason for giving their support and encouragement in many occasions and for creating a friendly working atmosphere.

Last but not least, a special and deep acknowledgement goes to my family. I am sincerely grateful to my parents, Armando and Anna, and my sisters, Sara and Lucia, for their love and for always being there for me. Finally I want to thank Stefano for giving his love, encouragement and unconditional support. To them I dedicate this thesis.

Table of Contents

1 INTRODUCTION

Mineral carbonation is one of the available options currently under investigation for storing anthropogenic carbon dioxide emissions in the framework of the actions aimed at climate change mitigation. The basic concept behind mineral CO_2 sequestration is to mimic natural weathering processes by which calcium- or magnesium- containing minerals are converted into the corresponding carbonates reacting with gaseous CO_2 (Huijgen et al., 2005):

$$(Ca, Mg)SiO_{3(s)} + CO_{2(g)} \rightarrow (Ca, Mg)CO_{3(s)} + SiO_{2(s)} \qquad \textbf{(1.1)}$$

Differently from other storage techniques based on the injection of carbon dioxide in geological formations or depleted oil fields (see Table 1.1), mineral carbonation does not require long term monitoring, since CO_2 is chemically incorporated into a mineral substance which remains naturally in the solid state avoiding any possibility of CO_2 release (Lackner et al., 1995). In addition, mineral carbon sequestration can be used in areas where other storage techniques, such as geologic carbon sequestration, are either not available or not feasible (Zevenhoven et al., 2010).

In order to apply carbonation as an ex situ storage option for fixing large amounts of CO_2, this reaction, that occurs spontaneously in nature in geological time frames, has to be accelerated by applying proper operating conditions. In the last decades several studies have investigated the possibility of storing CO_2 by accelerated carbonation of natural minerals. Considering the abundance on the earth crust of minerals such as olivine, wollastonite and serpentine, the storage of large amounts of CO_2 could be anticipated. However, in order to achieve a significant CO_2 uptake in shorter times (hours instead of thousands of years), the surface of the minerals needs to be activated by physical pre-treatments, such as size reduction, and thermal or steam treatment (to eliminate chemically-bound water). Upon activation, the mineral may be carbonated in aqueous phase by two different routes: a) the indirect route, where the alkaline metal is first extracted from the silicate matrix and then precipitated as carbonate in a separate step, in which CO_2 is also dissolved; b) the direct carbonation route, where CO_2 and alkaline metal dissolution and carbonation occur in the same step (Costa et al., 2007). Operating conditions for the carbonation of minerals are typically energy intensive; for example, direct carbonation of minerals is found to be effective at a temperature of 373-473 K and CO_2 pressure of 1-10 MPa (e.g. O’Connor et al., 2005; Sipilä et al., 2008).

Table 1.1: Summary of methodologies for CO_2 storage (adapted from Bobicki et al., 2012).

CO_2 STORAGE METHODS	ADVANTAGES	DISADVANTAGES
Geologic Sequestration	• Feasible on a large scale • Substantial storage capacity • Extensive experience • Low cost	• Monitoring necessary • Leakage possible
Ocean carbon sequestration	• Large storage capacity	• Temporary storage • Potential harmful effects on aquatic microbes and biota
Industrial use	• CO_2 incorporated into valuable products	• Limited storage capacity • Storage time short
Mineral carbon sequestration	• Only known form of permanent storage • Minerals required available in quantities capable of binding all fossil-fuel bound carbon • Carbonation products environmentally benign	• Energy intensive • High cost

An alternative feedstock suitable for mineral carbonation is also represented by some types of alkaline industrial residues characterized by high calcium or magnesium (hydr)oxide or silicate contents. The main types of alkaline residues that have been selected and tested so far for accelerated carbonation, due to their availability and/or chemical and mineralogical composition, are steelmaking slag, bottom ash and air pollution control (APC) residues generated by municipal solid waste incineration and cement kiln dust (Bobicki et al., 2012). Besides, these residues are typically available at CO_2 point-source emission locations, such as waste to energy facilities and steel and cement manufacturing plants and could be employed in niche applications in order to store at least part of the CO_2 emissions of the same industries from which they are produced. Figure 1.1 summarizes the average CO_2 uptakes obtained for several types of industrial residues as a function of the CaO content of the materials (for the specific operating conditions see Gunning et al., 2010; Pan et al., 2012; Costa, 2009). In many cases these residues present a particle size already suitable for the carbonation process allowing to reduce or avoid the need of a grinding step, that represents one of the most energy intensive stages of the whole carbonation process. Furthermore, several studies have demonstrated that carbonation of these residues may lead to an improvement of their environmental behaviour, thus making their reuse or disposal easier (e.g. Van Gerven et al., 2005; Baciocchi et al., 2009; 2010a).

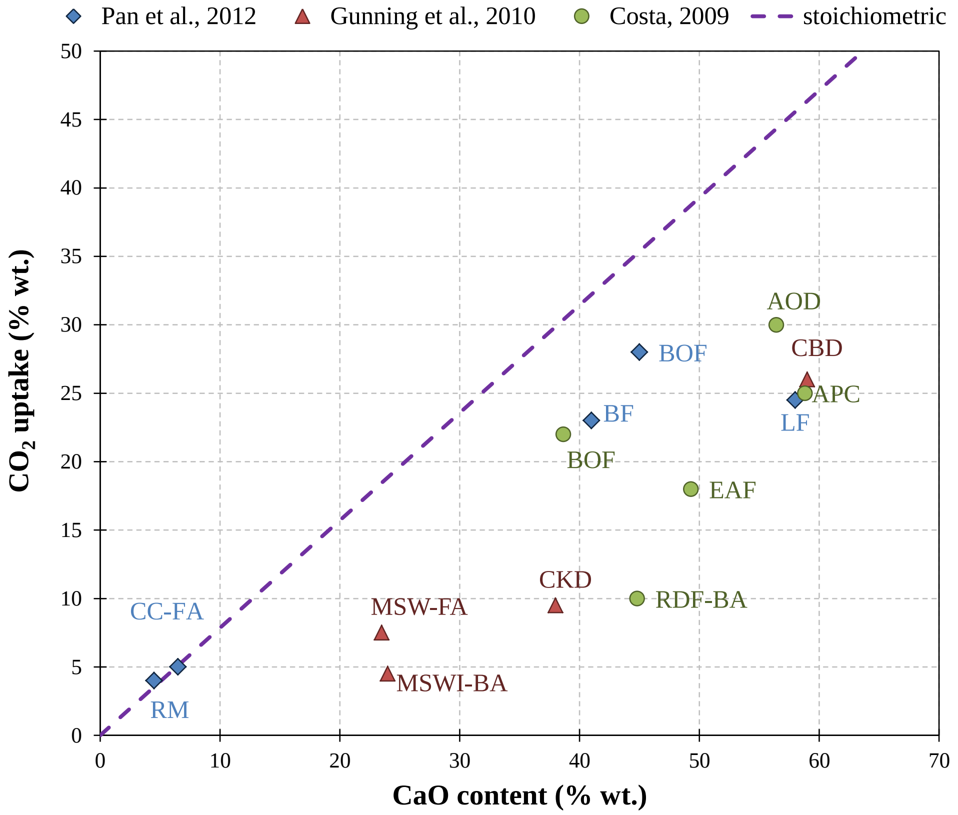

CKD = Cement Kiln Dust
CBD = Cement Bypass Dust
APC= Air Pollution Control residues
RDF-BA = Refuse Derived Fuel Bottom Ash
MSWI-BA = Municipal Solid Waste Incineration Bottom Ash
MSWI-FA = Municipal Solid Waste Incineration Fly Ash
RM = Red Mud

BOF = Basic Oxygen Furnace slags
EAF = Electric Arc Furnace slag
AOD = Argon Oxygen Desulfurization unit slag
BF = Blast Furnace slags
LF = Ladle Furnace slags
CC-FA =Coal Combustion Fly Ash

Figure 1.1: Comparison of the average CO_2 uptakes obtained for different types of residues as a function of the CaO content of the materials.

Although the amounts of residues produced each year are considered to be too small to substantially reduce CO_2 emissions, they could help to establish the mineral carbon sequestration technology and their use may be a stepping-stone towards the development of CCS processes utilizing natural minerals (Bobicki et al., 2012).

Most of the recent studies carried out in this field assessed the reactivity of the above mentioned residues applying the direct aqueous carbonation route (Sipilä et al., 2008; Huijgen et al., 2006a; Baciocchi et al., 2011b). This reaction route has been investigated using two different process layouts: the slurry phase route, at liquid-to-solid (L/S) ratios higher than 1 l/kg, and the wet route, using L/S ratios below 1 l/kg. This latter type of process avoids the treatment and disposal of the processing liquid, and has been also indicated to favor the dissolution kinetics of hydroxide and silicate phases under mild operating conditions, which may allow to more easily reach saturation conditions of carbonate mineral phases. (Baciocchi et al., 2011b).

Although the direct aqueous carbonation route is considered promising to store CO_2, its application at industrial scale was hindered so far by the energy and material requirements associated to the process. On the one hand the minerals require a mechanical, thermal or chemical pre-treatment in order to enhance the reactivity of these materials that otherwise require very energy intensive operating conditions. On the other hand, instead, industrial residues are more reactive thus requiring less energy intensive operating conditions but their availability is limited. Furthermore many studies so far investigated the feasibility of the accelerated carbonation of minerals and industrial residues using pure CO_2 gas stream thus requiring a carbon dioxide capture step that entails additional duty to the already high energy demand of the process.

The aim of this thesis is to make a step toward the application of the carbonation of alkaline materials at demonstrative or pilot scale, evaluating the effective energy and material requirements of the process proposed so far and investigating some viable options to make the process more sustainable reducing its energy penalty. In order to pursue these objectives some aspects of the aqueous carbonation process were analysed mainly for the application to industrial residues and activated serpentine.

As far as accelerated carbonation of minerals is concerned, a preliminary study was carried out in order to evaluate the carbonation potential of a sample of thermally activated serpentine. This study was performed in a 7 months research period carried out at the Process Engineering Department of the Swiss Federal Institute of Technology (ETH) in Zürich (Switzerland) and the main findings are reported in **Chapter 2**. The aim of this study was to evaluate the feasibility of performing accelerated carbonation of a thermally activated serpentine under flue gas atmosphere, thus avoiding the need of a CO_2 capture step. The focus of the first part of this study was to assess the dissolution kinetics of the tested material, that, as well known, represent the rate limiting step of the carbonation process. With this aim several experiments were performed at different temperature (T=30-90 °C) and partial pressure of CO_2 (p_{CO2}=0-100 bar) using a N_2/CO_2 gas mixture containing 10% CO_2 in order to simulate the typical carbon dioxide content of flue gases. At a later stage the carbonation potential of the tested activated serpentine was assessed performing direct aqueous carbonation experiments at different temperatures (T=30-90 °C), slurry densities (10-20% wt.) and 1 bar of carbon dioxide, monitoring the precipitation of different magnesium carbonates forms and estimating the achieved extent of carbonation.

In **Chapter 3,** instead, the main results of an experimental study carried out performing direct wet carbonation tests on three different types of industrial residues using a N_2/CO_2 gas mixture that simulates the typical composition of syngas (i.e. CO_2 content of 40%) are presented. The aim of this experimental research was to evaluate if the carbonation of industrial residues could be performed using directly CO_2 diluted sources, such as syngas, thus avoiding the CO_2 capture step. For this reason lab-scale tests were performed at different temperatures (20-50 °C) and CO_2 partial pressures (0.4-2.8 bar) using the APC residues from a waste incinerator and two types of steelmaking slags (i.e. BOF and AOD slag). For these materials the kinetics of carbonation was measured at different temperature and CO_2 partial pressure and compared with the results obtained using pure CO_2 at the same carbon dioxide partial pressure.

A further study carried out in this thesis was focused on the application of the carbonation of industrial residues within a CO_2 chemical absorption process for biogas upgrading. This study was performed within the framework of the UPGAS-LOWCO2 project (LIFE08 ENV/IT/000429) funded by the European Commission with the aim of developing innovative processes for biogas upgrading, allowing to store the separated CO_2 in a solid phase. One of the methods proposed in this project consists in the absorption of the CO_2 contained in the landfill biogas by means of an alkaline KOH or NaOH solution. The spent solution, rich in either sodium or potassium carbonates, is then regenerated to the hydroxide form by reaction with alkaline industrial residues containing $Ca(OH)_2$, whereas the CO_2 is stored as carbonate in a solid and stable form. Lab-scale tests were first performed in order to select the type of material more suitable for the process and the optimal operating conditions. On the basis of these results a pilot-scale carbonation/regeneration unit was designed, built and operated at a landfill site, allowing to perform tests using the landfill biogas and to evaluate the feasibility of the developed process. **Chapter 4** presents the main results of the tests performed in each phase of the project both in terms of CO_2 storage and spent solution regeneration, analysing also the effect of the tested treatments on the leaching behaviour of the residues.

As discussed above, mineral carbonation is considered an attractive process to permanently store anthropogenic carbon dioxide emissions using alkaline minerals or industrial residues. However, its full scale application may be hindered by the energy penalties associated to the operating conditions required to enhance reaction kinetics. So far, only a few studies have assessed the material and energy requirements of carbonation of industrial residues and the results reported differ significantly mainly owing to the differences in the considered assumptions and process schemes. In **Chapter 5** the assessment of the material and energy requirements for CO_2 storage by direct carbonation of minerals and alkaline industrial residues applying two different process routes (slurry phase and wet route) was carried out considering specific assumptions and process layouts. The results obtained using the approach developed in this study were also compared with the ones reported in previous works already published in literature in order to clarify the reasons behind the differences between these studies.

2 ACCELERATED CARBONATION OF ACTIVATED SERPENTINE

Partially taken from:

Werner M., Hariharan S.B., Bortolan A.V., Zingaretti D., Baciocchi R., Mazzotti M., 2013a. Carbonation of activated serpentine for direct flue gas mineralization. Energy Procedia (in press);

Hariharan S.B., Werner M., Zingaretti D., Baciocchi R., Mazzotti M., 2013a. Dissolution of activated serpentine for direct flue-gas mineralization. Energy Procedia (in press);

Werner M., Hariharan S.B., Zingaretti D., Baciocchi R., Mazzotti M., 2013b. Carbonation of activated serpentine using flue gas. In: Proceedings of Fourth International Conference on Accelerated Carbonation for Environmental and Materials Engineering (ACEME 2013), 9-12 April 2013 - Leuven, Belgium;

Hariharan S.B., Werner M., Zingaretti D., Baciocchi R., Mazzotti M., 2013b. Dissolution kinetics of thermally activated serpentine under flue gas atmosphere. In: Proceedings of Fourth International Conference on Accelerated Carbonation for Environmental and Materials Engineering (ACEME 2013), 9-12 April 2013 - Leuven, Belgium.

2.1 Introduction

Mineral carbonation is a reaction occurring between CO_2 and alkaline and alkaline-earth oxides, such as magnesium oxide (MgO) and calcium oxide (CaO), that leads to the precipitation of the corresponding carbonates (IPCC, 2005). This reaction is exothermic and occurs spontaneously within the processes of natural 'weathering' of the silicate rocks, such as olivine, serpentine and wollastonite (see Eq. (2.1)-(2.3) respectively).

$$Mg_2SiO_4 + CO_{2\,(g)} \rightarrow 2MgCO_{3\,(s)} + SiO_{2\,(s)} + 89\,kJ/mol\,CO_2 \tag{2.1}$$

$$Mg_3Si_2O_5(OH)_4 + 3CO_{2\,(g)} \rightarrow 3MgCO_{3\,(s)} + 2SiO_{2\,(s)} + 2H_2O + 64\,kJ/mol\,CO_2 \tag{2.2}$$

$$CaSiO_3 + CO_{2\,(g)} \rightarrow CaCO_{3\,(s)} + SiO_{2\,(s)} + 90\,kJ/molCO2 \tag{2.3}$$

Despite this reaction occurs very slowly in nature, it can be also carried out at controlled operating conditions in order to accelerate its kinetic, thus making possible to fix CO_2 in a solid and thermodynamically stable form in time frames suitable for industrial applications. The quantity of metal oxides in the silicate rocks that can be found in the earth's crust, in fact, exceeds the amounts needed to fix all the CO_2 that would be produced by the combustion of all available fossil fuel reserves (IPCC, 2005). Differently from other storage techniques based on the injection of carbon dioxide in geological formations or depleted oil fields, mineral carbonation does not require long term monitoring, since CO_2 is chemically incorporated into a mineral substance which remains naturally in the solid state avoiding any possibility of CO_2 release (Lackner et al., 1995) and, hence, without a need for post-storage surveillance and monitoring once the CO_2 has been fixed (Sipilä et al., 2008). Furthermore the products of this reaction are environmentally benign and could be potentially sold for profit (Maroto-Valer et al., 2005). In addition, mineral carbon sequestration can be used in areas where other storage techniques, such as geological carbon sequestration, are either not available or not feasible (Zevenhoven et al., 2010).

Among the calcium and magnesium silicates, the materials that proved to be suitable for carbonation processes are olivine (Mg_2SiO_4), serpentine ($Mg_3Si_2O_5(OH)_4$) and wollastonite ($CaSiO_3$). The advantage of Ca-silicates is that they tend to be more reactive towards carbonation than Mg-silicates. However, wollastonite resources are relatively small (Lackner, 2002). The Mg-silicates, instead, have the advantage of being available worldwide in large amounts and in relatively high purity compared to Ca-silicates (Huijgen and Comans, 2003).

As the kinetics of the gas-solid carbonation route was found to be too slow for industrial applications (Lackner et al., 1995), most of the works performed so far on mineral carbonation have addressed the aqueous route, where the process take place according to the following three steps ((see Eq. (2.4)-(2.6))

Step 1) Leaching of Ca/Mg from the mineral matrix:

$$(Ca,Mg)silicate_{(s)} + 2H^{+}_{(aq)} \rightarrow (Ca,Mg)^{2+}_{(aq)} + SiO_{2\,(s)} + H_2O_{(l)} \tag{2.4}$$

Step 2) Dissolution of CO_2 and subsequent conversion of (bi)carbonate species:

$$CO_{2(g)} + H_2O_{(l)} \rightarrow H_2CO_{3(aq)} \rightarrow \mathrm{H}^{+}_{(aq)} + HCO^{-}_{3\,(aq)} \tag{2.5}$$

Step 3) Nucleation and growth of calcium/magnesium carbonate:

$$(Ca,Mg)^{2+}_{(aq)} + HCO^{-}_{3\,(aq)} \rightarrow (Ca,Mg)CO_{3(s)} + \mathrm{H}^{+}_{(aq)} \tag{2.6}$$

Step 1 (dissolution of the mineral) and step 3 (precipitation of the carbonates) may either take place in the same reactor (direct route) or in separate reactors at different operating conditions (indirect carbonation) (Teir et al., 2005).

In the direct aqueous mineral carbonation a Ca/Mg-mineral is suspended in water to form slurry and afterwards carbonated directly at elevated CO_2 pressure and temperature (Baldyga et al., 2011). As described by Huijgen et al. (2006b), as in this route carbonation occurs in a gas–solid–water slurry, the reaction rate substantially increases compared to direct gas–solid carbonation. Since the dissolution of calcium or magnesium from the silicate matrix represents the rate limiting step for the mineralization process, in order to achieve a significant CO_2 uptake in shorter times (hours instead of thousands of years), the surface of the minerals needs to be activated by physical pre-treatments, such as size reduction, and thermal or steam treatment (to eliminate chemically-bound water).

The indirect aqueous route is based instead on the extraction of the reactive species (Ca or Mg) by using acids as extraction media, followed by their conversion to carbonates increasing the pH so that each reaction may be optimized by separately setting its operating conditions. As stated by Baldyga et al. (2011), the first indirect methods were based on using HCl, H_2SO_4 and NaOH (Blencoe et al., 2004; Butt et al., 1997; Maroto-Valer et al., 2004; Alexander et al., 2007). Several more acids including CH_3COOH, HCOOH and H_3PO_4 were investigated as well in attempt to produce magnesium-rich solutions (Maroto-Valer et al., 2005;Teir et al., 2007a). However the acidic condition that is required to enhance the dissolution of magnesium or calcium from the alkaline material hinders the quantitative precipitation of the alkaline metals in the carbonate form. For obtaining an effective carbonate precipitation a pH shift to basic conditions is required. Park and Fan (2004), for example, proposed a pH swing process in which, after the dissolution and internal grinding of the serpentine in a solution of orthophosphoric acid, oxalic acid and EDTA, NH_4OH is added to the liquid product, raising the pH to 8.6, thus causing the precipitation of iron oxide. CO_2 is then bubbled in the solution and the Mg^{2+} reacted to form $MgCO_3$. Both the two carbonation routes present some disadvantages that have hindered so far their application. In particular the addition of large amounts of additives required for the dissolution and subsequent carbonation have limited the development of indirect mineral sequestration (Wang et al., 2011). The direct carbonation route, instead, requires energy intensive operating conditions (e.g. 373-473 K and pressure of 1-10 MPa as reported by O’Connor et al., 2005; Sipilä et al., 2008). However, as reported by Bobicki et al. (2012), despite the fact that no direct aqueous mineral carbonation scheme has yet been proven economical, it is thought by many to be the most promising CO_2 mineralization technique (Huijgen and Comans, 2003; Sipilä et al., 2008; Lackner, 2003). Hence research in this field are focused on finding process routes that can achieve reaction rates viable for industrial purposes and make the reaction more energy-efficient.

So far the relatively simple silicate structure and dissolution mechanism of forsterite, the magnesium rich member of the olivine group, has resulted in extensive study of its dissolution under various conditions in view of the carbonation process (Hänchen et al., 2007, 2006; Pokrovsky and Schott, 2000; Prigiobbe et al., 2009). However the great abundance of the serpentine group makes it a more attractive feedstock for mineral carbonation than olivine. Nevertheless, it suffers from slow dissolution kinetics that makes thermal activation inevitable to accelerate the leaching of magnesium (IPCC, 2005; O'Connor et al., 2000). Thermal activation above 600°C removes enough chemically bound water to destabilize the crystal lattice into a pseudo amorphous structure. In early studies, where pure CO_2 was used, such heat activation was concluded to be economically unfeasible (McKelvy et al., 2004; O'Connor et al., 2005) since it adds substantially to the already high costs associated to the capture step required to increase the CO_2 concentration of the gas. Most researchers, in fact, have looked so far into processes where mineral carbonation takes place under an atmosphere of pure CO_2, either in a single or multi-step process. Recently the attention on mineral carbonation, instead, was focused on processes that combine the capture of CO_2 with its simultaneous conversion into stable carbonates. Capture is promoted by the dissolving feedstock, which provides alkalinity to the solution, enabling the latter to take up more CO_2. However, to dissolve under low partial pressures of CO_2, the feedstock material must be highly reactive. Hence, direct flue gas mineralization might only be successful if started from scarce feedstock materials such as special industrial wastes, or by means of pH-tuning additives that are difficult to recover or as proposed by Verduyn et al., (2009) using an activated serpentine.

The goal of the study presented in this chapter, hence, was to study the direct carbonation of thermally activated serpentine applying a novel approach where the costly capture step is avoided by the direct mineralization of flue gas CO_2 at the point source (Werner et al., 2011). With these aims a preliminary experimental study was carried out at the Swiss Federal Institute of Technology (ETH- Zürich) in order to analyse the kinetics of dissolution of magnesium from the mineral, that, as already discussed, represents the rate limiting step in the process and, then, to test the carbonation potential of this material. In this chapter, after a brief description of the main characteristics of the specific mineral used, the main findings regarding the dissolution kinetics of the thermally activated serpentine are reported (see Paragraph 2.3). In particular, dissolution experiments were performed using a CO_2/N_2 gas mixture with 10% of carbon dioxide in order to simulate the typical CO_2 content of a flue gas. Since in these experiments the dissolution proved to be quite fast even in the absence of additives, the focus of the second part of the study was to explore the carbonation potential of activated serpentine in its most simple process option, the single step carbonation, and in particular to analyse the precipitation of Mg-carbonates in the serpentine-CO_2-H_2O system at a CO_2 pressure of 1 bar (see Paragraph 2.4).

2.2 Material

Thermally activated serpentine was obtained from Shell Global Solutions International, Amsterdam, the Netherlands. The sample was received as a powder (sub 125 μm), thermally activated according to the provider's standard operating procedure. The thermal activation involved partial dehydroxylation (75% dehydroxylation) of crushed and ground natural crystalline serpentine that before heat treatment mainly consists of lizardite, with small amounts of clinochlore, tremolite, enstatite and hematite. The density of the activated material was determined by helium pycnometry (Micrometrics, AccuPyc 1330) to be 2629 ± 2 kg/m^3. The powder was dry-sieved into three fractions using 20 μm and 63 μm lab sieves. Dry product was characterized using x-ray diffraction (Bruker, AXS D8 Advance) and Figure 2.1 reports the results obtained for each fraction. As can be seen, the main mineralogical phases that were detected in the three fractions after the thermal activation are forsterite and hematite while only small amounts of lizardite, silica, tremolite and clinochlore were observed, demonstrating the effectiveness of the applied thermal pre-treatment.

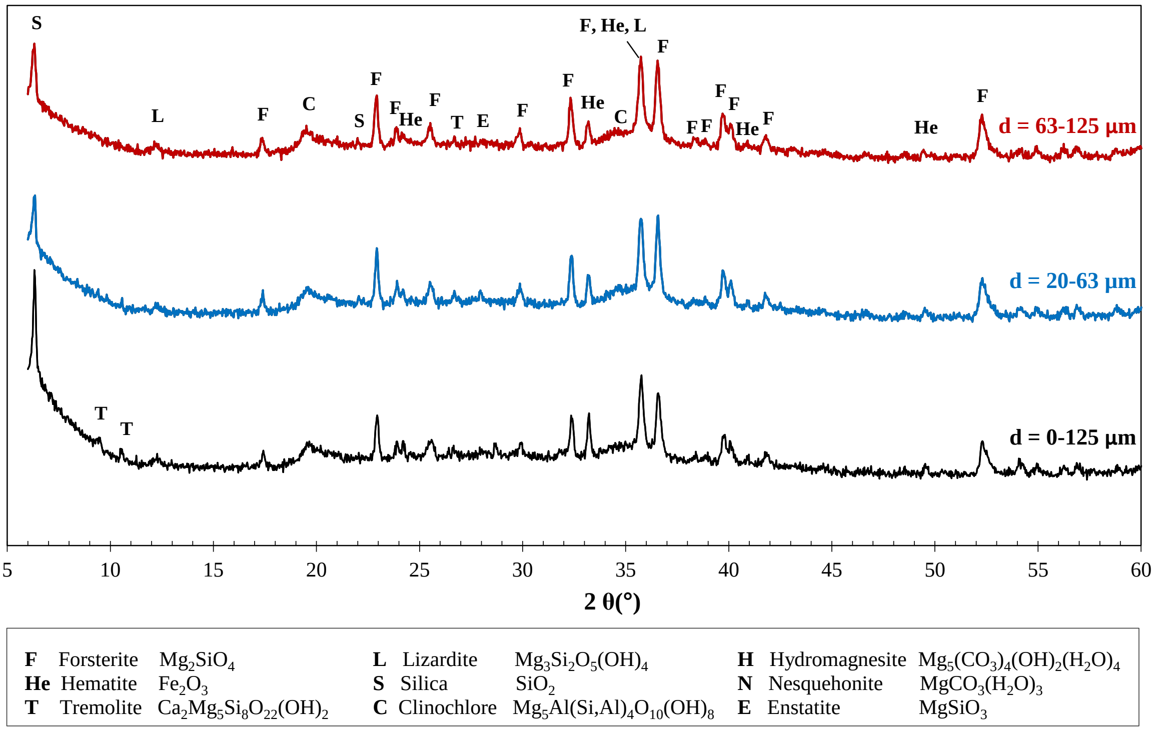

Figure 2.1: XRD of the different fractions of the activated serpentine.

The elemental composition of the different fractions of the activated serpentine (see Table 2.1) were determined by alkaline digestion with $Li_2B_4O_7$ in platinum melting pots at 1050 °C, followed by dissolution of the molten material in a 10% HNO_3 solution and measurement of element concentrations by inductively coupled plasma optical emission spectrometry (ICP-OES Agilent 710-ES).

Table 2.1: Elemental composition of the three fractions of activated serpentine.

	d< 125 µm %	20 < d< 63 µm %	63 < d< 125 µm %
Al	0.68	0.64	0.67
Ba	0.001	0.0005	0.0005
Ca	0.62	0.27	0.22
Co	0.01	0.01	0.00
Cr	0.19	0.21	0.17
Cu	0.02	0.01	0.01
Fe	5.76	6.27	6.21
K	0.17	0.10	0.10
Mg	23.73	23.74	24.10
Mn	0.09	0.08	0.08
Mo	0.0017	0.0007	0.0006
Na	0.14	0.12	0.10
Ni	0.18	0.17	0.17
Si	17.27	18.53	18.87
V	0.0035	0.0031	0.0040

The size fraction between 20 µm and 63 µm was selected for performing the dissolution tests and its particle size distribution was determined in a 0.15 M NaCl solution using a Coulter counter (Beckman, Coulter Multisizer 3).The size fraction between 20 µm and 63 µm was repeatedly washed with ethanol to remove fines and, then, dried overnight in an oven at 60 °C. Light microscope and scanning electron microscope (SEM) images (Figure 2.2) were taken to ensure proper sieving and complete removal of fines. Distribution data were averaged over nine measurements. The specific surface area of this fraction was 11.24±0.0165 m^2/g as determined by N_2 adsorption multi-point B.E.T method (TriStar 3000) and the particles were found to have a pore size distribution in the dimensions of mesopores.

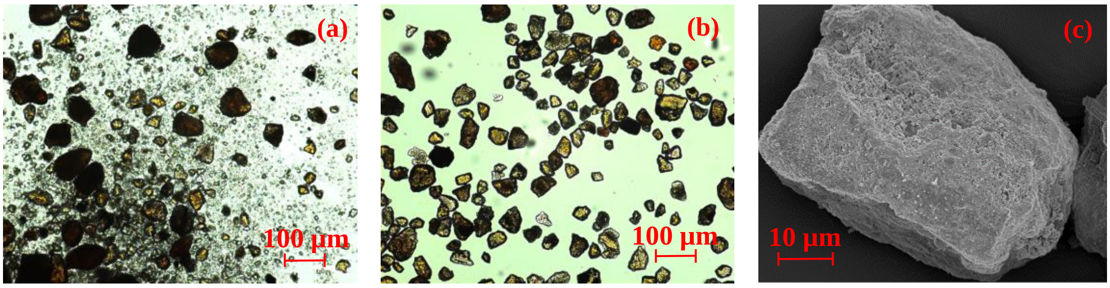

Figure 2.2: Thermal activated serpentine. a) sub 125 µm particles b) 20-63 µm size fraction after dry sieving and repeated washing with ethanol to remove fines. c) SEM image of a 20-63 µm size fraction particle.

2.3 Dissolution Experiments

This chapter reports the preliminary results of the far-from-equilibrium dissolution kinetics of thermally activated (75% dehydroxylated) serpentine. Preliminary flow-through experiments were carried out for three temperatures (i.e. 30, 60 and 90 °C) using 30 mg of the selected fraction of activated serpentine and applying CO_2 pressures within the range 0-100 bar in the specifically developed experimental setup described in Werner et al. (2011). The results of these preliminary dissolution experiments are reported and described in paragraph 2.3.2. Besides, in order to improve the accuracy of the performed dissolution measurements, several modification to the experimental setup were required and a series of experiments in the optimized experimental configuration were performed under lean partial pressures of CO_2 (0.1-2.0 bar) at moderate temperatures (30°C-90°C) using a lower amount of serpentine (5 mg instead of 30 mg) and some results of these tests are presented in paragraph 2.3.3.

2.3.1 Setup and Experimental procedure

The experimental setup (see Figure 2.3) used for performing the flow through dissolution experiments, first described in Werner et al. (2011), consists of a 300 ml titanium autoclave placed in an oil bath with external temperature control mounted on a high-capacity, low-readability balance (Mettler, XS64001LX).

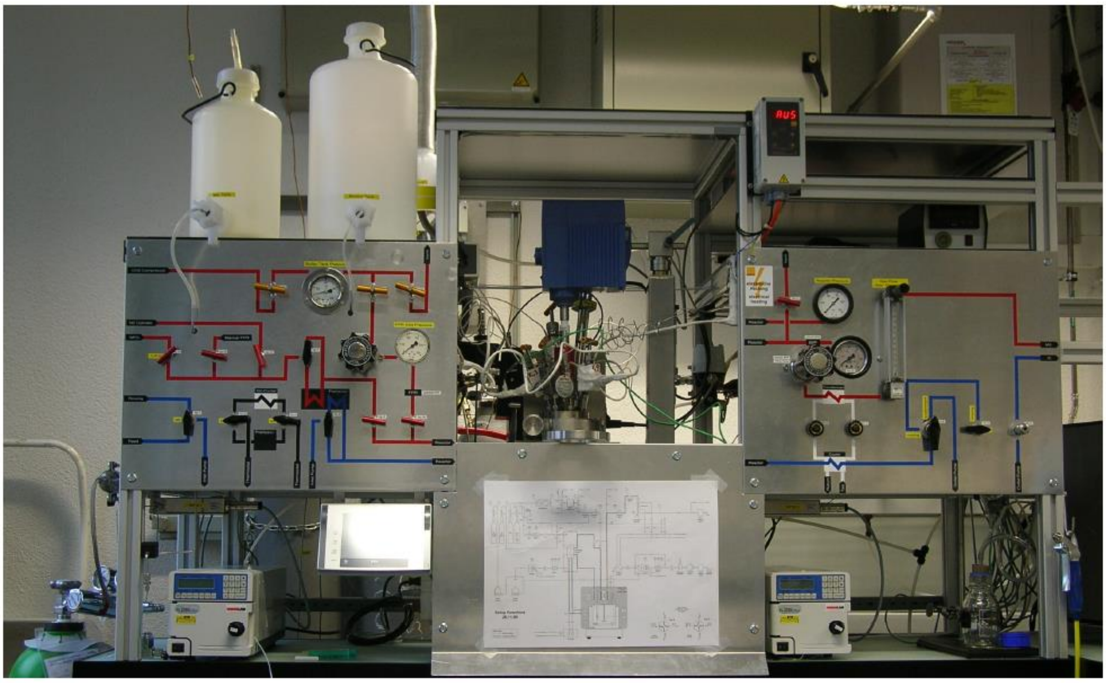

Figure 2.3: Picture of experimental setup used for the flow through dissolution experiments.

The lid of the reactor hosts inlet and outlet for liquid and gaseous flows, pressure and temperature sensors, a rupture disk, and a probe for in-situ monitoring via Raman spectroscopy (Kaiser, RXN1-789). The solution in the reactor is mixed with a blade stirrer suspended from the top of the reactor and driven by a magnetic coupling that entrains the gas mixture or nitrogen in the solution to facilitate gas diffusion into the solution. This stirrer is connected to two bottles: the nitrogen bottle is used for the heat up period prior to an experimental run, the second bottle contains a mixture of 10% mol CO_2 in N_2, resembling the average composition of flue gas from a coal and gas fired power plant. For experiments carried out at p_{CO2} higher than 11 bar, a gas bottle containing 100% CO_2 is used. Pressure is controlled by means of a backpressure regulator (BPR), while gas mass flow is set upstream via a mass flow controller. As the gas mixture does not contain any moisture, water stripping takes place from the reactor, thus requiring to heat the pipes downstream to prevent condensation. The excess water vapour is removed to a big extent in a condenser after the BPR, prior to online gas analysis via mass spectrometry further downstream (Pfeiffer Vacuum, GSD 301 C1). To measure the concentration of Mg^{2+} developing throughout an experimental run, a small liquid stream is withdrawn by means of an HPLC pump and fed to online analysis via ion chromatography (Dionex, ICS-2000, CS12A column). Total silica concentrations, instead, were determined from fractionated samples using the molybdate blue method. Upstream, another HPLC pump, delivers the necessary make-up of feed solution, in order to maintain a constant liquid level in the reactor. A constant flow is ensured via mass flow regulation at the inlet and the adjustment of the outlet pump rate according to the signal of the balance that detects weight changes in the reactor. The temperature and pH of the reactor solution are monitored continuously, and steady state is reached in less than an hour. In this setup preliminary dissolution experiments of thermally activated serpentine were carried out for temperature in the range 30-90 °C applying different CO_2 pressure values within 0.36 - 100 bar obtained using the N_2/CO_2 gas mixture (for p_{CO2} lower than 11 bar) or pure CO_2.

For each experiment, 30 mg of the selected fraction of activated serpentine were weighed and placed in the reactor which was thereafter firmly closed with the lid. The reactor was purged for three times with nitrogen up to 10 bar and filled with 170 ml of millipore water which was nitrogen purged overnight. Then, the gas mixture flow was initiated and after a waiting period of 30 minutes, also the liquid started to flow and downstream monitoring was enabled. During the dissolution experiments, the pH and the Mg concentrations were measured and the plant is operated with Labview. After the experiment, the reactor was depressurized in batch mode, the slurry is weighted to check if the liquid level was maintained and subsequently filtered. The solid product obtained at the end of each experiment was then dried overnight at room temperature.

As previously specified, after these tests the experimental setup and the operating procedure applied were partially modified (a simplified schematic diagram of this modified setup is shown in Figure 2.4). Specifically, the results obtained from the above mentioned series of experiments showed some critical aspects associated to the specific layout of the plant. In particular the long downstream piping network imply a large dead volume that entails a delay of around 1 hour between the outcome and the on line measurements of pH and Mg. Furthermore, the experimental procedure applied in the starting phase did not allow to measure the dissolution profiles in the initial phase (around 1 hour) where instead the conversion proved to be quite fast. For these reasons it was decided to modify the downstream piping network and to increase the flow rate of the pumps (from 1 ml/min to 5 ml/min) in order to reduce the dead volume and the delay in the measurements. Furthermore the experimental procedure was modified replacing the probe for in-situ Raman spectroscopy measurements with a gas-tight, tailor-made solid particle injection system that enabled the monitoring and measurement of initial, far-from-equilibrium dissolution kinetics of the activated serpentine. Before starting a dissolution experiment, the reactor was brought to equilibrium by having controlled liquid and gas flows. 5 mg of serpentine particles of the chosen size fraction were then carefully weighed, encapsulated in a small ice beaker (0.7 mL volume) and injected into this equilibrated, pressurized autoclave via the solid particle injection system. Gas mixtures of CO_2 and N_2 were used to simulate the flue gas composition for the experiments. Specifically in this optimized setup dissolution tests were performed at different temperatures (T=30-90°C) and partial pressures of CO_2 (p_{CO2}=0.1-2 bar) attained using a 2.5% and 10% CO_2 in N_2 gas atmosphere. The residence time for the liquid and the synthetic flue gas were set at 34 and 10 min respectively.

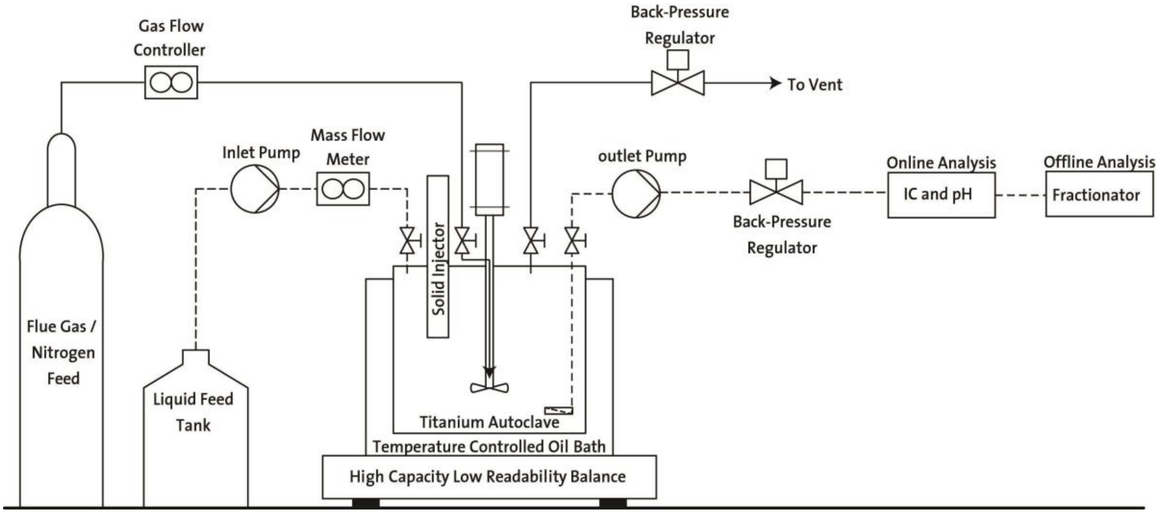

Figure 2.4: Simplified scheme of the modified experimental setup.

2.3.2 Preliminary results

Figure 2.5, Figure 2.6 and Figure 2.7 report the measured profiles of magnesium (a) and silicon (b) together with the estimated conversion based on Mg (c) and Si (d) measurements, the pH profiles (e) and the ratio between the Mg and Si conversion (f) obtained for each tested pressure at 30, 60 and 90 °C respectively (the lines in these plots have been produced by joining the experimental data points).

As can be seen in Figure 2.5(a), Figure 2.6(a) and Figure 2.7(a) magnesium dissolves rapidly in the initial phase of the experiment, where a maximum concentration of 554, 713 and 853 µM was reached for 30, 60 and 90 °C respectively, while after 2 hours a slow dissolution phase was observed. This trend is more evident observing the conversion plots reported in Figure 2.5(c), Figure 2.6(c) and Figure 2.7(c) where it is possible to note that in the first 2 hours of the experiments around 40, 60 and 70% of conversion was reached at 30, 60 and 90 °C respectively while after 10 hours a maximum value of 60, 70 and 90% was obtained. Initial elevated dissolution rates of minerals have been reported by several authors (Petrovich, 1981a, 1981b, Schott et al., 1981, Van Essendelft and Schobert, 2009). These have been attributed both to the presence of fines or surface defects and to the enhanced surface areas during sample preparation. Thermally activated serpentine, as reported in the previous section, has a very high BET surface area with mesopores. The fast initial dissolution rates could be the result of the high surface area available for dissolution through access from these pores.

Significant amounts of silicon are released during the experiment (see Figure 2.5(b), Figure 2.6(b) and Figure 2.7(b)) with a maximum concentration obtained after 2 hours at 30, 60 and 90°C of 158, 306 and 406 µM respectively, that correspond to a 15, 31 and 44% conversion (see Figure 2.5(d), Figure 2.6(d) and Figure 2.7(d)). However, the silicon conversion is found to be under-stoichiometric with respect to magnesium (as shown in Figure 2.5(f), Figure 2.6(f) and Figure 2.7(f) where the dotted line corresponding to a value of 1 indicates the stoichiometric cumulative release of magnesium and silicon), demonstrating that only a part of silicon is released into the bulk solution. Furthermore it can be seen that the dissolution becomes closer to the stoichiometric behaviour upon increasing the temperature.

For all the tested temperatures an increase in the CO_2 pressure resulted in an increase in the magnesium and silicon released in solution due to the exerted decrease in the pH of the solution (Figure 2.5(e), Figure 2.6(e) and Figure 2.7(e)). This effect is more evident for the tests performed at 30 °C, where the extent of conversion is anyhow lower. Hence the influence of the temperature on the dissolution of magnesium from the activated serpentine sample proved to be stronger than the one exerted by the carbon dioxide pressure.

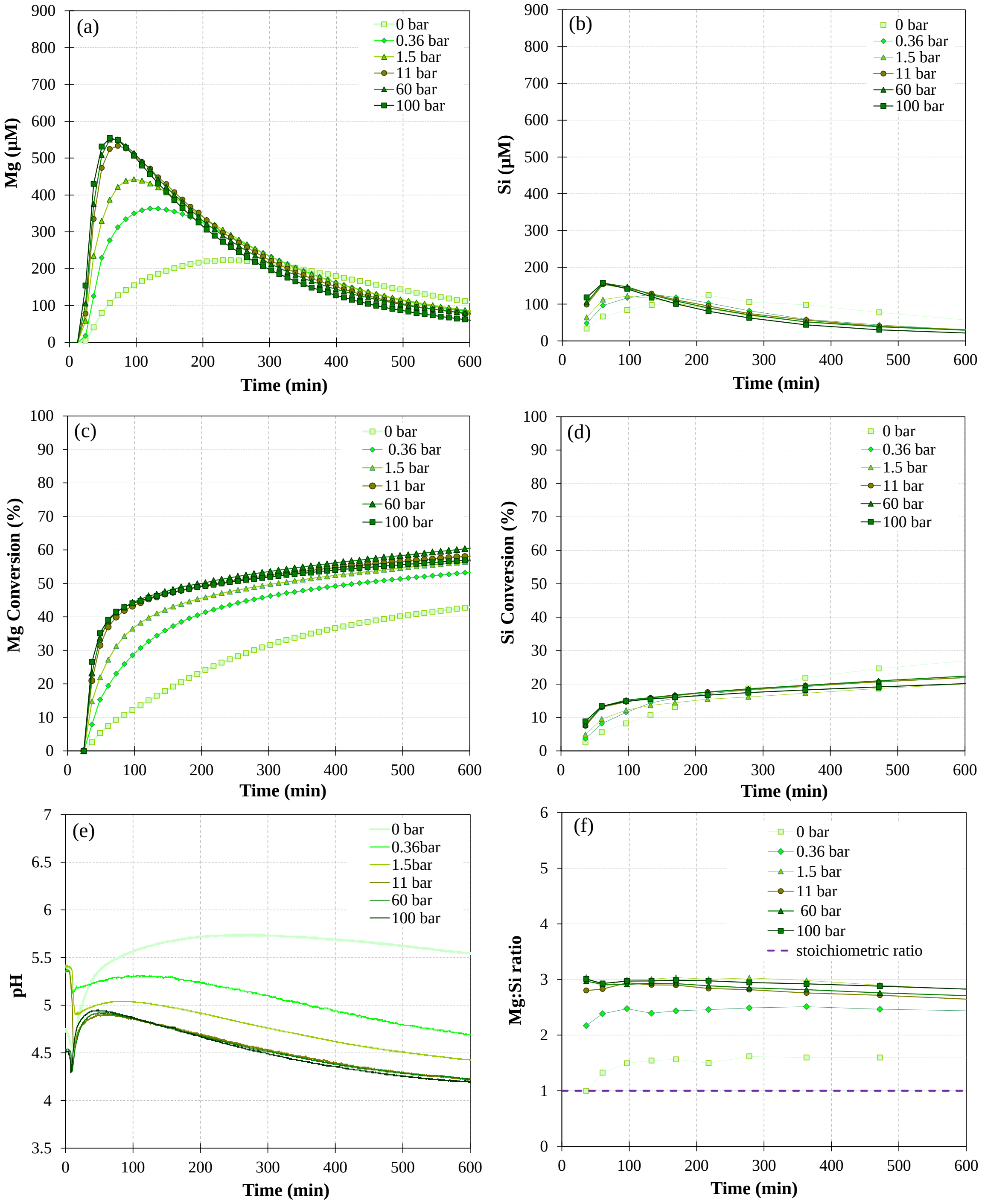

Figure 2.5: Dissolution profile for activated serpentine in flue gas atmosphere at 30 °C, mf = 30.0 mg. (a) magnesium concentration profile (b) silicon concentration profile (c) conversion profiles for magnesium, (d) conversion profiles for silicon, (e) downstream pH profile, (f) magnesium/silicon ratio.

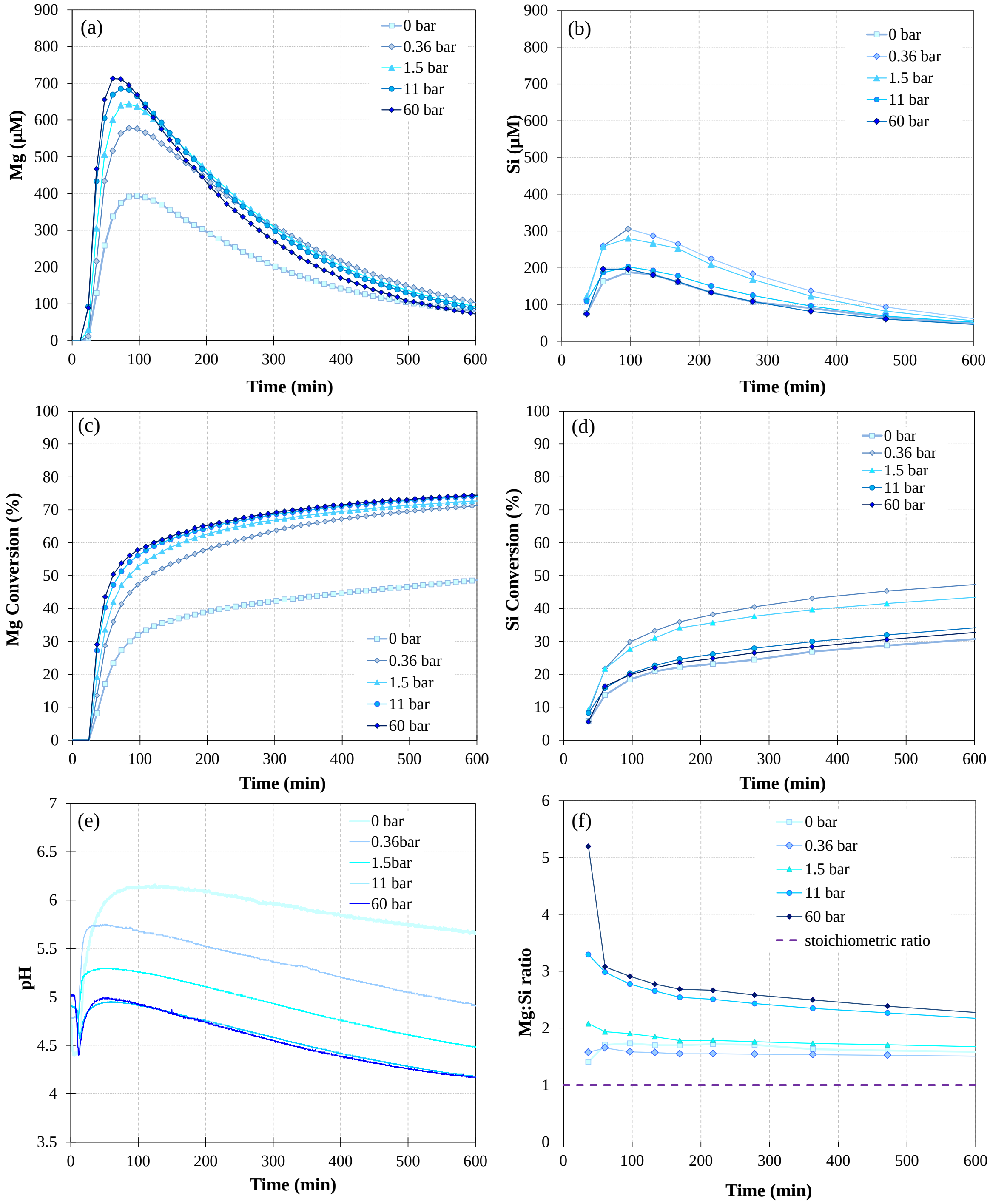

Figure 2.6: Dissolution profile for activated serpentine in flue gas atmosphere at 60 °C, mf = 30.0 mg. (a) magnesium concentration profile (b) silicon concentration profile (c) conversion profiles for magnesium, (d) conversion profiles for silicon, (e) downstream pH profile, (f) magnesium/silicon ratio.

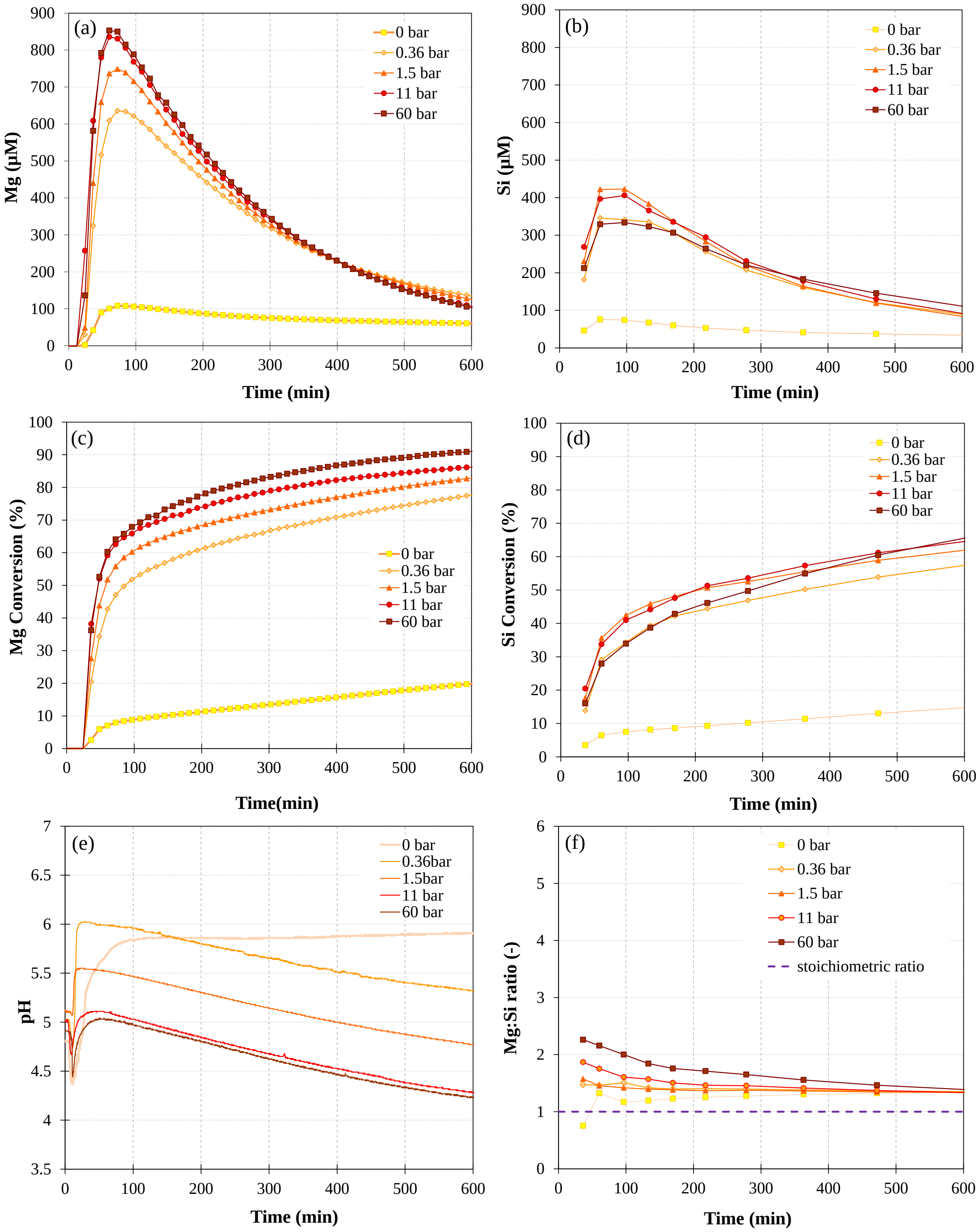

Figure 2.7: Dissolution profile for activated serpentine in flue gas atmosphere at 90 °C, mf = 30.0 mg. (a) magnesium concentration profile (b) silicon concentration profile (c) conversion profiles for magnesium, (d) conversion profiles for silicon, (e) downstream pH profile, (f) magnesium/silicon ratio.

2.3.3 Results obtained with the optimized experimental setup

Figure 2.8 reports the measured downstream concentration profiles of magnesium (a) and silicon (b), the estimated percentage of conversion based on Mg (c) and Si (d) measurements, the pH profile (e) and the ratio between Mg and Si conversion (f) for two experiments carried out in the modified experimental setup at 30 and 90 °C under a CO_2 partial pressure of 2 bar.

In the magnesium and silica concentration profile plots the markers indicate the experimental downstream concentration measurements while the lines in these plots have been produced by joining the experimental data points and accounting for a delay in concentration profile evolution due to the dead-volume of downstream piping network. The extent of conversion with respect to magnesium and silica (see Figure 2.8 (c) and (d)) has been calculated upstream at the reactor.

Although in a CO_2-water system, the resultant acidity is insufficient to dissolve natural serpentine (Park and Fan, 2004), thermally activated serpentine dissolves rapidly in moderate flue-gas operating conditions. From Figure 2.8(c), it can be seen that, as for the preliminary tests, rapid dissolution occurs initially, during the non-steady state period, and over 30 and 60% of the magnesium is leached in 1 hour (at 30 and 90°C respectively). This is followed by a dissolution period with very slow dissolution rates. This may be assumed to be steady state dissolution kinetics, although as the particle dissolves, its reaction surface and hence its dissolution rate decreases.

Unlike natural serpentine (see Van Essendelft and Schobert, 2009), a significant amount of silicon was released upon mineral dissolution (see Figure 2.8(b)). However, unlike forsterite (see Hänchen et al., 2006), the silicon release is non-stoichiometric with respect to magnesium as shown in Figure 2.8(f) where the ratio of the extent of dissolution between magnesium and silicon is plotted. This tests confirmed that the dissolution becomes less non-stoichiometric upon increasing the temperature. Such behaviour can be exhibited in systems where silicon dissolution rates are affected by equilibrium effects. However, the bulk concentrations of silicon are highly undersaturated with respect to amorphous silicon.

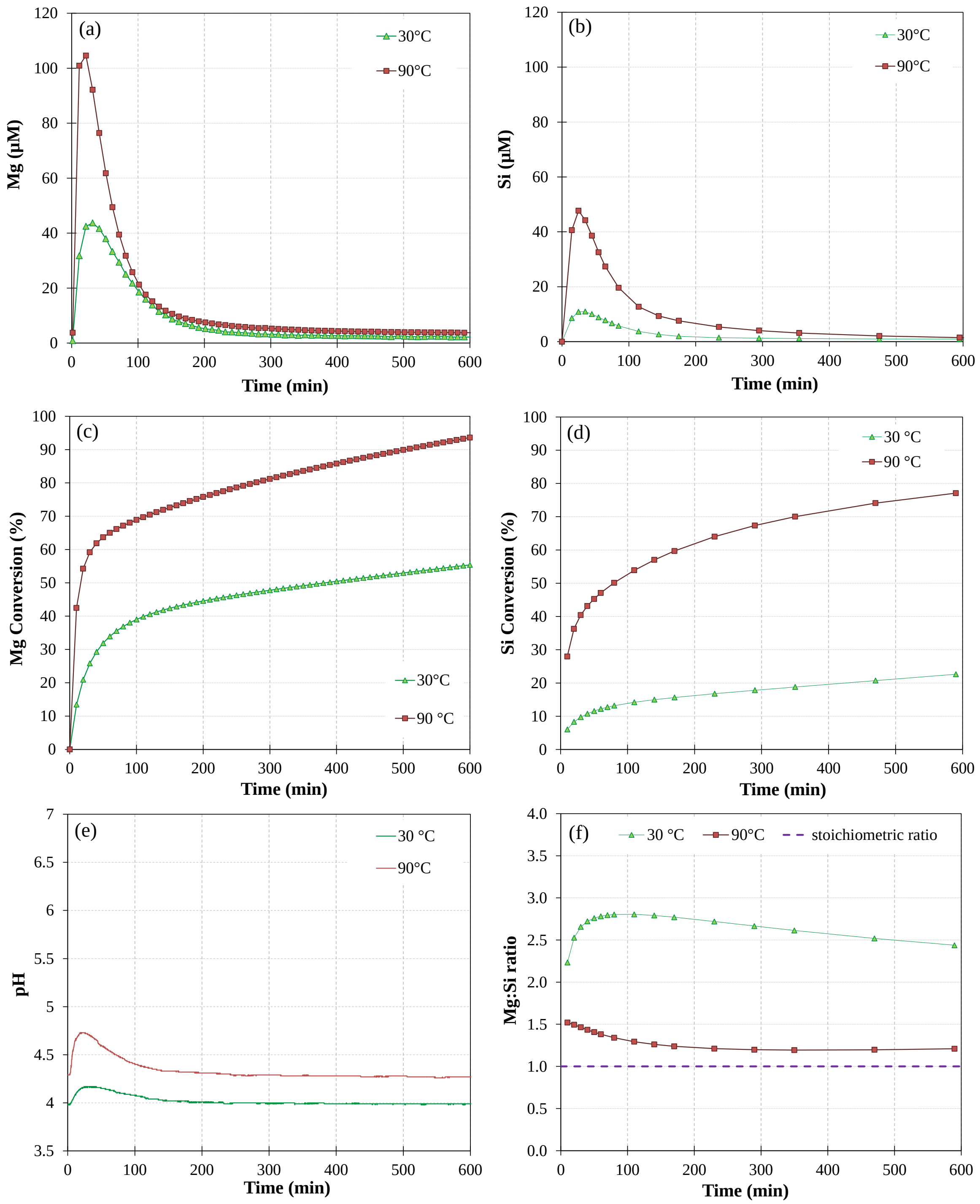

Figure 2.8: Dissolution profile for activated serpentine in flue gas atmosphere at 30 and 90 °C, mf = 5.0 mg. p_{CO2} = 2.0 bar (a) Downstream magnesium concentration profiles (b) silicon concentration profile (c) conversion profiles for magnesium (d) conversion profiles for silicon, (e) downstream pH profile, (f) ratio of the conversion obtained with respect of magnesium and silicon.

2.4 Carbonation Experiments

Starting from the promising results obtained from the above discussed dissolution tests performed with the 20-63 µm fraction, where the Mg release proved to be quite fast even in the absence of additives, in the second part of the study it was decided to perform direct carbonation experiments using the sub 125 µm fraction of the activated serpentine sample in order to analyse the precipitation of Mg-carbonates in the serpentine-CO_2-H_2O system and explore the carbonation potential of this material at mild operating conditions. In particular, the operating conditions to apply were chosen considering that typical flue gas CO_2 concentrations range from 4% for gas fired power plants up to over 20% for cement plants. Elevated partial pressures of CO_2, would require the co-compression of the other off gases, which is far from energetically efficient. Hence, the operating p_{CO2} for a flue gas mineralization process must not exceed levels close to ambient pressure or below. As to temperature, operating conditions are also limited to moderate levels, owing to the decreased solubility of CO_2 in water with increasing temperature.

2.4.1 Setup and Experimental procedure

Direct carbonation experiments were carried out using two 100 ml glass reactors in an EasymaxTM synthesis workstation for chemical and process development (Mettler Toledo, Switzerland) equipped with gas dip tubes and rotameters to control the flow of the process gas (see Figure 2.9). The reactor lids hosts ports for reflux-condensers, as well as for a pH- and Raman-probe to monitor dissolving and precipitating species in-situ. Upon filling the reactors with the designated amount of water, first nitrogen and then CO_2 have been bubbled through the solution for 30 min each, to remove oxygen and to establish the initial conditions with respect to temperature and p_{CO2}. The start of an experiment corresponded to the addition of activated serpentine powder through one of the lid ports using a funnel. The same port hosted also an adapter for a syringe that was used in some experiments to extract small samples of slurry at given time intervals.

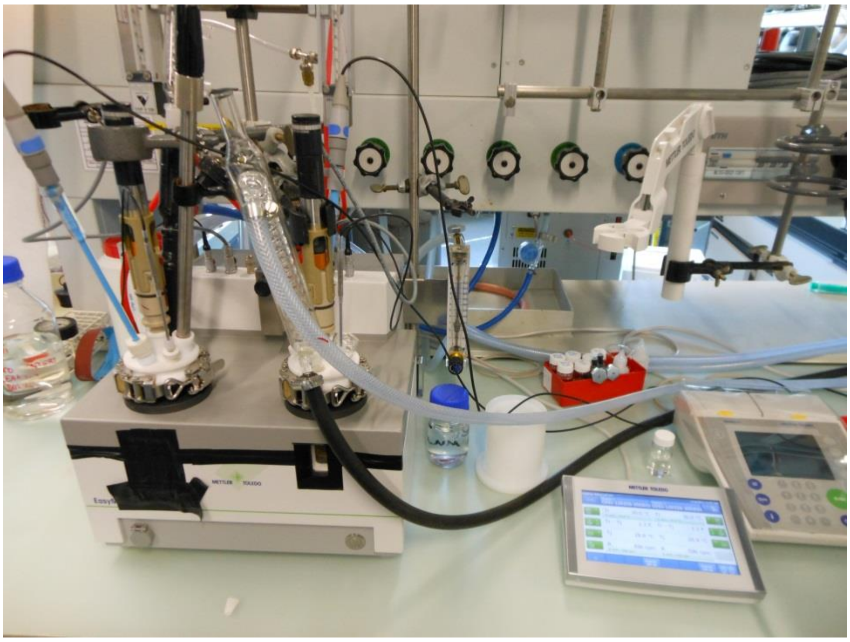

Figure 2.9: Picture of the experimental setup used for the batch carbonation experiments.

Experiments were performed at four temperatures (i.e. 30, 50, 60 and 90°C), with partial pressures of CO_2 in the range 0.1 - 1 bar applying a flow rate of 150 ml/min and different slurry densities (S/L = 10, 15, 20%wt.) and a stirring rate of 600 rpm. The tests were carried out for 9-15 hours monitoring in situ pH, temperature and the precipitation of the different Mg-carbonate species by Raman spectroscopy (Kaiser, RXN1-789). During the experiments a slurry sample was collected every 2 hours in order to estimate the extent of carbonation with time.

At the end of the experiment or after each sample collection, the slurry was immediately filtered and the solid sample was vacuum dried overnight at 40°C. The low drying temperature was chosen to prevent transformation of the product carbonates, and vacuum prevented potential further carbonation of the moist filter cake. Dry product was characterized using x-ray diffraction (Bruker, AXS D8 Advance) and scanning electron microscopy (Zeiss, LEO 1530). The carbonate content of the collected solid samples was determined by TOC analyser (Shimazu VCPH Anlyser equipped with SSM5000A solid sampler) and verified by Thermogravimetric analysis (Mettler Toledo, TGA/SDTA851). The mother liquor was instead acidified and the content of major elements were analysed by inductively coupled plasma optical emission spectrometry (ICP-OES Agilent 710-ES).

2.4.2 Mg carbonates precipitation

In the first phase of the activities, 15 hours long experiments were carried out in order to test the capacity of the performed analysis (Raman analysis, XRD measurements and SEM images) in determining the different forms of magnesium carbonates that precipitate during the experiment. Figure 2.10 shows Raman spectra of three preliminary experiments at 30, 60 and 90°C, together with SEM images of the acquired product.

Monitoring the reacting slurries with Raman allowed to observe the evolution of the products, despite the strong background in the spectra, which was caused by the presence of the pseudo amorphous serpentine feed. As expected, in fact, this analysis has shown the formation of nesquehonite (Raman shift 1099 cm^{-1}) in experiments carried out at 30-50°C while at higher temperature (i.e. 60-90 °C) only hydromagnesite (Raman shift 1119 cm^{-1}) was formed (see Figure 2.10).

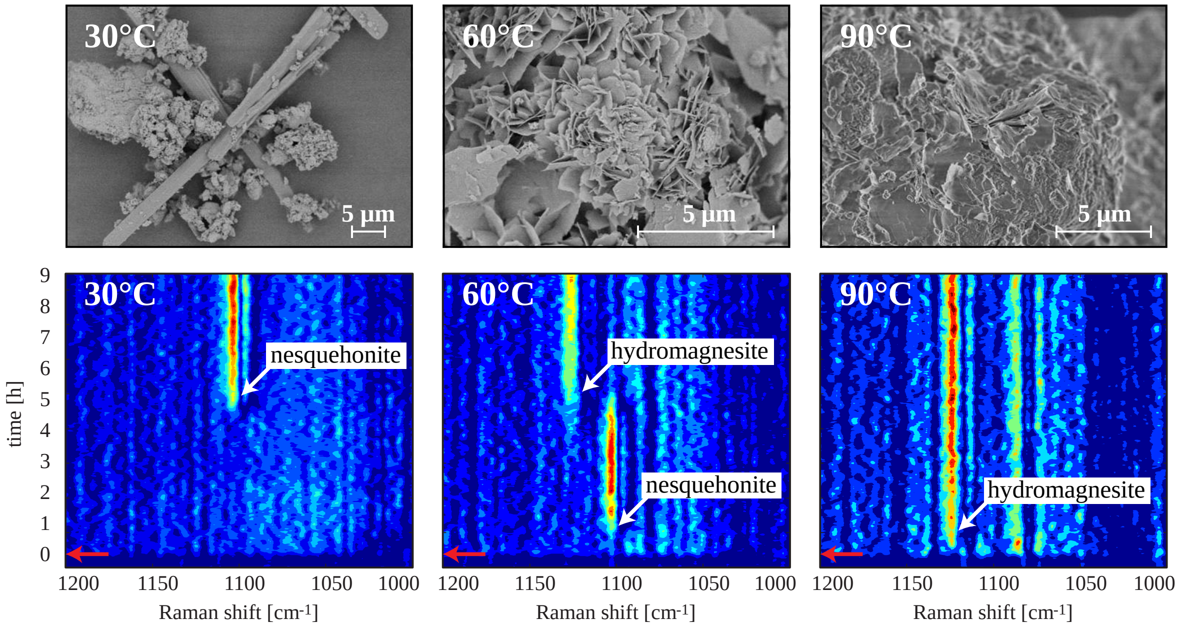

Figure 2.10: SEM images (top) of product for experiments at 30°C (left), 60°C (middle), and 90°C (right). Contour plots of Raman spectra (bottom), colour map relative to gradient of spectra in x-direction. Red arrows denote serpentine addition. Raman shift values for nesquehonite is 1099 cm-1, and for 1119 cm-1 for hydromagnesite. Experimental conditions: p_{CO2} = 1 bar, S/L = 10% wt.

SEM images also confirm these results showing that the solid product obtained at lower temperature consisted of the characteristic needle-shaped crystals of nesquehonite, while at 60-90°C the platelet-shaped hydromagnesite was formed (see Figure 2.10). These findings are in agreement with previous studies (e.g. Canterford and Tsambourakis, 1984) where the form of magnesium carbonate was observed to be strongly influenced by the temperature of the solution. Recently Hänchen and co-workers (2008) have studied the precipitation of magnesium carbonates calculating the solubilities of different magnesium carbonates (see Figure 2.11). As stated by Hänchen et al. (2008), despite being the stable carbonate form, the formation of magnesite at ambient temperature is virtually impossible and only nesquehonite ($MgCO_3$ $3H_2O$) can be precipitated from aqueous solutions at 25°C and moderate partial pressure of CO_2, i.e., close to ambient pressure or below (Dell and Weller, 1959; Davies and Bubela, 1973; Ming and Franklin, 1985; McKelvy et al., 2004 Kloprogge et al., 2003; Zhang et al., 2006,). At temperatures higher than 50°C, instead, various basic Mg-carbonates are usually formed by precipitation, mostly in the form of hydromagnesite ($Mg_5(CO_3)_4(OH)_2$ $4H_2O$) (Dell and Weller, 1959; Davies and Bubela, 1973; Fernandez et al., 2000; Zhang et al., 2006, Hänchen et al., 2008). Finally magnesite has been reported to form only at temperature higher than 60-100 °C and elevated p_{CO2} (e.g. Zhao et al., 2010, Sayles and Fyfe, 1973; Giammar et al., 2005).

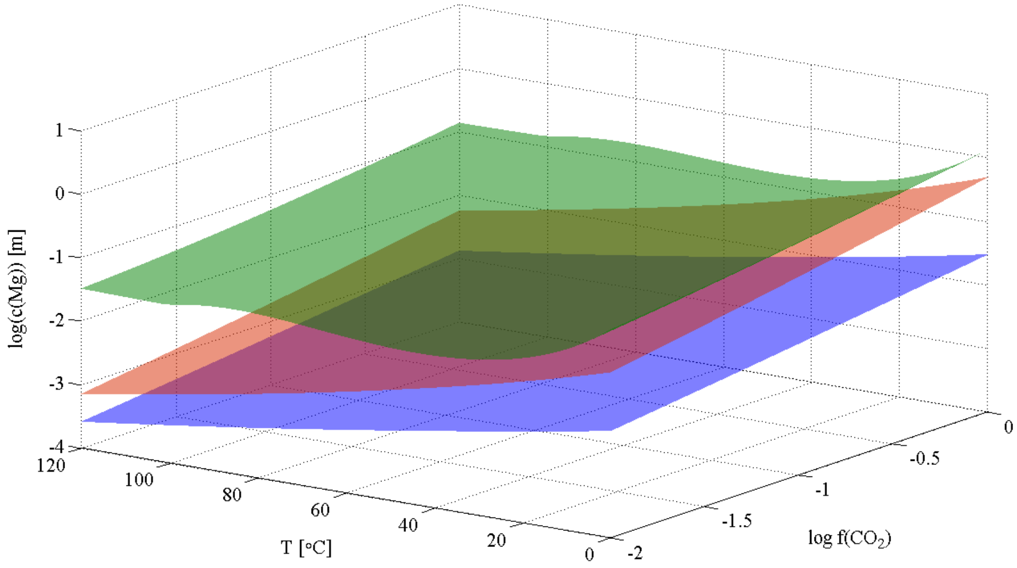

Figure 2.11: Solubilities of magnesite (blue), hydromagnesite (red), and nesquehonite (green) at flue gas mineralization conditions (from Hänchen et al., 2008).

Furthermore, as reported in Figure 2.10, the experiments carried out at 60 °C allowed also to observe the transformation from nesquehonite to hydromagnesite. In particular, at the beginning of the experiments nesquehonite was precipitated first, but after 5 hours its peak disappeared while the formation of hydromagnesite was observed. This transformation between the two Mg carbonates forms is also evident looking to the XRD analysis performed on the solid samples collected every 2 hours during this experiment (see Figure 2.12) that showed the disappearance of the characteristics peaks of nesquehonite with time and the formation of small peaks of hydromagnesite.

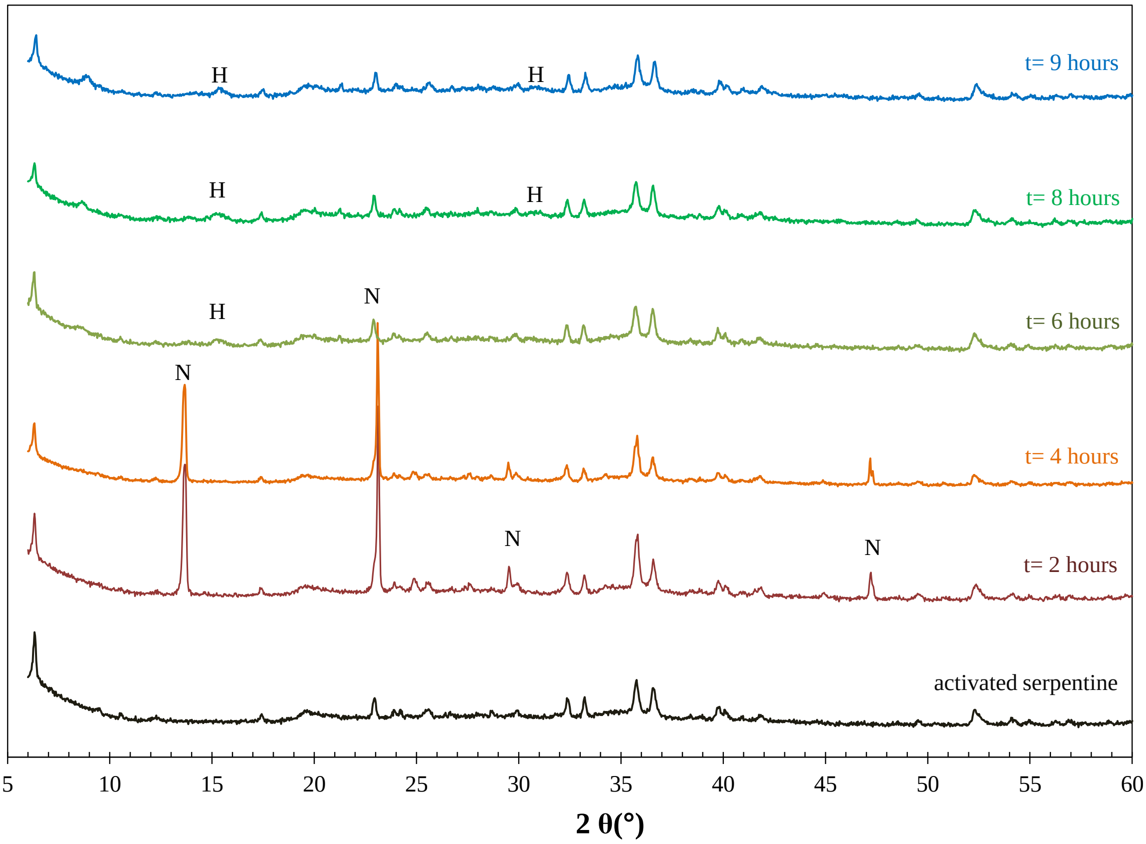

Figure 2.12: XRD analysis on the solid sample collected at different time during the experiment performed at 60 °C (N=nesquehonite, H=hydromagnesite).

2.4.3 Carbonation results

Based on the carbon content of the solid products measured by TOC, the CO_2 uptake and the extent of carbonation achieved in each tests were estimated. The former parameter was estimated according to Eq. (2.7) where C_{FIN} and C_{IN} represent the carbon content of the solid sample before and after the carbonation test respectively and M_C and M_{CO2} are the molar masses of carbon and CO_2. The extent of carbonation was then estimated considering the calculated CO_2 uptake and the total magnesium content of the activated serpentine accounting for the initial magnesium content as carbonates of the material (see Eq. (2.8)).

$$CO_{2\,UPTAKE}(\%) = \frac{\left(C_{FIN} - C_{IN}\right)\cdot\dfrac{M_{CO2}}{M_C}}{100 - \left(C_{FIN}\cdot\dfrac{M_{CO2}}{M_C}\right)}\cdot 100 \tag{2.7}$$

$$R_X(\%) = \frac{CO_{2\,uptake}(\%)\cdot\dfrac{M_{Mg}}{M_{CO2}}}{Mg_{REACTIVE}}\cdot 100 \tag{2.8}$$

Figure 2.13 reports the extent of carbonation of the solid product collected at different time in the experiments carried out at 30, 50, 60 and 90 °C. As can be seen at 30 °C Rx remained lower than 2% for the first 5 hours and then started to increase reaching around 10.2% after 8 hours. For 50 °C and 60 °C, instead, already after 2 hours the extent of carbonation proved to be around 9% and showed to slightly increase with time until around 15.7 and 17.7% respectively. At 90 °C the extent of carbonation after 2 hours was equal to 16 % and slightly increased for longer times up to 17.4%. From these results it is possible to observe that, as expected, an increase of the operating temperature accelerates the precipitation of carbonates and, hence, the extent of carbonation that anyhow did not exceed 18%.

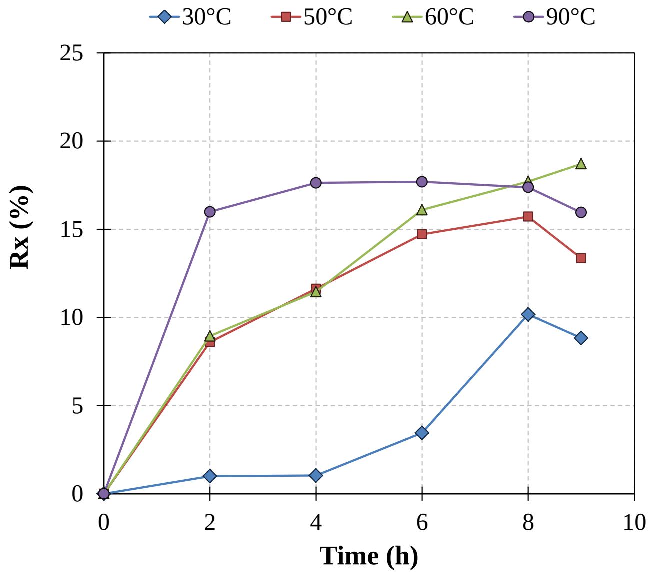

Figure 2.13: Extent of carbonation for different temperature (S/L=10% wt., p_{CO2}= 1 bar, 600 rpm).

Looking to the concentration of the main elements detected in the solutions collected in each experiment at different times and temperatures (see Figure 2.14), one can observe that magnesium is the major element detected in solution followed by silicon and calcium. Furthermore Figure 2.14 shows that the concentrations of magnesium and calcium in solution decrease for increasing temperature. This trend could be explained considering the results obtained by Hänchen and co-workers (see Figure 2.11) that showed a lower solubility of nesquehonite compared to hydromagnesite and a decrease of the solubility of both Mg carbonates forms with temperature (Hänchen et al., 2008). It can be also noted that a lower concentration of magnesium in solution was observed for higher extent of carbonation.

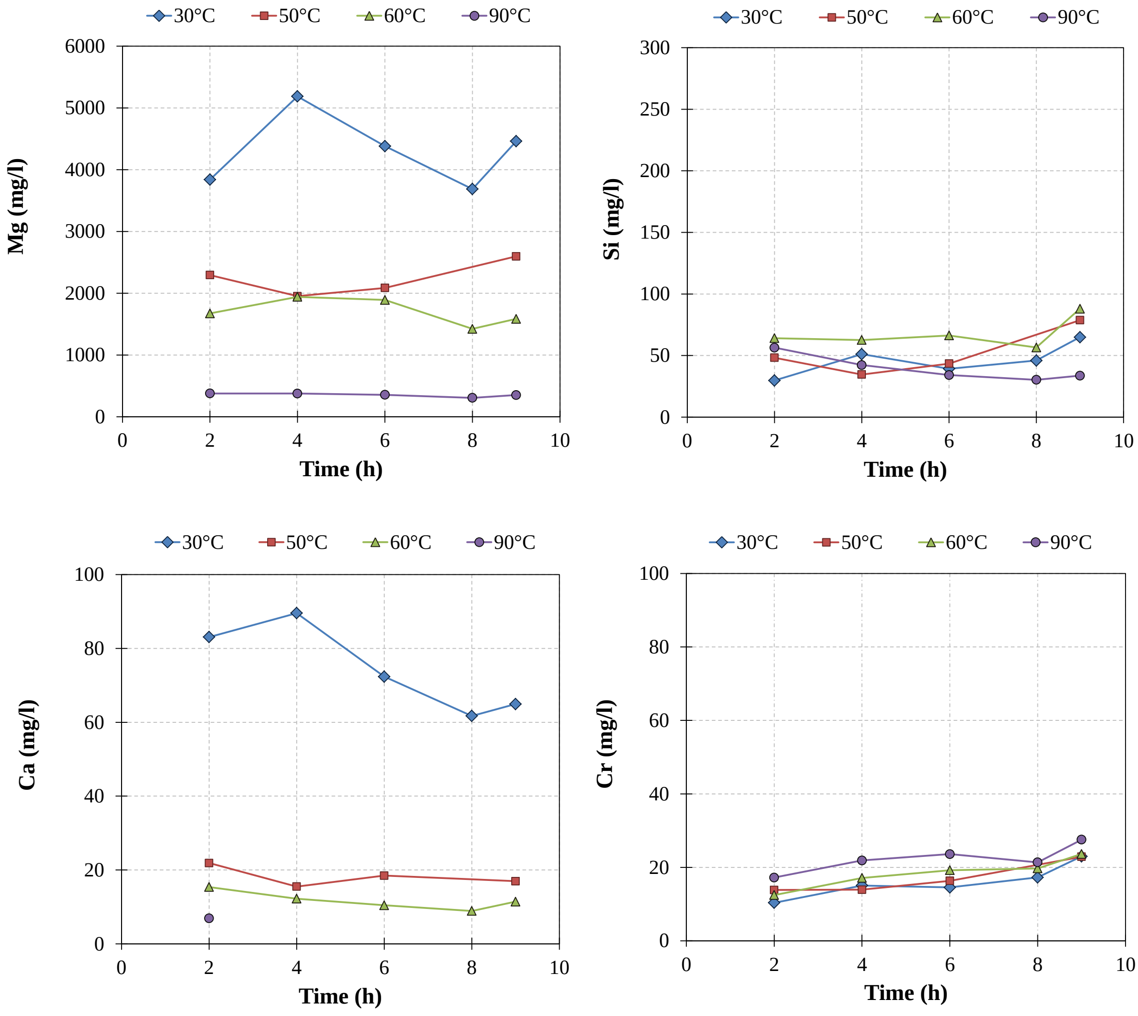

Figure 2.14: Concentration in solution of the main elements at different temperature (S/L=10% wt., p_{CO2}= 1 bar, 600 rpm).

However, the extent of carbonation obtained in all the tested operating conditions is anyhow low, remaining around values lower than 18%. In order to increase the extent of carbonation, some experiments were also performed at 30 and 90 °C applying higher slurry densities, i.e. 15 and 20% wt. and the results of these tests in terms of carbonation extent are reported in Figure 2.15. As can be seen an increase in the slurry density proved to affect mainly the extent of carbonation at 30 °C that after 8 hours reached around 17.1% instead of 10.2% passing from 10 to 20% wt. At 90 °C instead an increase in the slurry density from 10 to 15% wt. seems even to reduce the carbonation extent from 17.4 to 15.4%.

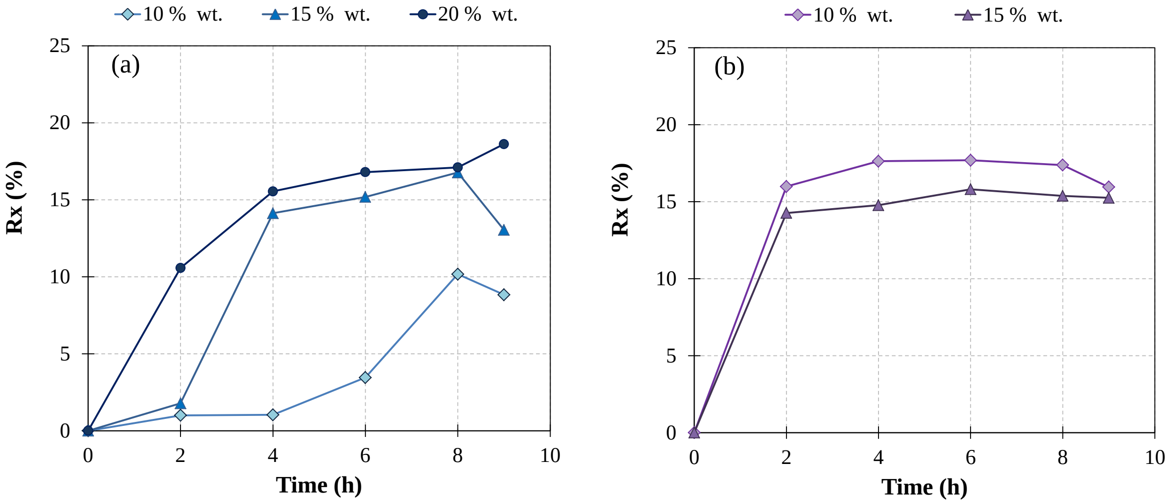

Figure 2.15: Extent of carbonation for different slurry densities at (a) 30 °C and (b) 90 °C (p_{CO2}= 1 bar, 600 rpm).

Based on these direct carbonation experiments one can observe that increasing the S/L ratio to 15 and 20% wt. entails a reduction of the time until onset of precipitation is reached and increases the carbonation efficiency at 30°C, but also in this case the Rx did not exceed 20% for the investigated temperatures. The higher the temperature and slurry density, the sooner this threshold was reached. At these high slurry densities, the pH jumped up to levels above 9, which was suspected to be too high for serpentine dissolution to proceed. Further reaction progress seemed to be hindered by either a diffusive barrier around the dissolving feed (silica-ash and/or secondary nucleation and growth of carbonates) or by equilibrium effects. In an attempt to prevent such high pH, one experiment was performed dosing serpentine step by step in 1 g portions at specific time intervals during the first 2 hours, and then letting the reaction proceed for another 2 h thereafter. However the extent of carbonation did not proved to be affected by the dosing strategy since a similar Rx value was obtained despite the pH trend was different. Therefore, it was hypothesized that further reaction progress could be hindered by the formation of a passivating layer around the dissolving mineral feed. This layer could either consist of an undissolved silica ash or it could form via heterogeneous nucleation and growth of carbonates on the serpentine surface. However some experiments were performed using a concurrent grinding by means of a ball mill that create fresh surface on the mineral or using some seeds but the obtained results showed only limited improvement in the carbonation extent (i.e. the R_X threshold increase from around 20% to around 25% and to 30% respectively). Such moderate increase suggests equilibrium effects to be more dominant and that an indirect process could be applied for further improvement of the carbonation extent of this material (Werner et al., 2013b).

2.4.4 Conclusions

The aim of the study presented in this chapter was to explore the possibility of performing direct carbonation of a thermally activated serpentine using a flue gas instead of pure CO_2 in order to avoid the CO_2 capture step that represent one of the most energy intensive stages in an ex situ carbonation process. In particular this chapter reports a preliminary study on the performance achievable in this process regarding both the dissolution of magnesium from the mineral, that, as well known, constitutes the limiting step in the mineralization process, and the carbonation potential of the tested material in the selected operating conditions.

In order to test the dissolution of the activated serpentine, several flow through tests were performed at a temperature within 30-90 °C applying different carbon dioxide pressure obtained by using a N_2/CO_2 gas mixture with 10% CO_2 and monitoring pH, temperature, magnesium and silicon concentrations for the entire duration of the experiment. Based on these results it was possible to measure the dissolution profiles of silicon and magnesium in all the tested conditions. It was observed that, as expected, the dissolution kinetics were faster for higher temperature and CO_2 pressure, although the effect exerted by temperature proved to be more evident. The dissolution kinetics is characterized by an initial non-steady state dissolution phase with high dissolution rates followed by a slow dissolution phase. The dissolution profiles at far-from-equilibrium operating conditions were dependent on the instantaneous pH of the aqueous system. Furthermore it was noted that the silica release rates were non-stoichiometric with respect to the magnesium release rates but became less under-stoichiometric with increasing temperature. Under-stoichiometric dissolution of silica can result in the formation of a diffusive barrier for further magnesium release. Thermal activation resulted in porous serpentine particles with a high surface area and enabled rapid dissolution of otherwise inert serpentine under mild acidic conditions. Based on these results, the colleagues of the ETH group are developing a model to describe the dissolution kinetics of the thermally activated serpentine in the tested conditions.

As for the assessment of the carbonation potential of this material, several experiments at different operating conditions relevant for flue gas mineralization (i.e. T=30-90 °C, p_{CO2}=1 bar) were carried out using the fraction with initial particle size under 125 µm. In its simplest process form, the single-step mode, the experimentally measured extent of carbonation was found to be lower than 20% under the conditions explored in this work. The use of a concurrent grinding or some seeds proved to exert only limited improvements in the process efficiency. The key challenge of the single-step process is the fact that dissolution of serpentine and precipitation of magnesite are favoured at the opposite ends of the pH range. Upon onset of precipitation, the equilibrium pH in the system activated-serpentine-CO_2-H_2O is too high for further dissolution, but too low for further precipitation. However the overall carbonation efficiency may be improved if serpentine dissolution and Mg-carbonate precipitation are separated. Currently, the ETH group is performing such indirect carbonations experiments applying a temperature swing in combination with a p_{CO2} swing and the obtained results look promising indicating substantial room for optimization.

3 ACCELERATED CARBONATION OF INDUSTRIAL RESIDUES USING 40% CO_2 GAS MIXTURE

3.1 Introduction

The results obtained so far in previous studies, as well as those reported in the previous chapter, show how difficult is to obtain relevant extent of carbonation of minerals in time scale of hours, suitable for industrial application. A possible way of bypassing some of the limitations of accelerated carbonation of primary alkaline earth minerals may rely on using alkaline industrial residues from thermal processes or from construction and demolition activities as a feedstock (Costa et al., 2007). These materials indeed are more reactive compared to natural minerals hence, generally, high CO_2 uptakes can be achieved applying less energy intensive operating conditions. Furthermore, in many cases these materials present a particle size already suitable for the carbonation process allowing to reduce or avoid the need of a grinding step, that represents one of the most energy intensive stages. In addition, although their total amount is quite limited when compared to silicate minerals, they are typically available at CO_2 point-source emission locations, such as coal-fired power plants, waste to energy facilities and steel manufacturing plants (Huijgen and Comans, 2003). Thus, these materials could be employed in niche applications in order to store at least part of the CO_2 emissions of the same industries from which they are produced. Besides, another important advantage that could be achieved applying the carbonation treatment to industrial residues is the improvement of the environmental behaviour of the residues, thus making their reuse or disposal easier (e.g. Van Gerven et al., 2005; Baciocchi et al., 2009, 2010a). Several works have applied accelerated carbonation both as a CO_2 sequestration technique and as a treatment strategy for improving the environmental behaviour of residues such as MSWI residues and steel slag (e.g. Fernández Bertos et al., 2004; Rendek et al., 2006; Huijgen and Comans, 2006).

The main types of alkaline residues that have been selected and tested for accelerated carbonation, due to their availability and chemical and mineralogical composition, are steelmaking slag (e.g.: Huijgen et al., 2005; Teir et al., 2007b; Lekakh et al., 2008; Kodama et al., 2008), bottom ash and air pollution control (APC) residues generated by municipal solid waste incineration (e.g. Rendek et al., 2006; Baciocchi et al. 2009), cement kiln dust (CKD) (Huntzinger et al., 2009), concrete wastes (e.g.: Iizuka et al., 2004; Shtepenko et al., 2005; Stolaroff et al., 2005), mining and mineral processing wastes.

The steel slags are considered a good candidate for mineral carbon sequestration considering their large availability, high alkalinity (pH around 12) and calcium content and the elevated carbon dioxide emission associated to the plants were they are produced. Steelmaking industries are responsible for 6-7% of total CO_2 emissions worldwide (Bonenfant et al., 2008) and from the different applied processes various types of slags are produced (e.g. blast furnace (BF), basic oxygen furnace (BOF), electric arc furnace (EAF) and ladle slags). Based on current steel production data and on the amounts of slags resulting from each specific process, it can be estimated that around 100 Mt/y of BOF slags and over 55 Mt/y of EAF slags are produced worldwide (World Coal Association, 2011; Siegmund et al., 2008). The chemical and mineralogical composition of steelmaking slags is strongly affected by the specific industrial process from which they are produced, but generally they are characterized by a high content of calcium (32-52% CaO according to Eloneva et al., 2008), iron, silicon, aluminium, magnesium and manganese oxides (Bonenfant et al., 2008). The carbonation of steel slags was proven to be effective both in the slurry phase direct route (e.g. Huijgen et al., 2005; Lekakh et al., 2008; Bonenfant et al., 2008; Baciocchi et al., 2011b) and in the indirect route (e.g. Teir et al., 2007b; Kodama et al., 2008).

The solid residues produced by a waste incineration plant consist mainly of two waste streams: bottom ash (80%) and air pollution control (APC) residues (around 20%). For APC residues, the high content of readily reactive calcium hydroxides makes carbonation potentially suitable for CO_2 sequestration purposes, with possible integration of the carbonation process with waste combustion in order to reduce the net CO_2 emissions of incinerator facilities. However, due to the relatively low amounts of such residues as compared to the original waste, a still limited reduction in CO_2 emissions can be anticipated (Costa et al., 2007). In the case of MSWI bottom ash, typical Ca and Mg contents are not high enough to render CO_2 sequestration through accelerated carbonation a viable option. For bottom ash, the application of accelerated carbonation is thereby applied with the aim to attain a chemically stable structure with improved leaching behaviour (Costa et al., 2007).

The CO_2 sequestration potential of CKD and concrete demolition waste has also been studied, owing to the high contents of both free lime and calcium silicates of these materials (e.g. Huntzinger et al., 2009; Iizuka et al., 2004; Shtepenko et al., 2005; Stolaroff et al., 2005). As stated by Bobicki et al. (2012) CKD and waste cement have the potential to be used for mineral carbon sequestration since both have a high mass fraction of CaO (20-60%), are available in large quantities and are highly reactive due to their small particle sizes. Bobicki et al. (2012) have estimated that, assuming a CO_2 uptake of 16.5% and considering the waste concrete produced in the European Union, China and United States to be approximately one third waste cement, these countries could collectively sequester nearly 61 Mt of CO_2 on an annual basis using cement waste alone, accounting for 0.2 % of global CO_2 emissions from fuel combustion (IEA, 2010) and about 3% of the CO_2 emissions from cement industry (IEA, 2009). Furthermore the carbonation of cement wastes not only sequesters carbon and recycles cement, but also mitigates the potential health hazards associated with CKD disposal (Huntzinger et al., 2009; Iizuka et al., 2004).

Most of the recent studies carried out in this field assessed the reactivity of the above mentioned residues applying the direct aqueous carbonation route (Sipilä et al., 2008; Huijgen et al., 2006; Lackner et al., 2003). This reaction route involves the dissolution of the reactive phases and the precipitation of carbonates in a single stage and has been performed using two different process layouts:

- slurry phase route at liquid-to-solid (L/S) ratios higher than 1 l/kg (typical operating conditions: T=100-150 °C and p_{CO2} = 1-20 bar) (Huijgen et al., 2006a);
- wet route, using L/S ratios below 1 l/kg (typical operating conditions: T=20-50 °C and p_{CO2} = 1-10 bar) (Baciocchi et al., 2011b).

This latter type of process avoids the treatment and disposal of the processing liquid, and has been also indicated to favour the dissolution kinetics of hydroxide and silicate phases under mild operating conditions, which may allow to more easily reach saturation conditions of carbonate mineral phases (Baciocchi et al., 2011b).

It is worth pointing out that although many types of residues proved to be reactive with CO_2 and could allow to store significant amounts of carbon dioxide, industrial scale application of the process are still missing. The energy demand of the process and the associated costs are commonly established to be the main drawbacks that hindered so far larger scale applications. For this reason now the researchers’ attention, as discussed already in the previous chapter for minerals, is focused on searching options that may allow to reduce the energy requirement of the process, for example trying to skip the need of a CO_2 capture stage that represents one of the most energy intensive step within the carbon capture and storage (CCS) process. Many studies carried out so far on accelerated carbonation, in fact, have investigated the performances of different types of industrial residues only using pure CO_2 stream, thus requiring a capture step before the carbonation process in order to concentrate the carbon dioxide content of the gas. It is therefore needed to collect experimental data aimed at testing the feasibility of performing the carbonation of alkaline material without a CO_2 capture step, hence using gas mixtures with lower contents of carbon dioxide directly produced at point sources, such as syngas or flue gas.

The goal of the study presented in this chapter was to evaluate the feasibility of performing carbonation of industrial residues using a N_2/CO_2 gas mixture with 40 % of CO_2, that simulates the typical carbon dioxide concentration of a syngas. In particular an experimental study was carried out performing wet-route carbonation tests using three types of industrial residues previously characterized and used to perform carbonation tests with pure CO_2 (see Baciocchi et al., 2009; 2010b). Specifically for each residue the effect of the main operating conditions on the achieved extent of carbonation was analysed and, then, the performances obtained with the N_2/CO_2 gas mixture were compared with the ones already observed for the same material, using pure carbon dioxide basically at the same CO_2 partial pressure.

3.2 Materials and methods

Three types of industrial residues were used to test the CO_2 uptake achievable with each material using a N_2/CO_2 gas mixture with 40% of CO_2 instead of pure carbon dioxide, i.e.:

- the APC residues sampled from the baghouse section of a hospital waste incinerator located near Rome (Italy) at the outlet of the flue gas dry treatment section where pulverized hydrated lime and activated carbon are added to remove acid gases and organic micropollutants;
- the ladle slags produced at the outlet of the argon oxygen decarburization and desulfurization unit (AOD) in a stainless steel making plant;
- the basic oxygen furnace slags collected from an integrated steel manufacturing plant site in Italy.

The main characteristic of each residue in terms of water content, loss on ignition (LOI), element and major anion content, carbonate content, mineralogical and morphological composition, acid/base neutralization capacity (ANC/BNC) as well as leaching behaviour are published elsewhere (i.e. Baciocchi et al., 2011b; 2011c; 2010b). Table 3.1 reports the main mineralogical phases detected in each residues by XRD analysis. Before starting the experimental campaign the residues were oven dried at 105 °C and their carbonate content was measured again in order to take in account the effect of the natural weathering of the material. Specifically, the measured $CaCO_3$ content was equal to 4.6% for the AOD slags, 10.8% for the APC residues and 4% for the BOF slags.

Table 3.1: Main mineralogical phases detected in each residue.

Residue	Main phases
APC residues	CaOHCl, $Ca(OH)_2$, NaCl, $CaCO_3$
AOD slags	Ca_2SiO_4, $CaCO_3$, MgO
BOF slags	Ca_3SiO_5, $Ca_2Fe_2O_5$, Ca_2SiO_4, CaO, FeO, $(MgO)_{0.59}(MnO)_{0.41}$, $CaCO_3$

The carbonation experiments were carried out in a 150 ml stainless steel reactor placed in a thermostatic bath to operation at different temperatures in the range 20-50 °C. Three 1 g samples of dry residues were placed in aluminium foil containers and, then, mixed with distilled water at the desired L/S ratios. Namely, for each residue it was decided to apply the liquid to solid ratio that, based on the results of previous experiments, demonstrated to lead to the highest carbonation extents. In particular 0.2 l/kg was applied for tests performed with APC residues, 0.4 and 0.3 l/kg in case of AOD slag and BOF slags respectively.

The carbonation experiments were performed using a gas mixture made up by 40% carbon dioxide and 60% nitrogen in order to simulate the typical CO_2 content of a syngas. The carbon dioxide partial pressures (p_{CO2}) tested in these experiments were 0.4, 1.6 and 2.8 bar. Furthermore some tests were also performed using pure CO_2 with a pressure of 3 bar in order to compare the performances obtained with this gas and the N_2/CO_2 mixture for each material. Temperature was monitored with a thermocouple, while gas humidity was maintained at 75% using a saturated NaCl solution in the reactor. The reactor was flushed with CO_2 at the beginning of each run to ensure air expulsion. The experiments were conducted for reaction times from 15 min to 24 h to study the CO_2 uptake kinetics under different operating conditions.

The carbonate content of the solid product before and after carbonation were estimated by calcimetry analysis of HCl-digested ash using a Dietrich–Früling calcimeter.

The amount of stored CO_2 was assessed by measuring the weight gain upon carbonation and the CO_2 uptake of the ash. This latter parameter was estimated on the basis of the calcimetry measurements performed on both untreated and carbonated samples, subtracting from the $CaCO_3$ content of the treated samples ($CaCO_{3FIN}$) the amount of $CaCO_3$ measured in the residues prior to carbonation ($CaCO_{3IN}$) and accounting for the weight increase upon carbonation, as shown in Eq. (3.1)

$$CO_{2\,UPTAKE}(\%) = \frac{\left(CaCO_{3\,FIN} - CaCO_{3\,IN}\right)\cdot\frac{M_{CO2}}{M_{CaCO3}}}{100-\left(CaCO_{3\,FIN}\cdot\frac{M_{CO2}}{M_{CaCO3}}\right)}\cdot 100 \tag{3.1}$$

$$R_X(\%) = \frac{CO_{2uptake}(\%)\cdot\frac{M_{Ca}}{M_{CO2}}}{Ca_{REACTIVE}}\cdot 100 \tag{3.2}$$

The performance achieved in each test were also estimated in terms of the extent of carbonation R_X, applying Eq. (3.2) in which $Ca_{REACTIVE}$ is the difference between the total calcium content of the residues and the initial calcium content as $CaCO_3$ of the material; M_{Ca} and M_{CO2} are the molar mass of calcium and carbon dioxide respectively.

3.3 Results

Figure 3.1 reports the CO_2 uptake kinetics (Figure 3.1 (a)) and extent of carbonation, R_X, (Figure 3.1 (b)) obtained for each type of residues at 50 °C under a CO_2/N_2 gas atmosphere applying a CO_2 partial pressure of 2.8 bar (i.e. total pressure of 7 bar). The highest CO_2 uptakes were achieved by the AOD slag with values ranging from 20% (i.e. 200 g CO_2/kg residue) after 1 hour of reaction to 27.1% after 24 hours. The APC residues, as expected, proved to be highly reactive, allowing to obtain a CO_2 uptake of 17.2% already after 15 minutes of reaction. However, Figure 3.1 (a) shows that for reaction times longer than 2 hours the CO_2 uptake achievable by the APC residues remained almost constant around a value of 20 %. Finally, it may be observed that the CO_2 uptakes achieved by the BOF slags were significantly lower compared to the ones resulting for the other two residues, with a maximum value of 13.3% reached after 24 hours.

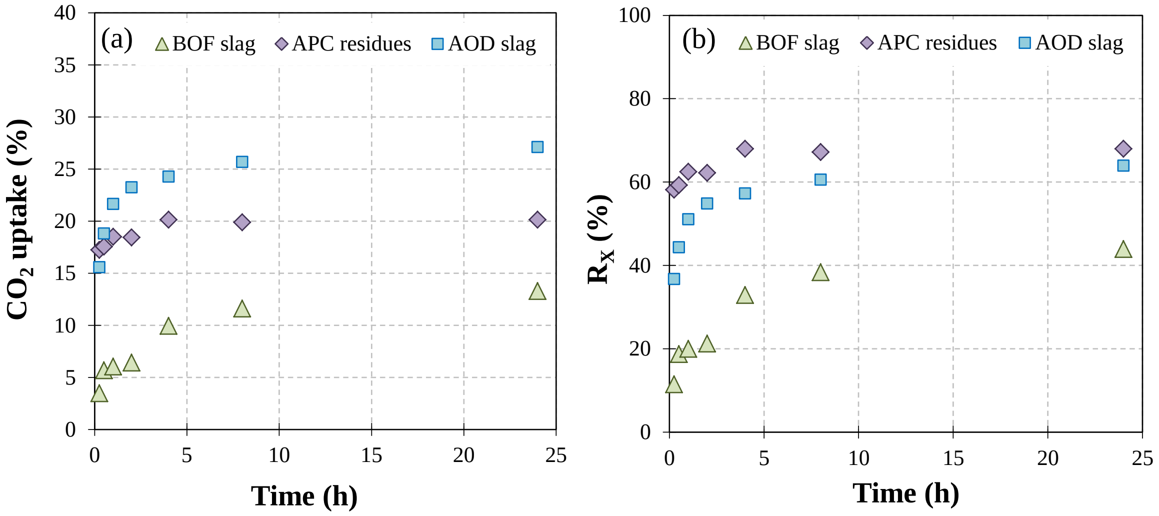

Figure 3.1: Kinetics of (a) CO_2 uptake and (b) extent of carbonation observed for each residues at 50 °C (p_{CO2}=2.8 bar, p_{TOT}=7 bar, L/S of 0.2 l/kg for APC residues, 0.4 l/kg for AOD slag and 0.3 l/kg for BOF slag).

Considering the extent of carbonation (R_X) achieved by each type of residue (see Figure 3.1(b)), one can observe that the APC residues and the AOD slags allowed to reach the highest R_X values (i.e. 68 and 63% respectively) while a lower extent of carbonation was obtained for the BOF slags, i.e. 44%. These results could be explained considering the chemical composition of the materials and namely the specific mineralogical composition of the residues (see Table 3.1). The APC residues in fact are mainly made up by calcium hydroxide and calcium hydroxychloride (CaOHCl) that can rapidly react with CO_2 also at mild operating conditions. For this reason, hence, the extent of carbonation resulting for this material proved above 60% also for short reaction times. The other two types of residues are instead characterized by a prevalence of calcium silicate phases which are generally reported to present a slower reactivity with CO_2 and require higher temperature or carbon dioxide partial pressure to achieve better carbonation performances. However, the CO_2 uptakes and extent of reaction resulting for the two types of tested steelmaking slags differed considerably; these differences in reactivity may be mainly related to the mineralogy of the two types of residues. As reported in Table 3.1, the AOD slags were made up primarily by Ca_2SiO_4, while the main mineralogical phases detected in the BOF slags were Ca_3SiO_5, $Ca_2Fe_2O_5$, $Ca(OH)_2$ and Ca_2SiO_4. For the AOD slags, that were characterized by a high calcium content (i.e. around 40%), as already mentioned, high CO_2 uptake values were achieved, however the Rx values resulting for reaction times shorter than 5 hours were significantly lower compared to the ones obtained for the APC residues; this behaviour may be associated to the slower reaction kinetics of dicalcium silicate compared to calcium hydroxide at the tested conditions. For longer reaction times the Rx values obtained by the two types of residues were instead quite similar. The BOF slags, presented a lower calcium content (around 28%wt.) and were characterized by reactive phases presenting a lower reaction kinetics, such as Ca-Fe oxides, thus entailing both lower CO_2 uptakes and extents of carbonation, probably requiring more energy intensive operating conditions for obtaining better performances.

Figure 3.2 reports the influence of the carbon dioxide partial pressure (Figure 3.2 (a)) and of the temperature (Figure 3.2 (b)) on the extent of carbonation observed in 1 hour tests performed using a gas mixture with 40% CO_2.

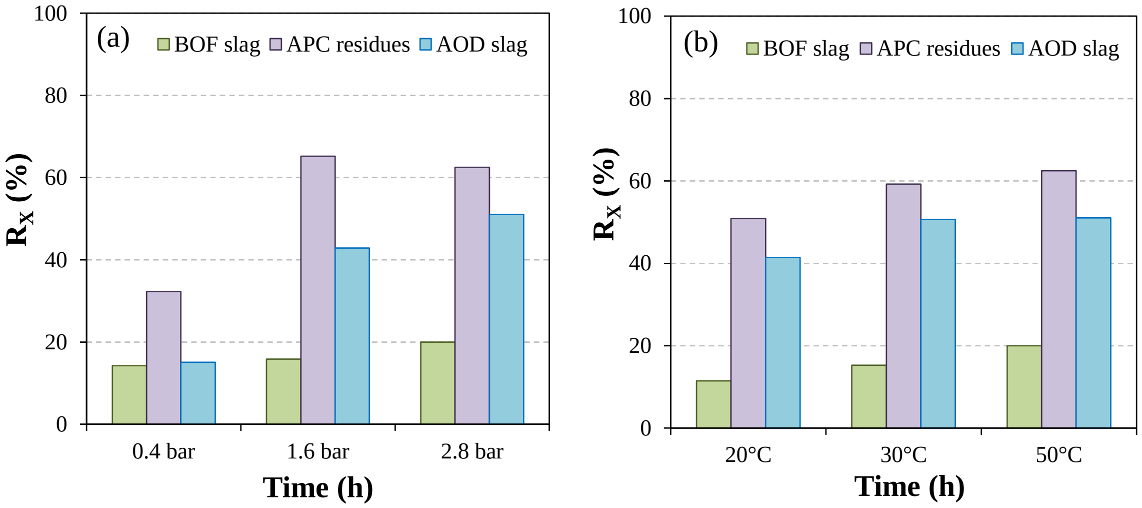

Figure 3.2: Influence of (a) p_{CO2} at 50 °C and (b) temperature with p_{CO2}=2.8 bar (7 bar of gas mixture) on the carbonation extent (R_X) observed for each residues (t=1 h, L/S of 0.2 l/kg for APC residues, 0.4 l/kg for AOD slag and 0.3 l/kg for BOF slag).

As can be seen from these results, for all the tested CO_2 partial pressures, the BOF slags demonstrated a low extent of carbonation that, although slightly influenced by an increase in the applied p_{CO2}, anyhow remained lower or equal to 20% (see Figure 3.2 (a)). For the other two types of residues, instead, a significant increase in the extent of carbonation (i.e. from 32.3 to 65.2% for the APC residues and from 15 to 43% for the AOD slags) was observed passing from 0.4 to 1.6 bar, while a further increase in the applied CO_2 partial pressure to 2.8 bar resulted in a slight increase in the extent of carbonation for the AOD slag (i.e. 51 instead of 43%), whereas no remarkable effect was observed for the APC residues. Regarding the effect of the operating temperature on the performance obtained by each type of residue, looking at Figure 3.2 (b), one can observe that the reactivity of the BOF slags, differently from the APC residues and the AOD slags, proved to be significantly influenced by an increase in the applied temperature. For this material, in fact, although only a limited extent of carbonation was observed, an increase from 11.5 to 20% was obtained increasing temperature from 20 to 50 °C. The extent of carbonation of the APC residues and of the AOD slags, instead, showed only a slight increase with temperature, i.e. from 51 to 62.5% and from 41.4 to 51% respectively.

Finally, the effect of the gas composition on the performance of the carbonation process at the same CO_2 partial pressure was assessed by comparing the results obtained for different experimental durations at 50 °C with the gas mixture (p_{CO2}=2.8 bar) and with pure CO_2 (p_{CO2}=3 bar). The results of this evaluation are reported in Figure 3.3 for (a) BOF slags, (b) APC residues and (c) AOD slags. As can be seen, for the APC residues and the AOD slags no significant differences were observed in the CO_2 uptake kinetics resulting for experiments carried out with the 40% CO_2 gas mixture compared to those obtained under a 100% CO_2 atmosphere, even considering the slight difference in the applied CO_2 partial pressure (see Figure 3.3(b) and (c) respectively). In particular, the APC residues and the AOD slags showed a carbonation extent of 68 and 64% respectively under the N_2/CO_2 atmosphere, while Rx values of 71% and 68% were reached using pure carbon dioxide. For the BOF slags, instead, a difference in the CO_2 uptake of the residues was observed depending on the composition of the gas phase. In particular, at the same reaction time the CO_2 uptake obtained when the N_2/CO_2 gas mixture was used was consistently lower than the one resulting for 100% CO_2; for example, after 24 hours the maximum value of 13% (corresponding to a Rx of 44%) was obtained in the experiments carried with 40% CO_2, while the use of pure carbon dioxide led to a maximum uptake of 16% (corresponding to a Rx of around 53%).

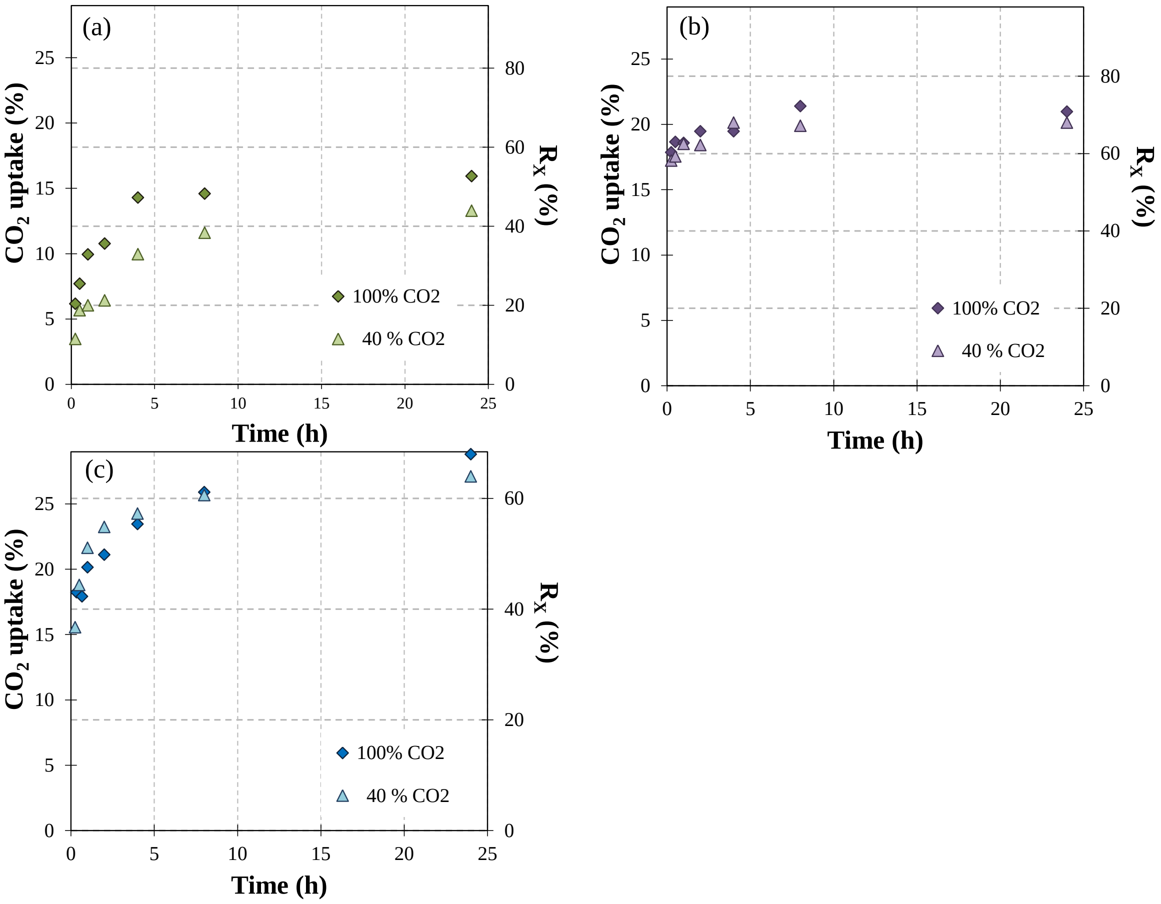

Figure 3.3: Comparison of CO_2 uptake and extent of carbonation obtained at 50°C using 7 bar of the gas mixture (p_{CO2}=2.8 bar) or 3 bar of pure CO_2 with (a) BOF slag at L/S= 0.3 l/kg, (b) APC residues at L/S= 0.3 l/kg and (c) AOD slag L/S= 0.4 l/kg T=50 °C,p_{CO2}=3 bar).

It is worth pointing out that in a previous study (Costa, 2009) the extent of carbonation of APC residues at a p_{CO2} of around 1 bar proved also to be influenced by the composition of the gas phase, exhibiting a significantly slower reaction kinetics when a 10% CO_2, 20% O_2 and 70% N_2 mixture was employed. This result was ascribed to CO_2 diffusion limitations that were related to the specific experimental setup (static batch reactor with down-flow gas supply) adopted for the tests in which a physical inhibition of CO_2 diffusion due to the N_2 and O_2 content of the gas feed may have occurred. The results of this study indicate that the hindering effect on CO_2 uptake kinetics exerted by the composition of the gas phase is not related only to the experimental set up but may depend also on the specific morphology and mineralogy of the treated residues. Hence, it appears that for the tested reaction mode the carbonation reaction kinetics of materials such as APC residues and AOD slag, characterized by a fine particle size and significant content of phases reactive at mild operating conditions, may not be affected by variations in gas composition for CO_2

contents ≥40%. For residues such as the BOF slag, that showed a slower reaction kinetics at the tested operating conditions, the use of CO_2 diluted gas mixtures may further hinder the extent of carbonation.

3.4 Conclusions

The aim of the study presented in this chapter was to evaluate the feasibility of performing carbonation of industrial residues directly employing a gas mixture characterized by a composition similar to that of the syngas produced by many industrial processes, such as coal or waste gasification and steam reforming, so to avoid the need of the energy intensive CO_2 capture step. In this context a preliminary experimental study was performed carrying out a set of lab-scale wet route carbonation tests using a gas mixture made up by 40% carbon dioxide and 60% nitrogen in order to simulate the typical composition of syngas. These experiments were performed using three types of industrial residues already characterized and employed in previous carbonation tests carried out using pure CO_2. Specifically, the APC residues collected from a hospital waste incinerator and two types of steelmaking slags, i.e. AOD and BOF slags, were tested. Among the materials used in the experiments performed with the N_2/CO_2 gas mixture, the APC residues showed the highest extent of carbonation, with a maximum R_X value of 68% after 24 hours, followed by the AOD and BOF slag that after 24 hours presented a carbonation extent of 64% and 44% respectively. Furthermore, for these materials some 1 hour tests were also performed in order to investigate the effects of two key factors that may influence the extent of carbonation, i.e. temperature and CO_2 partial pressure. The performed tests showed that the reactivity of the APC residues and the AOD slags was only slightly influenced by a variation of these parameters since these materials proved to be quite reactive already at mild operating conditions ($T=20$ °C and $pCO_2=1.6$ bar). The CO_2 uptake resulting for the BOF slags, instead, showed to be significantly influenced by a variation of the applied temperature and CO_2 partial pressure. However, even at the most enhanced conditions ($T=50$ °C and $pCO_2=2.8$ bar) and longest reaction time (24 hours) tested the maximum CO_2 uptake and Rx values obtained for this material were considerably lower than those resulting for the other two types of residues. The differences in the reaction yields achieved adopting the three types of materials were mostly related to the differences in the main mineralogical composition of the residues.

In order to evaluate if the gas composition could exert an effect on the observed extent of carbonation, the results obtained for different experimental durations at 50 °C with the gas mixture (p_{CO2}=2.8 bar) where compared with those achieved using pure CO_2 at basically the same CO_2 partial pressure (p_{CO2}=3 bar). This comparison showed that for the APC residues and the AOD slag the CO_2 uptakes measured at different reaction times did not seem to be influenced by the use of the gas mixture instead of 100% CO_2, while for the BOF slags lower Rx values were measured when the N_2/CO_2 gas mixture was used. These results demonstrate that for the specific experimental setup applied in this study the use of direct carbonation of a gas phase with a CO_2 concentration similar to that of syngas, is feasible although the achievable performance is significantly affected by the chemical and physical characteristics of the type of alkaline residues employed.

4 CARBONATION OF INDUSTRIAL RESIDUES FOR BIOGAS UPGRADING

Adapted from:

Baciocchi R., Carnevale E., Costa G., Gavasci R., Lombardi L., Olivieri T., Zanchi L., Zingaretti D., 2013c. Performance of a biogas upgrading process based on alkali absorption with regeneration using APC residues (submitted to Waste Management)

Baciocchi R., Carnevale E., Costa G., Lombardi L., Olivieri T., Paradisi A., Zanchi L., Zingaretti D., 2013b. Pilot-scale investigation of an innovative process for biogas upgrading with CO_2 capture and storage. Energy Procedia (in press);

Baciocchi R., Carnevale E., Corti A., Costa G., Lombardi L., Olivieri T., Zanchi L., Zingaretti D., 2013a. Innovative process for biogas upgrading with CO_2 storage: results from pilot plant operation. Biomass & Bioenergy 53, 128-137;

Baciocchi R., Costa G., Gavasci R., Lombardi L., Zingaretti D., 2012a. Regeneration of a spent alkaline solution from a biogas upgrading unit by carbonation of APC residues. Chemical Engineering Journal 179, 63-71;

Baciocchi R. Costa G. Faraoni G. Lombardi L. Olivieri T. Zingaretti D. 2011c Pilot-scale carbonation of APC residues for CO2 storage and alkali regeneration downstream an absorption column for biogas upgrading. Proceedings of Sardinia 2011 Thirteenth International Waste Management and Landfill Symposium 3 - 7 October 2011 S. Margherita di Pula (Cagliari). Sardinia. Italy.
ISBN 978-88-6265-000-7;

Baciocchi R., Corti A., Costa G., Lombardi L., Zingaretti D., 2011a. Storage of carbon dioxide captured in a pilot-scale biogas upgrading plant by accelerated carbonation of industrial residues. Energy Procedia 4, 4985-4992;

Lombardi L., Corti A., Carnevale E., Baciocchi R., Zingaretti D., 2011. Carbon dioxide removal and capture for landfill gas up-grading. Energy Procedia 4, 465-472.

4.1 Introduction

As reported in the previous chapter, several studies and applications proved the possibility of using different types of industrial residues to store CO_2 point source emissions by means of a direct carbonation process in which these materials react with pure CO_2 or a gaseous mixture containing CO_2. In this chapter instead the possibility of applying carbonation of residues within a specific upgrading process carried out to remove CO_2 from landfill biogas is analysed. The EU's commitment to achieving a low-carbon economy, pursued through the adoption of increasingly ambitious targets for the reduction of greenhouse gas (GHG) emissions and for the increase in the use of renewable energy sources (e.g. Directive 2009/29/EC, Directive 2009/28/EC and Directive 2003/87/EC), has recently sparked a great interest in technologies that allow to obtain energy and vehicle fuels from renewable sources such as energy crops, algae and different types of waste and wastewater treatment residues. Among renewable energy sources, biogas generated from anaerobic digestion of biowaste, wastewater treatment sludge, manure or energy crops as well as municipal solid waste landfills, mainly made up by CH_4 (40-75% vol.) and CO_2 (15-60% vol.) plays an important role (Persson et al., 2006). Besides the substitution of fossil fuels, which yields a reduction in anthropogenic GHG emissions, exploitation of biogas generated from waste materials, presents other environmental advantages, such as the reduction of landfill CH_4 emissions to the atmosphere. The most adopted utilization strategies for biogas are heat, steam and/or electricity production, which do not require specific pre-treatment of the gas apart from the removal of water vapour, dust and contaminants such as hydrogen sulphide that may induce corrosion and mechanical wear of the equipment and machinery. However, the application of upgrading treatments mainly aimed at reducing the CO_2 concentration of biogas, such as e.g. water or amine scrubbing, membrane separation and pressure swing adsorption, may allow to obtain a product with an increased methane content, thus termed biomethane, which can be used as vehicle fuel or fed into the natural gas distribution grid (Ryckebosch et al., 2011). CO_2 removal, in fact is one of the first measures required to increase the energy content of the gas; the lower heating value of biogas, typically ranging between 15 and 25 MJ/Nm^3 for biogas with a 50-

60% vol. CH_4 content, can be raised to values typical of natural gas (35 MJ/Nm^3) when a methane content of more than 96-97% is achieved (Ryckebosch et al., 2011).

Within the framework of the European Life+ project “UPgrading of landfillGAS for LOWering CO_2 emissions” (UPGAS-LOWCO2, LIFE08 ENV/IT/000429) two innovative biogas upgrading processes aimed at achieving multiple environmental benefits were developed and tested at pilot scale (Lombardi et al., 2011). The distinctive feature of the proposed processes is that they are aimed not only at reducing the CO_2 content of the biogas but also at permanently storing the separated CO_2 in a solid form using alkaline industrial residues. Specifically, the method presented in this chapter, Alkali absorption with Regeneration (AwR), is based on chemical absorption of CO_2 with alkaline (KOH or NaOH) solutions followed by regeneration of the spent solutions (mainly containing K_2CO_3 or Na_2CO_3) by contacting them with industrial residues characterized by a significant content of calcium hydroxide. Alkali absorption was proven to be a feasible method to obtain biomethane from biogas; however, its applicability is hindered by its high requirement of alkali reagents, the production of which is characterized by high costs and environmental impacts (Tippayawong and Thanompongchart, 2010). Specifically in a former LIFE+ project (GHERL-GreenHouse Effect Reduction from Landfills, LIFE05 ENV/IT/000874) the feasibility of a process based on chemical absorption (see Eq.(4.1)) with an aqueous solution of potassium hydroxide (KOH) for upgrading landfill gas and capturing CO_2 was demonstrated with the construction and operation of a pilot-scale plant in a landfill site in Italy (Lombardi et al., 2008).

$$2KOH_{(aq)} + CO_{2(g)} \rightarrow K_2CO_{3(aq)} + H_2O \qquad \textbf{(4.1)}$$

However in this process no further CO_2 storage processes or reuse options for the K_2CO_3 solution were investigated. For this reason, in the above mentioned project a regeneration process based on the caustic recovery treatment employed in several industrial applications (e.g. lima-soda water softening process), but making use of a waste material as calcium hydroxide source, was developed in order to reduce the consumption of alkali reagents and improve the economical and environmental performance of this biogas upgrading technique. In this process the carbonate/bicarbonate ions contained in the solution react with calcium hydroxide, leading to the precipitation of calcium carbonate (carbonation reaction shown in Eq. (4.2)) and the regeneration of the alkali reagents dissolved in the solution (Baciocchi et al., 2012a). As a result of the carbonation reaction, the CO_2 separated in the absorption stage may be therefore stored in a solid and permanent form.

$$Ca(OH)_2 + K_2CO_{3(aq)} \rightarrow CaCO_{3(\downarrow)} + 2KOH_{(aq)} \qquad \textbf{(4.2)}$$

Furthermore, besides as a CO_2 sequestration technique, carbonation has been applied to alkaline industrial residues such as waste incineration bottom and fly ash as a treatment to improve their environmental behaviour (Costa et al., 2007). This reaction has shown in fact to affect in particular the mineralogy and pH of these materials, resulting in a modification of their leaching behaviour in terms of the release of metals and oxyanion forming elements (see e.g.: Fernández-Bertos et al., 2004; Van Gerven et al., 2005; Zhang et al., 2008; Baciocchi et al., 2009). Hence, the additional environmental benefits targeted by this upgrading technique are the reduction of carbon dioxide landfill gas or biogas emissions, which are of biogenic origin and thus may be taken into account in the overall greenhouse balance as negative emissions, as well as the improvement of the leaching behaviour of the alkaline residues employed in the regeneration stage.

In the first phase of the project, preliminary laboratory scale experiments allowed to select the type of residues to employ for the regeneration process as well as to define the unit processes and operating conditions required by the AwR process in order to achieve the targeted objectives (see section 4.2). Specifically, Air Pollution Control (APC) residues resulting from the treatment of waste incineration flue gas with calcium hydroxide were selected since, due to their chemical, physical and mineralogical composition, they exhibited the highest regeneration capacity among the tested waste materials. Based on the preliminary experiments, a new series of lab-scale tests were performed using freshly sampled APC residues in order to verify the operating conditions selected and to define the conditions to adopt in the pilot-scale plant using spent absorption solutions produced in the already existing absorption column (see section 4.3). On the basis of these results, the sizing, design and construction of a pilot-scale regeneration/carbonation unit was performed. In the second phase of the project, AwR tests were carried out in pilot-scale absorption and regeneration units installed in an operating landfill site in order to verify the technical feasibility of the proposed process and to identify the composition of the load solution to use in the absorption treatment that may allow to achieve all of the objectives targeted by the process, i.e. biomethane production, permanent storage of the separated

CO_2 and improvement of the leaching behaviour of the solid product compared to the untreated residues (see section 4.4).

4.2 Lab scale activities

In the first phase of the project $Ca(OH)_2$ was used as reference material for carrying out preliminary carbonation experiments with the aim of evaluating the effect of the main operating parameters on KOH regeneration and calcite precipitation (see section 4.2.3). At a later stage, the performance achievable using different types of industrial residues were analysed and compared and among the available different types of alkaline residues, such as waste incineration bottom ash, stainless steel slag and APC residues, the latter material was selected due to its chemical, physical and mineralogical composition that allowed to achieve a higher KOH regeneration capacity (see section 4.2.4). Several tests were then carried out in order to identify the conditions that allow to maximize the extent of K_2CO_3 conversion to KOH and the CO_2 uptake of the solid residues, analysing also the effects on the leaching behaviour of the residues (see section 4.2.5). Based on these preliminary tests the process layout and the operating conditions to apply in each unit of the proposed process were defined (see section 4.2.6).

4.2.1 Materials

Three types of industrial residues were tested in the carbonation/regeneration experiments:

- air pollution control (APC) residues sampled from the baghouse section of a hospital waste incinerator located near Rome (Italy) at the outlet of the flue gas dry treatment section where pulverized hydrated lime and activated carbon are added to remove acid gases and organic micropollutants;
- stainless steel slag sampled at the outlet of the argon oxygen decarburization (AOD) unit of an electric arc furnace plant;
- the finest size fraction (d < 0.425 mm) of the waste incineration bottom ash (BA) disposed of at the landfill where the absorption pilot plant is situated (Casa Rota landfill, Arezzo, Italy).

Detailed chemical, physical and mineralogical characterization data and an analysis of the leaching behaviour of the residues tested in the carbonation experiments, as well as a description of the employed analytical methods, are reported elsewhere (APC residues

(Baciocchi et al., 2009) AOD slag (Baciocchi et al., 2010b), Casa Rota BA (Baciocchi et al., 2010c)).

In Table 4.1, the main composition of the three tested residues is summarized. As can be noted, the amount of calcium available for the carbonation reaction, obtained as the difference between the total Ca and the $CaCO_3$ contents of the residues, were quite similar for the first two types of residues, whereas the bottom ash presented a significantly lower available Ca content.

Table 4.1: Estimated available calcium content (% wt.) and main mineralogy of the residues examined in this study.

Residue	Ca reactive (% wt.)	Main phases
APC residues	33.4	$Ca(OH)_2$; CaOHCl, NaCl, KCl, $CaCO_3$
AOD slags	38.3	Ca_2SiO_4; CaF_2; MgO; Fe_3O_4
Casa Rota Bottom Ash (fraction d<0.425 mm)	21.9	$Ca(OH)_2$; $Ca_2Al_2SiO_7$; $CaCO_3$; SiO_2

It is worth pointing out that the materials considered in this chapter are collected from different batches with respect to those considered in Chapter 3. As can be seen in Table 4.1, the APC residues are mainly made up by calcium hydroxide, calcium hydroxychloride, sylvite and halite. The main mineralogical phases detected in the AOD slag and in the bottom ash differed completely from those retrieved in the APC residues. Namely the AOD slag was prevalently made up by dicalcium silicate while the bottom ash sample presented an intermediate composition to that of the other two materials, containing both Ca hydroxide phases (i.e. portlandite, hydrocalumite and ettringite), and Ca silicate phases (dicalcium silicate, gehlenite, etc.).

4.2.2 Regeneration experiments Procedure

Lab scale batch regeneration experiments of a 2 eq/l K_2CO_3 solution were carried out in a 300 ml beaker placed in a thermostatic water bath for temperature control. This concentration was selected on the basis of the typical values expected in the spent solution generated from an alkali absorption process (Baciocchi et al., 2006). On the basis of the composition of the residues (or of $Ca(OH)_2$), the amount of calcium phases available for the regeneration reaction (Ca_R) was estimated as the difference between the total Ca and the Ca as $CaCO_3$ content of each material (see Table 4.1). Namely regeneration experiments were carried out dosing different amounts of residues or $Ca(OH)_2$ in order to set the equivalent ratio of Ca_R to K_2CO_3, indicated as R, at specific values in the range 0.7-1.9 eq Ca_R/eq K_2CO_3.

At the beginning of the experiment a 100 ml distilled water slurry of the residues (or of $Ca(OH)_2$) was poured into the reactor. During the entire duration of the experiment the suspended solution was stirred with a paddle-type impeller at a constant rate of 250 rpm and the pH and the temperature of the solution were continuously measured with a Hanna Instruments benchtop pH/T meter and recorded with a data logger. After 5 minutes, in order to obtain a 2 eq/l initial concentration of potassium carbonate, 100 ml of a 4 eq/l aqueous solution of K_2CO_3 was added to the slurry of alkaline residues and from this moment on the reaction time was taken. Different experiment durations (from 15 to 240 minutes) and reaction temperatures (from 25 to 55°C) were tested in order to study reaction kinetics. At the end of each experiment, the solution was quickly filtered under reduced pressure. A 100 ml filtered sample was then titrated with a 10 eq/l HNO_3 solution in order to quantify the different species in solution based on its buffering capacity at specific pH ranges, i.e. hydroxides ($12 \leq pH \leq 14$), carbonates ($8 \leq pH \leq 11$) and bicarbonates ($5 \leq pH \leq 7$). The separated solid sample was dried over night at 105 °C and then its main properties, i.e. calcite content, mineralogy, microstructure and leaching behaviour, were analysed. Specifically, the calcite content of the ash was measured with a Dietrich–Frühling calcimeter that allows to determine the volume of evolved gas from HCl-digested solid samples. To assess the release of metals, metalloids and soluble salts at the natural pH of the solid samples, the leaching compliance test (EN 12457-2) was carried out. The concentrations of metals and metalloids were analysed by Atomic Absorption Spectroscopy (AAS Perkin Elmer 3030B), whereas the leachate content of chloride and sulphates were measured by titration with $AgNO_3$ and spectrophotometric analysis, respectively. The obtained concentrations were compared with the current EU landfill acceptance criteria (Council Decision 2003/33/EC).

4.2.3 Results: Regeneration experiments with $Ca(OH)_2$

Figure 4.1 shows the titration curves of the filtered solutions resulting from experiments carried out with $Ca(OH)_2$ at 25 °C for different experiment durations and for two specific R values among the tested ones: 1 (see Figure 4.1(a)) and 1.2 eq Ca_R/eq K_2CO_3 (see Figure 4.1(b)).

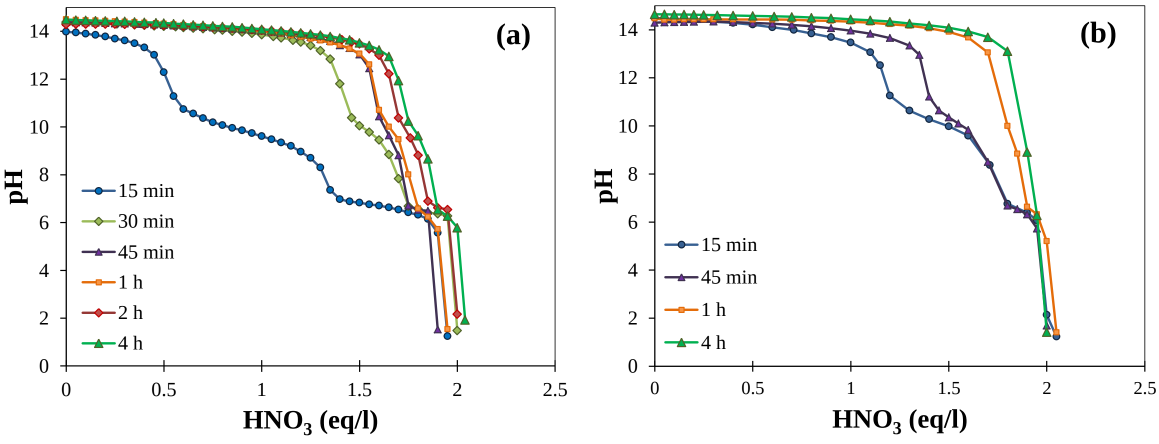

Figure 4.1: Titration curves of the regenerated solution obtained with $Ca(OH)_2$ at 25 °C at different reaction times and R values: (a) 1; (b) 1.2 eq Ca_R/eq K_2CO_3.

For both of the tested R values, a significant KOH regeneration was achieved after 1 hour of reaction; however, only for the highest R value tested, complete conversion of the carbonate/bicarbonate phases to KOH could be observed for reaction times above 1 hour, (see Figure 4.1(b)). Furthermore, the R value of 1.2 eq Ca_R/eq K_2CO_3 exhibited an enhancing effect on reaction kinetics, doubling the amount of regenerated KOH at short reaction times (i.e. 15 minutes) compared to the one obtained for R equal to 1 eq Ca_R/eq K_2CO_3. Concerning the effects of the R value on the CO_2 uptake of the solid phase (calculated based on Eq. (3.1) and shown in Figure 4.2), as expected, the highest uptakes (520 g CO_2/kg material, corresponding to a complete conversion of the available Ca to $CaCO_3$) were measured for the lowest R value tested (0.9 eq Ca_R/eq K_2CO_3). An increase in the amount of $Ca(OH)_2$ added to the solution above the stoichiometric value (R>1 eq Ca_R/eq K_2CO_3) resulted in a decrease of the CO_2 uptake of the material.

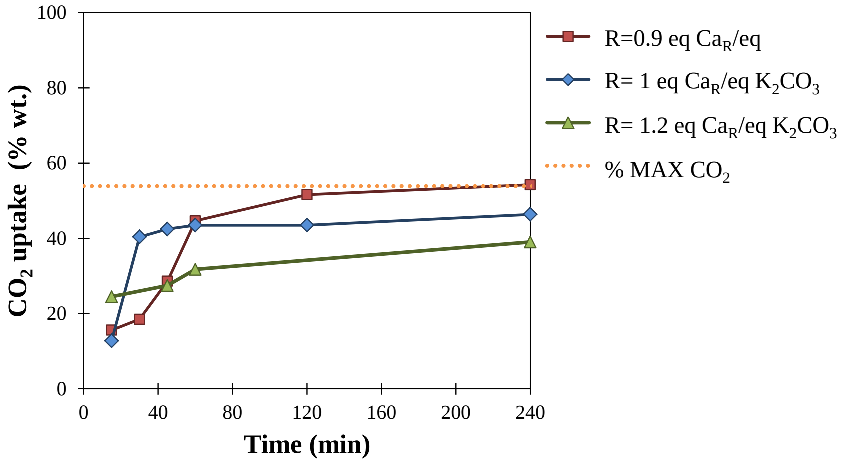

Figure 4.2: CO_2 uptake kinetics of the solid material at 25 °C as a function of the Ca to K_2CO_3 molar ratio at different reaction times.

These results evidenced that no R value can allow to maximize both the amount of KOH regenerated in the solution and the CO_2 uptake of the solid phase. For this reason it was decided to perform the next experiments with alkaline industrial residues using R values above the stoichiometric ones, so to maximize the KOH regeneration yield

4.2.4 Results: Regeneration experiments with alkaline industrial residues

In Figure 4.3(a), the titration curves of regenerated solutions obtained adding different types of industrial residues while keeping an R value equal to 1.2 eq Ca_R/eq K_2CO_3 are exhibited and compared to the results obtained for the reference material. For these experiments, the reaction time was of 2 hours and the operating temperature was set at 55 °C, which as described below, was the investigated temperature that allowed to obtain the best results both in terms of KOH regeneration and of CO_2 storage. In this test a washing pre-treatment was applied to the APC residues in order to remove most of the soluble phases, chlorides in particular, contained in the ash that can hinder the regeneration yield (as explained in details in section 4.2.5). The pre-treatment consisted in washing the APC residues for 15 minutes with distilled water at a liquid to solid (L/S) ratio of 10 l/kg. After washing, the residues were filtered under reduced pressure and dried at 105 °C before using them in the regeneration experiment.

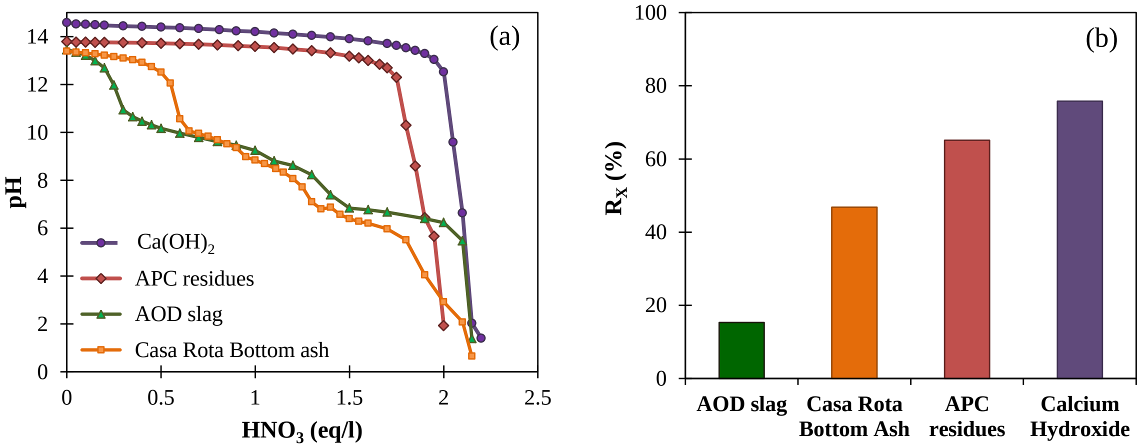

Figure 4.3: Comparison between (a) the titration curves of the regenerated solutions and (b) the extent of carbonation obtained for tests performed using $Ca(OH)_2$ and the three different types of tested industrial residues (R=1.2 eq Ca_R/eq K_2CO_3, time=2 h, T=55 °C).

As can be noted, for the washed APC residues, a significantly higher concentration of KOH was retrieved in the filtered solution than for AOD slag or the tested bottom ash. This result was due mainly to the different mineralogical composition of the three types of tested residues. The washed APC residues, in fact, were characterized by a rather high

$Ca(OH)_2$ concentration, whereas, the AOD residues and Casa Rota bottom ash were mainly made up by calcium silicates which do not provide enough alkalinity in the solution to react with potassium carbonate and hence allow to regenerate a much lower amount of KOH. Casa Rota BA actually showed a higher amount of regenerated KOH compared to AOD slag, and this was correlated to the presence of Ca hydroxide phases (portlandite and hydrocalumite) in this type of slag.

Also the extent of carbonation (R_X) of the tested material, estimated considering the CO_2 uptake of the residues measured by calcimetry analysis divided by the initial available Ca content of each material (see Eq. (3.1) and (3.2)), was significantly higher for the APC residues compared in particular to that of the AOD slag, (see Figure 4.3(b)). Hence, APC residues were selected as the type of industrial residues to be used in the pilot-scale regeneration/carbonation reactor.

4.2.5 Results: Regeneration experiments with APC residues

In order to test the performance achievable using this type of residues in the upgrading process and to choose the optimal operating condition, the residues were first characterized and, then, used for performing a series of lab-scale tests. Firstly, several tests were performed in order to confirm the value of the equivalent ratio R to apply in each test carried out with APC residues. Besides, it was decided to assess the effect of a washing pre-treatment of the residues applied before the regeneration step. Specifically, the APC residues were washed for 15 minutes with deionized water at a liquid to solid (L/S) ratio of 10 l/kg. After washing, the residues were filtered under reduced pressure and dried at 105 °C, while the washing water composition was analysed employing the same methods used to characterize the leaching solutions. In addition, the effect of the operating temperature was also investigated by carrying out experiments at 40 and 55 °C. Some experiments were then performed with the initial addition of potassium hydroxide to analyse the effect on KOH regeneration and CO_2 storage induced by the presence of unreacted potassium hydroxide in the spent absorption solution. Specifically, a 1 eq/l KOH concentration, which corresponds to a 67% conversion efficiency of KOH to K_2CO_3 in the absorption step, was tested. Finally, a second washing treatment was also tested in order to improve the leaching behaviour of the final solid product. This treatment consisted in washing the solid sample obtained from the regeneration reaction for 15 minutes with deionized water at a liquid to solid (L/S) ratio of 5 l/kg. After washing, the residues were filtered under reduced pressure and dried at 105 °C.

<u>Characterization of the APC residues</u>

To evaluate the exact amount of residues to use in each regeneration experiment, the composition of the APC residues was examined in order to assess the types and amounts of potentially reactive phases. The elemental composition of the APC residues was determined by alkaline digestion with $Li_2B_4O_7$ in platinum melting pots at 1050 °C, followed by dissolution of the molten material in a 10 % HNO_3 solution and measurement of element concentrations using an atomic absorption spectrometer (AAS Perkin Elmer 3030B) equipped with an air-acetylene flame, a graphite furnace and a hydride generation system. The major constituents of the APC residues, accounting for more than 60% of total ash mass, proved to be calcium and chloride. Significant concentrations of metals (Zn, Cu and Pb) and sulphates were also observed in agreement with the average composition values reported in the literature for these types of residues (Quina et al., 2008). In addition, the results of leaching tests indicated the high mobility of most of the above mentioned contaminants (i.e. Cl, Pb, Zn, Cu, Cr, SO_4 and Sb) in agreement with prior findings reported for this type of residues (e.g. IAWG, 1997). In particular Cl and Pb eluate concentration resulted higher than the limits for hazardous waste disposal implying the need of pre-treatment before landfilling (Baciocchi et al., 2009).

The main mineralogical phases were determined by powder XRD analysis using a Zeiss diffractometer (model LEO 1530) equipped with a Cu anode and Kα radiation; an angular step of 0.021° and 2θ range from 6 to 65° was used. The microstructure of the solid samples was analysed by Scanning Electron Microscopy SEM (Bruker AXS, model D8 Advance). In accordance with previous studies on these residues (e.g. Bodenan and Deniard, 2003, Quina et al., 2008), as shown in Figure 4.4, the main mineralogical phases detected by XRD analysis in the untreated APC residues were calcium hydroxides ($Ca(OH)_2$ and CaOHCl), calcite ($CaCO_3$) and soluble salts (NaCl, KCl and $CaSO_4$). These results were also confirmed by SEM images of the material (see Figure 4.5(a)-(b)). In particular, in Figure 4.5(a) the presence of cubic NaCl and KCl crystals and of $CaSO_4$ prismatic to needle crystals can be noted, while in Figure 4.5(b) hexagonal plates of $Ca(OH)_2$ partly covered by $CaCO_3$ and CaOHCl fine grains plus $CaSO_4$ prismatic to needle crystals are in evidence.

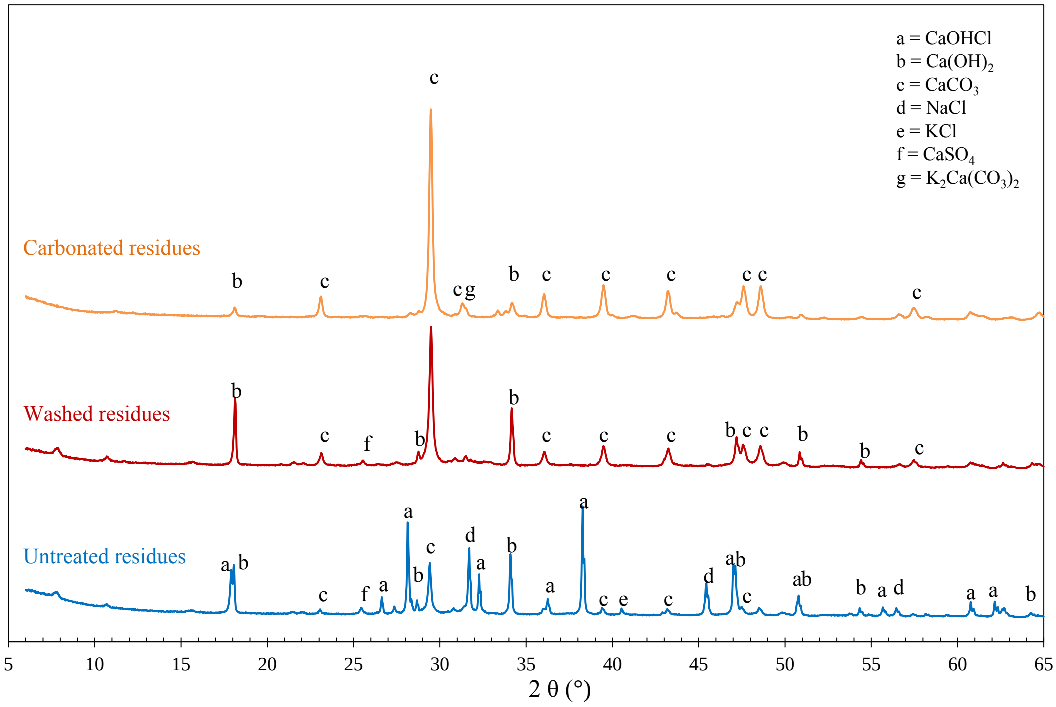

Figure 4.4: Comparison between the mineralogical composition of the untreated, washed and carbonated (R=1.2 eq Ca_R/eq K_2CO_3, time=1 h and T=55 °C) residues.

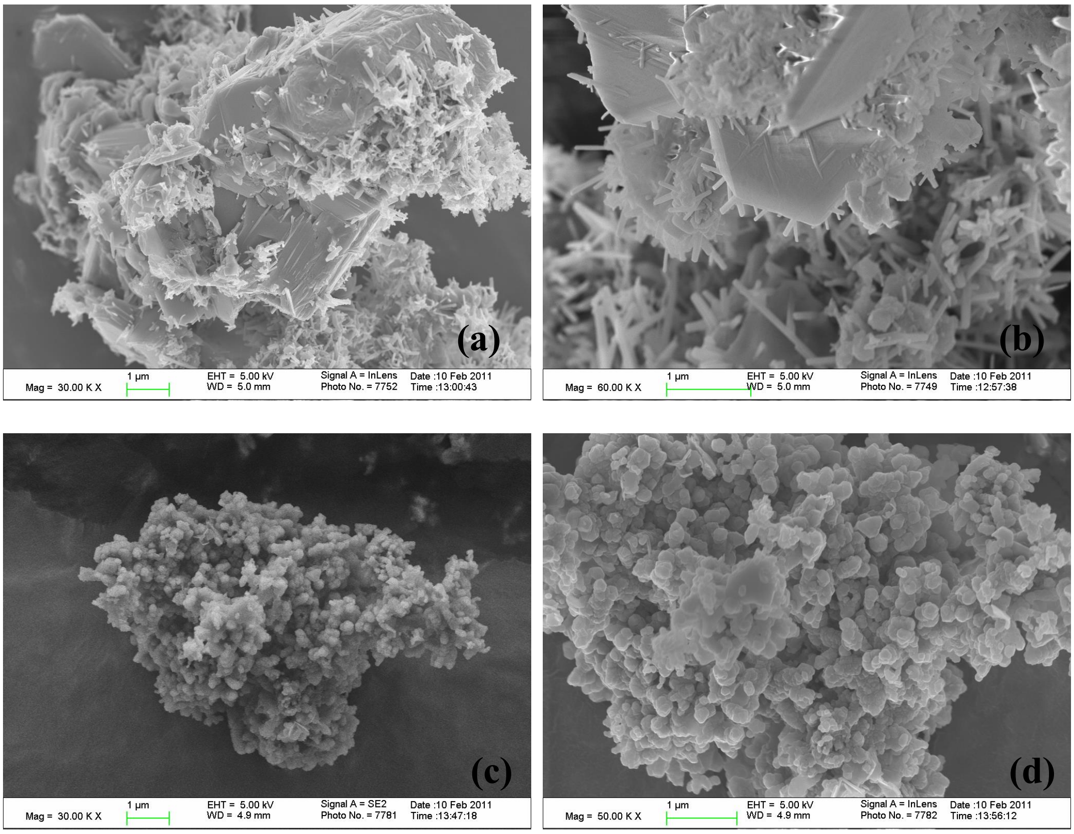

Figure 4.5: SEM images of the: (a-b) untreated and (c-d) carbonated (R=1.2 eq Ca_R/eq K_2CO_3, time=1 h and T=55 °C) residues at different magnifications.

Effect of the Ca/K_2CO_3 equivalent ratio (R)

From the characterization discussed above the reactive phases for the regeneration process were identified as $Ca(OH)_2$ and CaOHCl. Based on the total calcium and $CaCO_3$ contents of the ash, the amount of calcium available for the carbonation reaction (Ca_R) was estimated equal to 33.4% weight of the residues. On the basis of this estimation, the amounts of residues to use in these preliminary experiments were calculated. Specifically, 16.5, 23.5, 25.7, 28 and 44.3 g of APC residues were added in 200 ml of 2 eq/l K_2CO_3 solutions to achieve R values of 0.7, 1, 1.1, 1.2, 1.9 eq Ca_R/eq K_2CO_3, respectively.

Figure 4.6 exhibits the titration curves of the filtered solutions resulting from regeneration experiments carried out on as received APC residues at 25 °C for different experiment durations and for specific R values: 0.7 (see Figure 4.6(a), 1.0 (see Figure 4.6(b)) and 1.2 eq Ca_R/eq K_2CO_3 (see Figure 4.6(c)). As can be noted, all the tested R values allowed to achieve a significant KOH regeneration in the solution (from 0.9 to 1.35 eq/l) already after a reaction time of 30 minutes. As expected, an increase in the R value showed to reduce the amounts of unreacted carbonates and bicarbonates in the solution. As shown in Figure 4.6(c), for reaction times above 1 hour and an R value of 1.2 eq Ca_R /eq K_2CO_3, the buffering capacity of the solution could be correlated only to hydroxide phases.

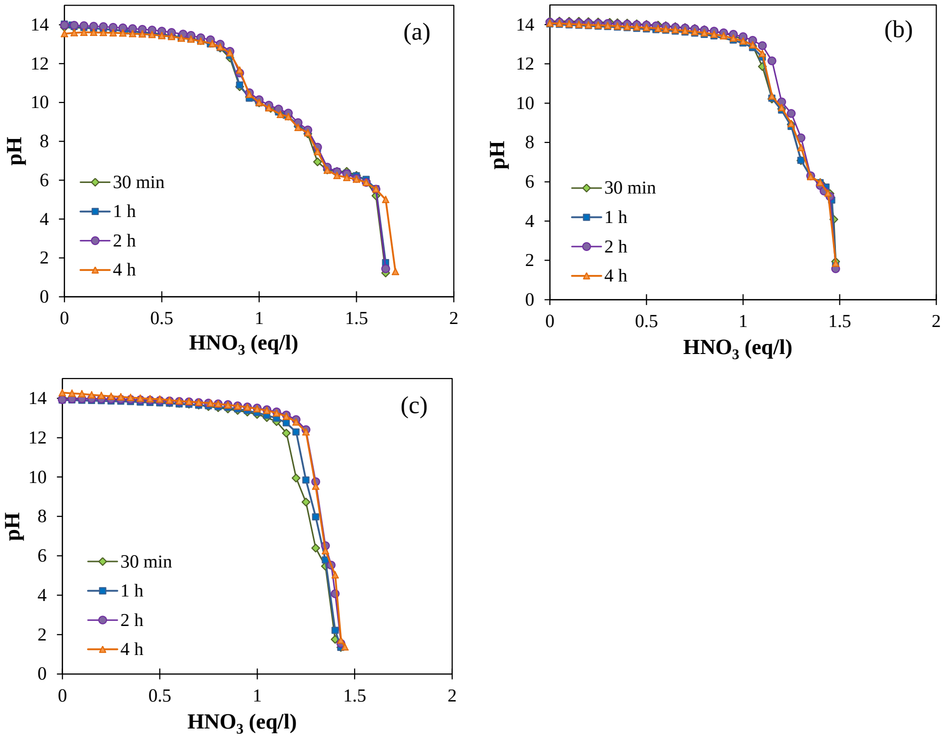

Figure 4.6: Titration curves of the K_2CO_3 solution regenerated with APC residues at 25 °C for different reaction times and R values: (a) 0.7, (b) 1.0 and (c) 1.2 eq Ca_R/eq K_2CO_3.

On the other hand, it is also important to highlight that for all the experiments carried out on as received APC residues, the total buffering capacity of the carbonated solution was considerably lower than the value of 2 eq/l resulting from the initial composition of the solution. In particular, Figure 4.6 shows that an increase in the amount of APC residues used in the experiments produced a decrease in the total buffering capacity of the solution. This behaviour was explained with the very high chloride content of the residues (around 22% by weight), mainly as calcium hydroxychloride and halite (see Figure 4.4). For every mole of CaOHCl, as shown in Eq. (4.3), only 1 mole of KOH can be produced, differently from calcium hydroxide that allows to regenerate 2 moles of potassium hydroxide (see Eq. (4.2)).

$$CaOHCl + K_2CO_{3(aq)} \rightarrow CaCO_{3(\downarrow)} + KOH_{(aq)} + KCl_{(aq)} \qquad \textbf{(4.3)}$$

Since CaOHCl is more soluble than $Ca(OH)_2$, it is probably more readily available for reacting with potassium carbonate than $Ca(OH)_2$; hence an increase in the amount of ashes added to the solution produced a reduction of the total buffering capacity of the solution due to the formation of more KCl which does not exert any pH buffering capacity.

Figure 4.7(a) reports the influence of the R value on the amount of KOH that can be regenerated in the solution. As already pointed out, an increase in the amounts of residues used in the experiments showed to improve KOH regeneration considerably, although for R values above 1.2 eq Ca_R/eq K_2CO_3, the amount of regenerated KOH decreased due to the increasing amount of chlorides that, as previously discussed, hindered KOH regeneration. Hence, under the tested conditions, the R value that was found to maximize the KOH regeneration was confirmed to be 1.2 eq Ca_R/eq K_2CO_3.

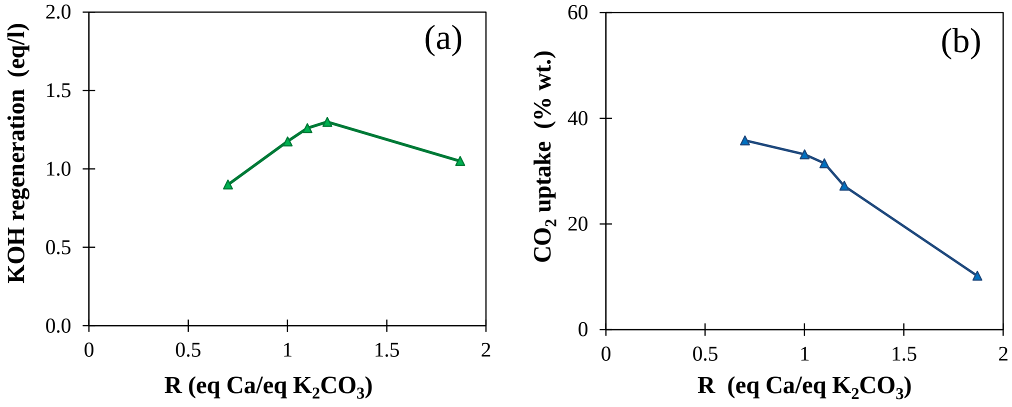

Figure 4.7: Influence of the R value on the carbonation (time=2 h and T=25 °C) of untreated residues in terms of: (a) KOH regeneration of the solution and (b) CO_2 uptake in the solid product.

Figure 4.7(b), instead, reports the CO_2 uptakes (% wt.) achieved at different R values as calculated based on the difference between the final ($CaCO_{3FIN}$) and initial ($CaCO_{3IN}$) calcite contents (% wt.) of the residues accounting for the weight increase of the sample obtained upon carbonation (see Eq. (3.1)). As expected, the highest uptakes (35% wt., corresponding to a 98% conversion of Ca_R to $CaCO_3$) were measured for the lowest tested R value (0.7 eq Ca_R/eq K_2CO_3). An increase in the amount of residues added to the solution above the stoichiometric value (R>1 eq Ca_R/eq K_2CO_3) resulted in a decrease of the CO_2 uptake of the ash, (e.g. 27.2% wt. for R=1.2 eq Ca_R/eq K_2CO_3).

These results confirmed that, as for the experiments performed with $Ca(OH)_2$, no R value can allow to maximize both the amount of KOH regenerated in the solution and the CO_2 uptake of the residues. In view of the integration of this process with the CO_2 absorption step, it was decided to operate the next experiments using an R value of 1.2 eq Ca_R/eq K_2CO_3 that allows to maximize the KOH regeneration yield minimizing the amount of KOH make up eventually required at the inlet of the absorption unit.

Washing pre-treatment

A washing pre-treatment of the APC residues was tested in order to remove most of the phases responsible of decreasing the total buffering capacity of the solution, with the aim of increasing the KOH regeneration yield.

This treatment determined a weight loss of about 25% dry wt. of the material, mainly correlated to the dissolution of chloride containing phases. From mineralogy analysis in fact the main phases detected for the washed ash were calcite and portlandite (see Figure 4.4), whereas CaOHCl, NaCl and KCl were hardly detectable. The composition of the washing solution confirmed these results exhibiting a high concentration of soluble components, chloride in particular. From these data a chloride removal efficiency of 81% was determined while the Ca_R value in the residues showed to slightly increase amounting to 35.6% upon washing.

As shown in Figure 4.8, this pre-treatment allowed to recover about 25% of the total buffering capacity of the solution; thus, in order to enhance KOH regeneration, all the other regeneration experiments were carried out on washed APC residues.

However, although the total buffering capacity of the carbonated solution increased significantly for the washed ash, the amount of regenerated KOH was roughly the same as that retrieved for the non pre-treated ash (see Figure 4.8). This result may be ascribed to the fact that for the washed residues the main reacting phase was $Ca(OH)_2$ which, as previously mentioned, presents slower reaction kinetics than CaOHCl. For this reason, in order to enhance the completion of the carbonation reaction, the effect of increasing reaction temperature was examined.

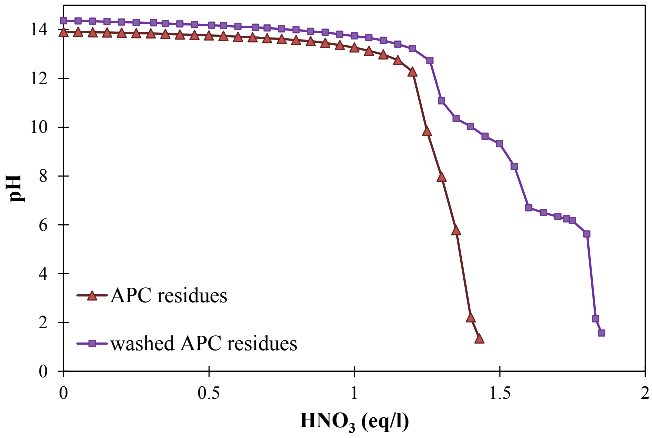

Figure 4.8: Comparison between the titration curves of the solution regenerated with untreated and washed residues (R=1.2 eq Ca_R/eq K_2CO_3, t=1 h, T=25 °C).

Temperature increase

As shown in Figure 4.9, temperature showed to exert a noteworthy enhancing effect on the amount of KOH regenerated in the carbonated solution. A temperature rise from 25 to 55 °C resulted in a KOH regeneration increase from 1.35 to 1.85 eq/l KOH, corresponding to over 90% KOH recovery for experiment durations of 1 hour.

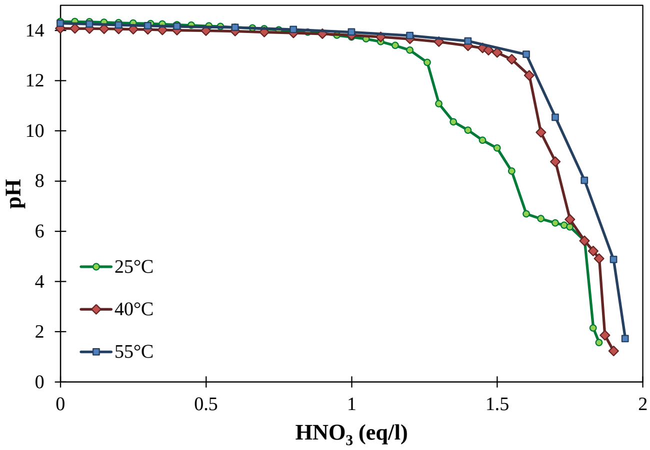

Figure 4.9: Influence of the reaction temperature on the titration curves of the regenerated solution (washed APC residues, R=1.2 eq Ca_R/eq K_2CO_3, t=1 h).

The CO_2 uptake obtained at these operating conditions (washed APC residues, R=1.2 eq Ca_R/eq K_2CO_3, T=55°C, t=1 h) was 30% wt. In this sample, as for the other carbonated residues, the main crystalline phase detected by XRD analysis was calcite (see Figure 4.4). Figure 4.5(c)-(d) reports the corresponding SEM images in which mainly calcite crystals (rounded grains) can be noted, confirming that almost complete conversion of $Ca(OH)_2$ to $CaCO_3$ was attained.

Regeneration experiments with an initial KOH concentration

The effect exerted by the presence of 1 M of KOH in the K_2CO_3 spent solution on the net extent of KOH regeneration is reported in Figure 4.10. As previously mentioned, the aim of these experiments was to assess if an incomplete conversion of KOH to K_2CO_3 during the CO_2 absorption process (i.e. 67%) could hinder the KOH regeneration. Several studies (e.g. Konno et al., 2002) have in fact shown that the presence of an alkaline hydroxide phase such as KOH reduces the solubility of $Ca(OH)_2$ and hence the precipitation of calcite.

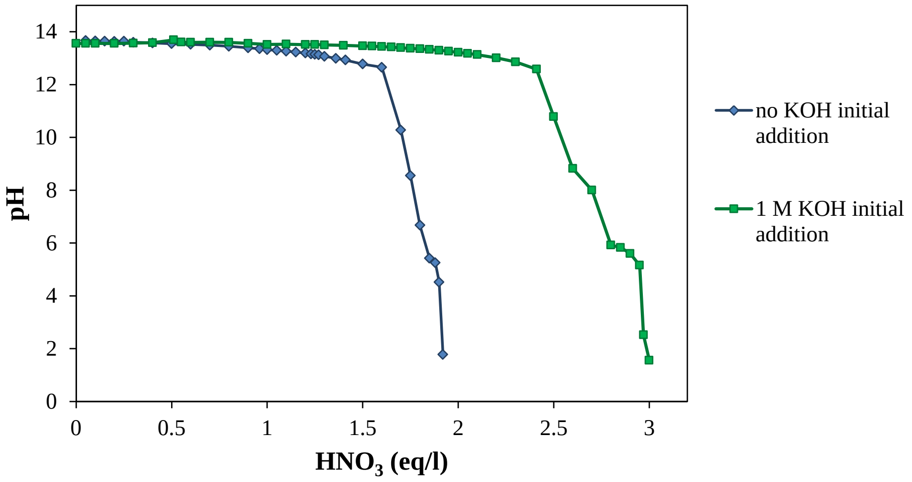

Figure 4.10: Comparison between the titration curves of the regenerated solution (washed APC residues, R=1.2 eq Ca_R/eq K_2CO_3, t=1 h, T=55 °C) with and without an initial addition of KOH.

Analysing Figure 4.10, it may be noted that the net amount of KOH regenerated in the carbonated solution with an initial addition of potassium hydroxide was lower than that obtained with K_2CO_3 only (1.45 compared to 1.85 eq/l KOH). This effect can be observed also for longer experiment duration, as reported in Figure 4.11(a). The hindering effect caused by the initial presence of KOH was even more evident on the CO_2 uptake of the residues (see Figure 4.11(b)) that resulted about 25% lower than the values measured without initial KOH addition (22.3% compared to 30%).

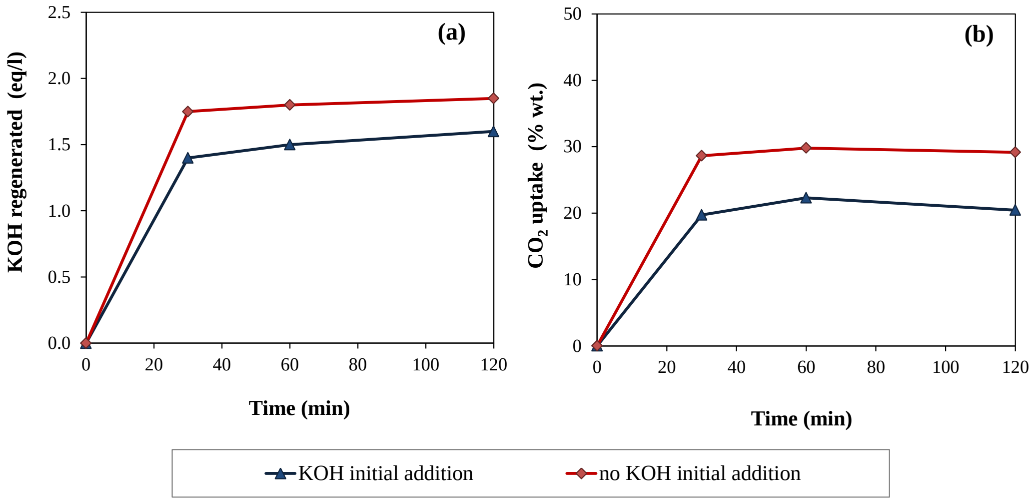

Figure 4.11: Results of regeneration experiments (washed APC residues, R=1.2 mol Ca/mol K_2CO_3, T=55 °C) with and without initial addition of KOH: (a) KOH regeneration efficiency; (b) CO_2 uptake of APC residues (% wt.).

Leaching behaviour of the treated residues

To assess the effects of the tested treatments (washing and regeneration) on the environmental properties of the corresponding solid products, the concentrations of specific components in the leachates obtained applying the EN 12457-2 test were analysed. It was decided to evaluate the leaching behaviour of the solid product resulting from the regeneration experiments carried out under optimized conditions (R=1.2 eq Ca_R/eq K_2CO_3, t=1 h, T=55 °C) and with an initial concentration of KOH. This latter condition was selected since it was considered a worst case scenario given that at higher pH of the leachate, an increased release of most components would be expected. The results are reported in Figure 4.12 together with the corresponding pH values.

The washing pre-treatment, which did not appear to modify the pH of the residues, showed to exert a significant effect in reducing the mobility of all the considered components (in particular Cu, Cl, Sb, Pb and Zn) due to the decrease of their total content. After this pre-treatment, however, Cl and Pb leachate concentrations resulted still higher than the limits for hazardous waste disposal (2500 mg/l and 5 mg/l respectively). For the carbonated ash a higher pH value (i.e. 13.4) was found, which was attributed to the presence of a residual amount of KOH in the ash after filtration. The applied carbonation treatment showed to decrease the mobility of Cl, SO_4 and Pb, but to increase the release of Sb, Zn and Cr; Cu leaching instead appeared to be unaffected by this treatment.

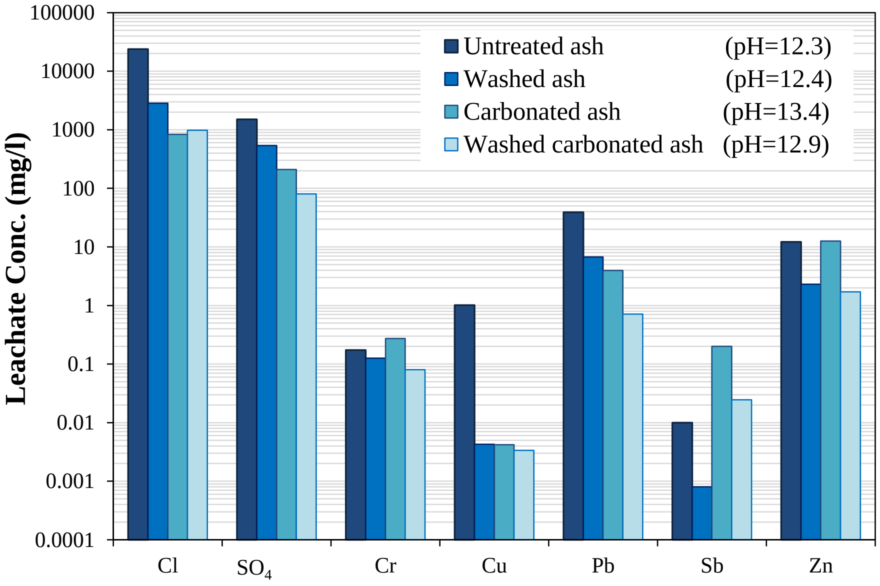

Figure 4.12: Leaching test results (EN 12457-2) for the different types of tested residues. Carbonation conditions: washed APC residues, 1 eq/l KOH, R=1.2 eq Ca_R/eq K_2CO_3, t=1 h, T=55 °C.

While for the most soluble components (Cl^- and SO_4^{2-}) this behaviour may be simply ascribed to the decrease in total concentration resulting from the slurry phase treatment, for metals and metalloids other effects should be considered. For these types of residues, in fact, carbonation has been generally found to cause the decrease of the mobility of amphoteric elements such as Cu, Zn and Pb and this has been mainly related to its effects in lowering the pH of the material (see e.g. Costa et al., 2007 and references therein). For the treatment tested in the present work, though, notwithstanding the significant degree of carbonation obtained, the pH of the material increased. Hence, the leaching behaviour of Zn may be tentatively related to the pH variation, while the mobility of Cu and Pb may be explained by different mechanisms such as metal carbonate precipitation (see e.g. Baciocchi et al., 2009) or decrease in total concentration resulting from the slurry phase treatment. The effects of carbonation on the leaching of oxyanion forming elements (such as Cr and Sb) have been less elucidated so far (e.g. Cornelis et al., 2008). However, the enhancing effect of carbonation on Sb leaching was already found for APC residues and ascribed to the incorporation of this metalloid in portlandite, which reacts upon CO_2 treatment (Baciocchi et al., 2009).

In order to improve the overall leaching behaviour of the solid material so to comply with the disposal criteria for non hazardous waste landfilling, the effects of a second washing treatment applied to the carbonated residues were investigated. In this case, due to the removal of part of the KOH contained in the ash, the pH of the residues decreased, but remained still well above values indicating solubility control by calcite. The mobility of most of the tested compounds (Zn, Pb, Sb, Cr and SO_4) appeared anyhow to decrease after this latter treatment, resulting lower than the limit values for non hazardous waste disposal.

4.2.6 Process layout and operating conditions

Figure 4.13 reports the scheme of the integrated alkali absorption and regeneration process developed on the basis of the lab-scale experimental results discussed above while the operating conditions to apply in each unit to maximize the regeneration of KOH for the absorption step and to store significant amounts of CO_2 in the solid residues are reported in Table 4.2.

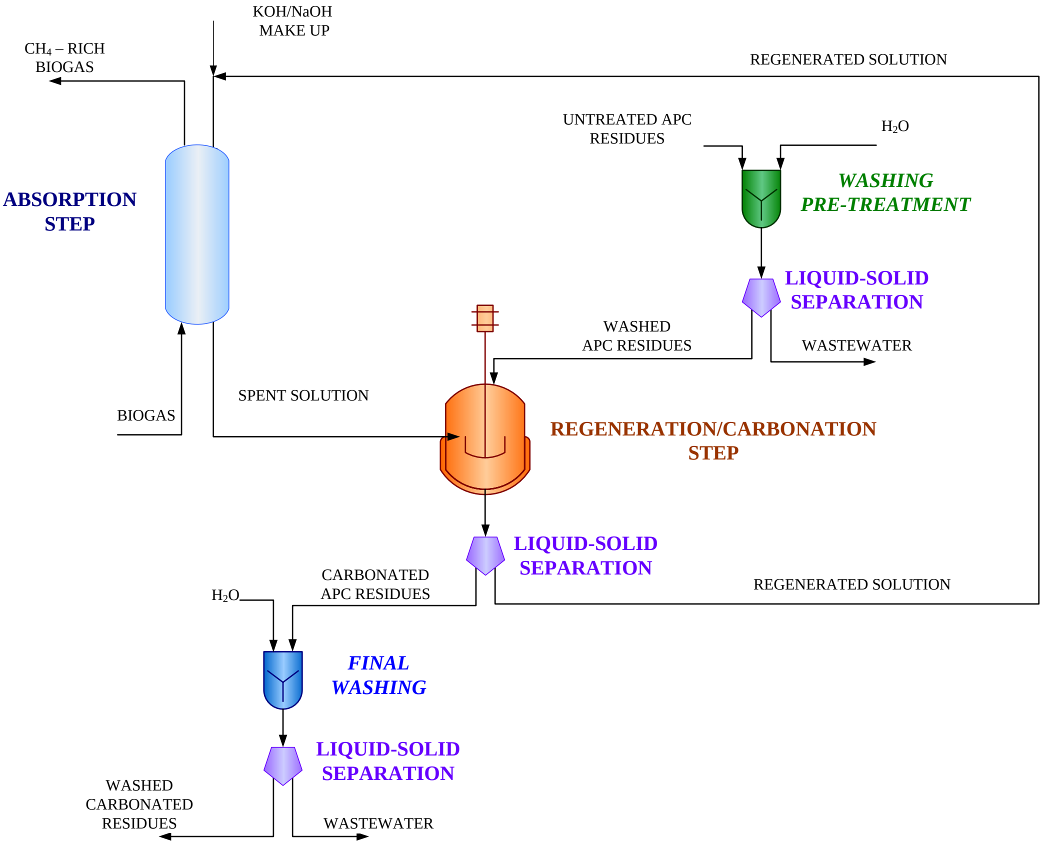

Figure 4.13: Scheme of the proposed alkali absorption and regeneration process.

The proposed regeneration process is mainly made up by a washing unit, a regeneration/carbonation reactor and a final washing unit each followed by a liquid-solid separation step. In particular the spent solution is conveyed from the outlet of the absorption unit to the carbonation reactor, where it is mixed with a stream of APC residues previously treated in a washing unit to remove soluble salts, in particular chlorides. The washed residues readily dissolve in the carbonation reactor, releasing calcium hydroxide which reacts with the potassium carbonate contained in the spent solution, leading to the regeneration of the KOH required for CO_2 absorption. As shown in the experimental section, the regeneration of K_2CO_3 to KOH is not complete, due to a limited yield of the chemical reaction and to the loss of solution with the wet solid. Hence, a partial make-up of KOH is necessary to obtain the required KOH concentration at the inlet of the absorption unit. A further washing treatment is then applied to the solid product obtained after carbonation in order to improve the leaching behaviour of this material.

Table 4.2: Operating conditions selected for the proposed regeneration process.

PRE-TREATMENT		
TYPE	Washing	
L/S	10	l/kg
TIME	15	minutes
REGENERATION		
R	1.2	mol Ca_R/mol K_2CO_3
TEMPERATURE	55	°C
TIME	60	minutes
FINAL TREATMENT		
TYPE	Washing	
L/S	5	l/kg
TIME	15	minutes

4.3 Optimization tests

Before the final design of the pilot-scale carbonation reactor, a new series of lab-scale tests were performed for each unit operation using freshly sampled APC residues in order to verify the operating conditions selected on the basis of the results of the preliminary lab-scale tests and to define the conditions to adopt in the pilot-scale plant. Furthermore regarding the regeneration reaction, experiments were carried out using the spent solution samples collected at the outlet of the already operating pilot-scale absorption column. Finally, the properties of the solid product of each treatment step were analysed to evaluate the possibility of their direct disposal or the need for a further treatment to comply with legislative requirements.

4.3.1 Characterization of reagents and products

In the first months of 2011 approximately 20 kg of APC residues were sampled from the baghouse section of the same plant, a hospital waste incineration facility located near Rome, from which the residues used in the previously discussed lab-scale experiments had been collected.

The APC residues were characterized in terms of humidity, main composition, calcite content, mineralogy, acid neutralization capacity and leaching behaviour.

The concentration of main and trace components was determined by fusion of ash samples with $Li_2B_4O_7$ in platinum melting pots at 1050 °C, followed by dissolution of the molten material in a 10% HNO_3 solution and measurement of element concentrations using inductively coupled plasma optical emission spectrometry (ICP-OES). The chloride content of the ash was determined by titration of the eluate solutions obtained from the compliance leaching test (EN 12457-2) with $AgNO_3$. The calcite content was measured by calcimetry analysis of HCl-digested samples using a Dietrich-Frühling calcimeter. The mineralogy of the ash was determined by X-ray diffraction (XRD) with Cu Kα radiation using a Philips Expert Pro diffractometer (equipped with a copper tube operated at 40 kV and 40 mA) with an angular step of 0.02° held for 2 seconds and a 2θ value spanning from 5 to 85°. The acid neutralization capacity (ANC) of APC residues was evaluated by contacting several subsamples of the material, applying a liquid to solid (L/S) ratio of 10 l/kg, with solutions containing increasing concentrations of HNO_3 in an end over end tumbler for 48 hours. The EN 12457-2 batch compliance leaching test was conducted to analyse the types and amounts of trace contaminants released by the APC residues at natural pH, by contacting samples of the material with distilled water at a L/S ratio of 10 l/kg in an end over end tumbler for 24 hours. The pH of the filtered solutions was measured and their elemental composition was analysed by ICP-OES. The obtained results were then compared to landfill compliance criteria.

The same analyses were also carried out to characterize the solid products obtained after the washing pre-treatment, the regeneration/carbonation reaction and the final washing treatment.

4.3.2 Experimental procedure

Regarding the washing pre-treatment, lab-scale experiments were carried out in order to evaluate if a similar removal of the chloride content of the ash could be achieved reducing the volume of water required for this treatment. For this reason several tests were performed washing the APC residues for 15 minutes with distilled water at a L/S ratio of 10 or 5 l/kg and at ambient temperature or at 55 °C applying a stirring rate of 250 rpm. The efficiency of the treatment was evaluated by analysing the chloride content of the wastewater so to determine the amount removed from the ash.

Since for the pilot-scale plant drying and milling of the solid product of each stage of the regeneration process were considered unfeasible, the new regeneration experiments were carried out using the washed APC residues directly resulting from the liquid-solid separation treatment without drying the solid product.

For the regeneration/carbonation stage, lab-scale experiments were carried out using washed APC residues and spent solution samples produced from the pilot-scale absorption tests with KOH and NaOH solutions. Different tests were carried out to evaluate the effect of the amount of residues used to regenerate a specific solution sample, i.e. the molar ratio of Ca as $Ca(OH)_2$ to K_2CO_3 or Na_2CO_3, on the achieved regeneration efficiencies. Lab-scale batch regeneration experiments were carried out in a 600 ml beaker that was placed in a thermostatic water bath for temperature control. At the beginning of each experiment the selected amount of washed APC residues was placed into the reactor and contacted with 200 ml of spent absorption solution. The experiments were carried out at 55 °C for 1 hour (the conditions selected during the preliminary evaluations phase) and for the entire duration of the experiment the suspended solution was stirred with a paddle-type impeller at a constant rate of 250 rpm. The solutions produced from the regeneration/carbonation experiments were titrated with a 10 eq/l HNO_3 solution so to allow to quantify the different species in the solution as already described in paragraph 4.2.2

Also after the regeneration/carbonation reaction, the residues separated from the solution were directly fed to the final washing treatment and the amount of water to add was calculated taking into account the humidity of the solid material in order to obtain a L/S of 5 l/kg. The operating conditions applied were the same as those used for the washing pre-treatment.

Vacuum filtration was selected as the liquid-solid separation method to use after each treatment stage; for the lab-scale experiments a Büchner filtration system was adopted. As for the filter media, a SEFAR propylene fabric presenting a mesh opening of 14 μm and a thickness of 200 μm was chosen for the pilot-scale unit and therefore tested in the lab-scale experiments.

4.3.3 Results

Characterization of the APC residues

The analysis carried out on the freshly sampled APC residues (see Table 4.3) confirmed the results previously obtained for this material, with calcium and chloride representing the major constituents of the ash since they account together for over 55% of the total ash mass. Significant alkali and metal concentrations, namely Na, K, Zn, and Cu, were also retrieved. The initial calcite content of the residues was around 9.8%.

Table 4.3: Concentration values of major and trace components in the freshly sampled APC residues.

MAJOR COMPONENTS		TRACE ELEMENTS	
	(g/kg)		(mg/kg)
Al	0.9	Be	<0.6
Ca	307.2	Cd	14.8
Cu	1.1	Co	<0.4
Fe	0.6	Cr	41.9
K	7.7	Mn	20.5
Mg	3.2	Mo	8.7
Na	49.5	Ni	16.7
Zn	3.2	Pb	160.9
Cl^-	255.0	Tl	<20
$CaCO_3$	98.0	V	2.1

The diffraction pattern resulting for the untreated APC residues, shown in Figure 4.14, indicated the presence of the same phases that had been detected for the previously analysed APC residues, i.e. Ca hydroxide phases (i.e. portlandite ($Ca(OH)_2$) and calcium hydroxychloride (CaOHCl)), halite (NaCl) and calcite ($CaCO_3$). The results of the acid neutralization capacity (ANC) test, not shown here for sake of brevity, confirmed the significant content of hydroxide phases in the ash, as indicated by the large acid buffering capacity exhibited by the residues at pH 12 (11 meq. H^+/g ash).

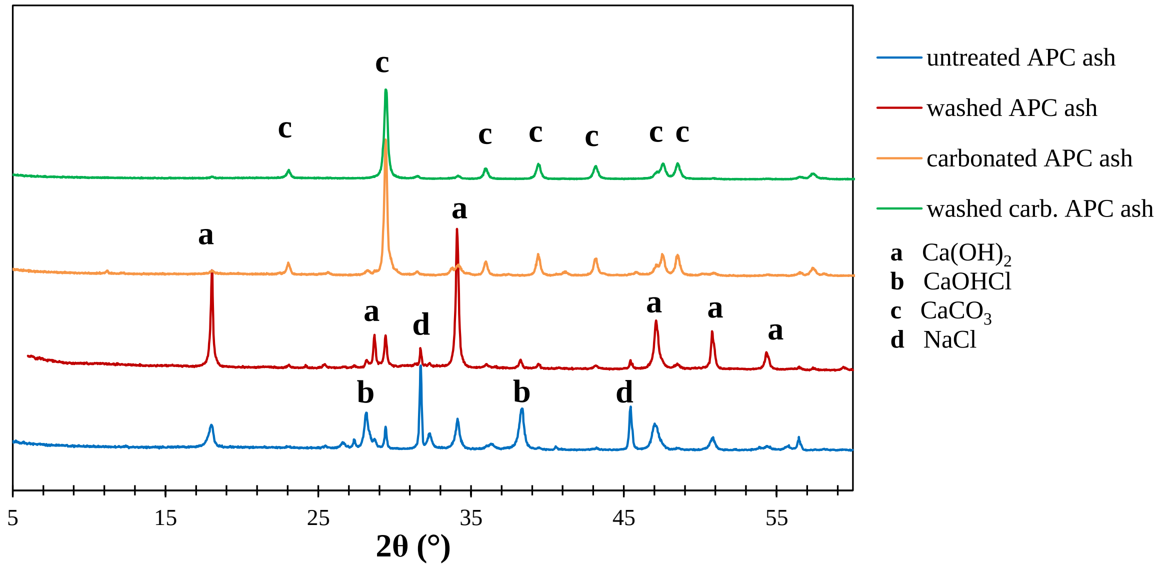

Figure 4.14: Comparison of the XRD of the untreated APC residues sampled in 2011 and the one of the solid sample obtained after each required treatment (pre-washing, carbonation and final washing).

As for the leaching behaviour of the untreated residues (see Figure 4.15), the pH of the eluates proved alkaline (12.4), while the critical elements, as compared to the landfill compliance criteria currently in force in Italy and the EU, were Cl, Pb and Zn. In particular, leachate concentrations of Cl and Pb proved higher than the limits for hazardous waste disposal, whereas Zn concentration resulted higher than the non-hazardous waste disposal limit.

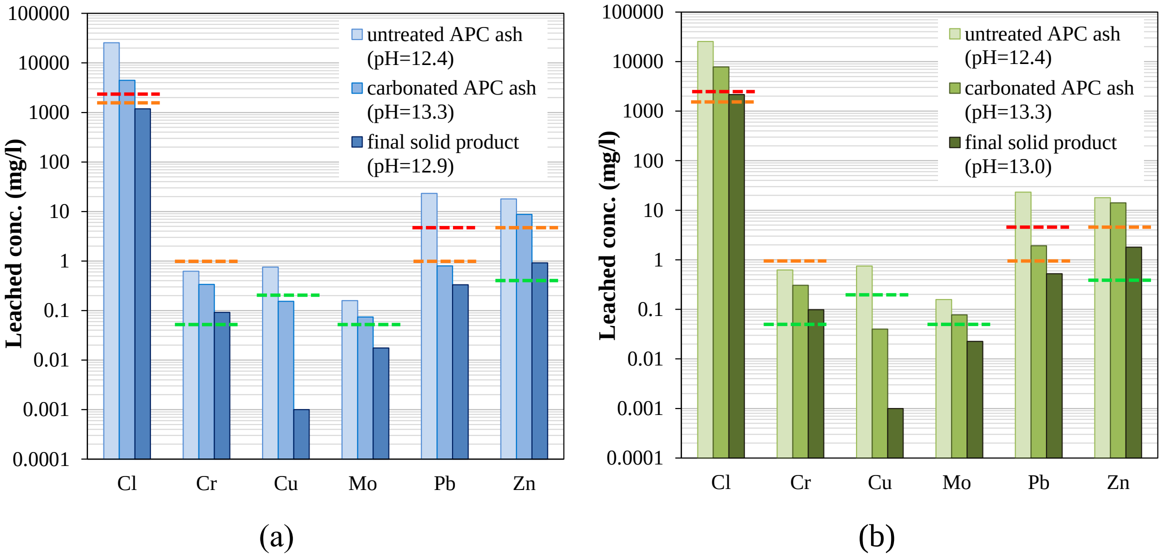

Figure 4.15: Comparison of eluate concentrations obtained in tests carried out with (a) KOH or (b) NaOH solutions for the untreated, carbonated and washed carbonated APC residues with the acceptance criteria of inert (green line), non-hazardous (orange line) and hazardous (red line) waste landfills.

Regeneration experiments

For the washing pre-treatment, the results of the lab-scale experiments allowed to select a L/S ratio of 5 l/kg and ambient temperature as the operating conditions to use in the pilot-scale unit. Under these conditions in fact the chloride removal efficiency resulted higher than 90% although the liquid to solid ratio was reduced from 10 to 5 l/kg. After the washing pre-treatment a significantly higher weight loss (around 40%) of the solid material was measured compared to the previously analysed residues (around 25%), owing probably to the differences in the chemical composition of the residues. The composition of the washed residues was analysed to calculate the amount of residues to use in the regeneration experiments. As shown in Figure 4.14, upon the washing pre-treatment the residues were mainly made up by portlandite since the NaCl and CaOHCl content of the ash showed to decrease significantly. From the buffering capacity of the washed residues at pH=12 measured by the ANC test (18.5 meq. H^+/g ash), the calcium content as $Ca(OH)_2$ of the material was estimated (37% wt.).

Figure 4.16(a) and (b) report the titration curves of two solutions obtained from the absorption column (i.e. 2.35 eq/l KOH and 3.15 eq/l NaOH) and of the corresponding solutions obtained after regeneration carried out at optimal operating conditions, i.e. 55 °C, R=1.2 eq Ca/eq K_2CO_3 and R=1.1 eq Ca/eq Na_2CO_3 respectively. In both cases the spent solution contained only potassium or sodium carbonates and bicarbonates, indicating that complete conversion was achieved in the absorption column, whereas, after the regeneration step, the buffering capacity of the solution showed that just potassium or sodium hydroxide was present. From these results, hence, it may be observed that also the regeneration reaction was almost complete. However, as shown in Figure 4.16(a), the normality of the obtained regenerated solution amounted to only 1.95 eq/l, against the 2.35 eq/l of the K_2CO_3 initial solution, due to the dilution effect caused by the use of wet residues. As a consequence, the KOH regeneration efficiency achieved was equal to 78%. Similarly, one can observe that also for the NaOH solution (Figure 4.16(b)) the dilution effect caused by the use of wet residues entails a lower normality of the regenerated solution compared to the spent one (2.45 eq/l against of 3.15 eq/l NaOH) and hence a regeneration efficiency of around 75%. Accordingly, the solid product obtained in the two tests was mainly made up by $CaCO_3$ (e.g. see Figure 4.14 for the solid product obtained from regeneration of KOH solution) with a CO_2 uptake of 45 and 46% wt. for KOH and NaOH respectively.

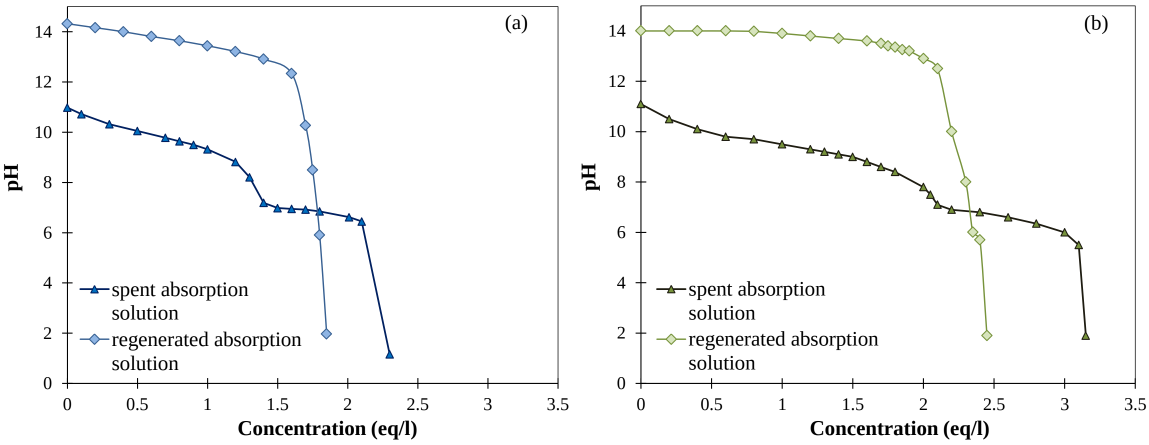

Figure 4.16: Comparison of the acid titration curves obtained for (a) the KOH or (b) NaOH absorption solution before and after the regeneration reaction (R=1.2 eq Ca/eq CO_3, 55°C and 1 h contact time).

Regarding the final washing treatment, XRD results (e.g. see Figure 4.14) showed that the solid product presented a similar mineralogical composition to the carbonated residues (i.e. predominance of calcite) but a lower content of halite and portlandite. The material presented in fact a 13% weight loss upon the final washing process.

As for the effects of this treatment on the leaching behaviour of the residues, in Figure 4.15 leachate concentrations of critical components before and after the carbonation reaction carried out with KOH (Figure 4.15 (a)) and NaOH (Figure 4.15 (b)) are compared to those of the untreated material and to landfill acceptance criteria.

The effects of the treatment on the decrease of the mobility of all of the investigated elements after carbonation, but especially after the final washing treatment are evident. In particular, the final solid product of the regeneration process carried out with KOH solution showed to comply with the limits for non-hazardous waste landfilling, with Cu and Mo even complying with the limits for inert waste landfilling. The solid product obtained in the test performed with NaOH solution showed a similar behaviour except for chlorides whose concentration proved to be higher than the limit for non-hazardous waste landfilling.

The humidity values (52-58%) achieved by the lab-scale vacuum filtration tests proved similar if not lower than the values that are typically achieved with commercial separation devices such as filter presses (55-60% wt.). Humidity showed to increase after the carbonation reaction and also after the final washing treatment.

4.4 Pilot scale activities

4.4.1 Pilot-scale units

Based on the results reported in the previous paragraph, the final operating conditions to adopt in each phase of the process were selected and the sizing, design and construction of the regeneration unit were carried out. In particular, in order to demonstrate the technical feasibility of the proposed process, the already existing absorption column was integrated with the pilot-scale regeneration/carbonation unit in the research laboratory hosted at the Casa Rota landfill site and several pilot-scale tests were performed. In the following, each unit of the pilot plant is described and the main findings of the pilot-scale absorption and regeneration tests are reported and discussed.

Absorption column

The absorption pilot plant (Figure 4.17 (i)) consists of a packed column where an aqueous KOH or NaOH solution is fed counter-currently to the landfill gas, extracted from a collection station in the landfill and fed to the column by means of a side channel blower. The column, built in stainless steel and characterized by an overall height of 990 mm and a diameter of 80 mm, is packed with Sulzer laboratory DX packing. The pilot plant, suitable to process about 20-25 m^3/h (gas at standard conditions of 273 K and 1001 kPa) of landfill gas and 40-60 l/h of absorbing solution, was built within a previous LIFE + project (Lombardi et al., 2011) and modified in the current UPGASLOWCO2 project. Input and output gas flow rates are measured by means of a volumetric flow meter (Fluidwell e F110) able to work in the range from 2.5 to 35 m^3/h. The input and output volumetric gas composition is also measured by means of portable gas analysers (Geotechnical Instruments e GA 94 for the input gas and Geotechnical Instruments-GA2000 for the output gas) which measure CH_4 and CO_2 by infra-red absorption (3% absolute accuracy for volumetric concentration >15%) and O_2 by internal electro-chemical cells. Input and output differential pressure is measured by a diaphragm pressure transducer (Delta Ohm-HD 408T 100MBG) able to work in the range from -10 to +10 kPa relative pressure. Atmospheric pressure is measured by means of a barometric pressure transducer (Delta Ohm-HD 9908 BARO) able to work in the range from 70 to 110 kPa. Input and output gas temperature is measured by means of K-type thermocouples. The gas flow rate, pressure and temperature are measured and registered in a quasi-continuous manner (every 10 s).

The measurement instruments are controlled by a programmable automation controller (Compact Field Point e National Instrument) composed by rugged I/O modules and intelligent communication interfaces. The composition is measured every 60 s and is directly registered by the gas analysers.

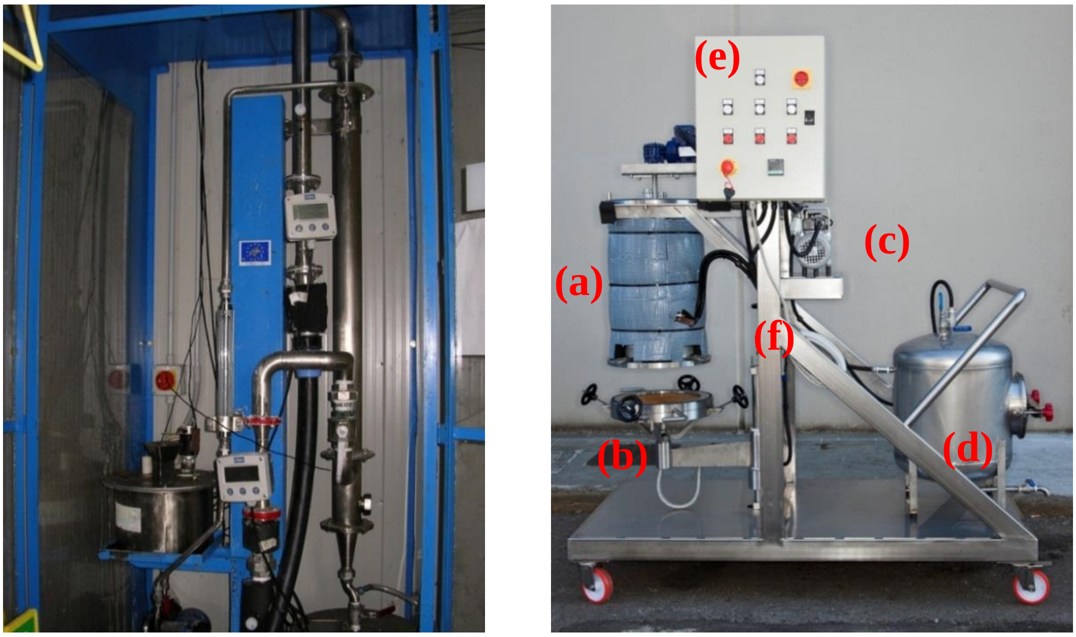

(i) (ii)

Figure 4.17: Pictures of the pilot plant: i) absorption column; ii) regeneration reactor and its main components: a) regeneration reactor with mixer and heating jacket, b) bottom section of the reactor with filter tensioning system, c) vacuum filtration pump, d) liquid collection tank, e) control panel and f) steel frame.

Regeneration unit

The regeneration pilot plant was designed and built with the aim of using the same reactor to perform in batch mode the pre-washing treatment of the residues, the regeneration/carbonation reaction and the post-washing treatment, as well as the liquid/solid separation step needed after each of the three unit operations. Namely the pilot-scale unit was designed in order to treat a maximum spent absorption solution volume of 10 l, i.e. the amount that can be stored in the tank of the existing pilot-scale absorption column considering the maximum concentration of carbonate phases measured for the spent absorption solutions produced by the pilot-scale plant (3.15 eq/l). In order to carry out the final design of the pilot scale regeneration reactor it was decided to consider a volume greater than the maximum value required by each of the three treatment stages, i.e. 20.6 l (volume required for the washing pre-treatment stage). Besides, the height of the reactor was chosen to grant a height/diameter (H/D) ratio of 2, which was considered as a compromise condition for optimizing mixing requirements (high H/D value) and filtration demands (low H/D value). For the separation step it was decided to apply vacuum filtration, the same method adopted for the lab-scale experiments discussed in section 4.2. As shown in Figure 4.17 (ii), the plant is made up by: the regeneration reactor (a), which includes a paddle type mixer and an external heating jacket; the filter medium (b), which is fitted on the bottom of the reactor in a custom made tensioning system; the vacuum filtration system, made up by the pump (c) and the filtered liquid collection tank (d); the control panel (e) with switches for activating all equipment (mixer, heating system and vacuum pump) and a display for setting the heating temperature; a stainless steel support system (f) on wheels on which all units and equipment are placed and manoeuvred. The regeneration reactor has an internal diameter of 300 mm and height of 600 mm. It is made of stainless steel (AISI 316), with a wall thickness of 2 mm. The filtration media is a monofilament propylene fabric (SEFAR TETEX MONO 05-1100 SK 014) with a 14 μm pore size and a thickness of 2 mm. The vacuum pump (Core Equipment RC4D-E-V) has a flow rate of 67 l/min and can achieve a total final pressure of 1 Pa, with a motor power of 0.37 kW.

4.4.2 Materials

For carrying out the pilot-scale tests, 45 kg of APC residues were collected in the end of 2011 from the same incineration plant where the previous samples were collected and these residues were characterized using the methods already described for the lab-scale tests. This sample of APC residues presented a slightly higher calcite content, around 13% by weight and the results of the XRD analysis (see Figure 4.18) indicated that the mineralogy of the material was quite similar to that of the residues used in the previous lab-scale tests. In particular the newly sampled APC residues were characterized by a prevalence of NaCl and CaOHCl and also significant amounts of $Ca(OH)_2$. The results of the leaching compliance tests carried out on the untreated APC residues proved in good agreement with the ones obtained for the residues used for the lab-scale tests, with Cl, Pb and Zn still representing the critical elements. However, comparing the results it is possible to note that the calcium and chloride concentration in the newly sampled APC residues proved to be higher than in the previously tested residues, while the lead and zinc concentrations and pH of the eluate were lower (see Figure 4.23). Overall, similarly to what observed for the residues used in the lab-scale tests, lead and chloride leachate concentrations proved to be higher than the limits for disposal in hazardous waste landfills.

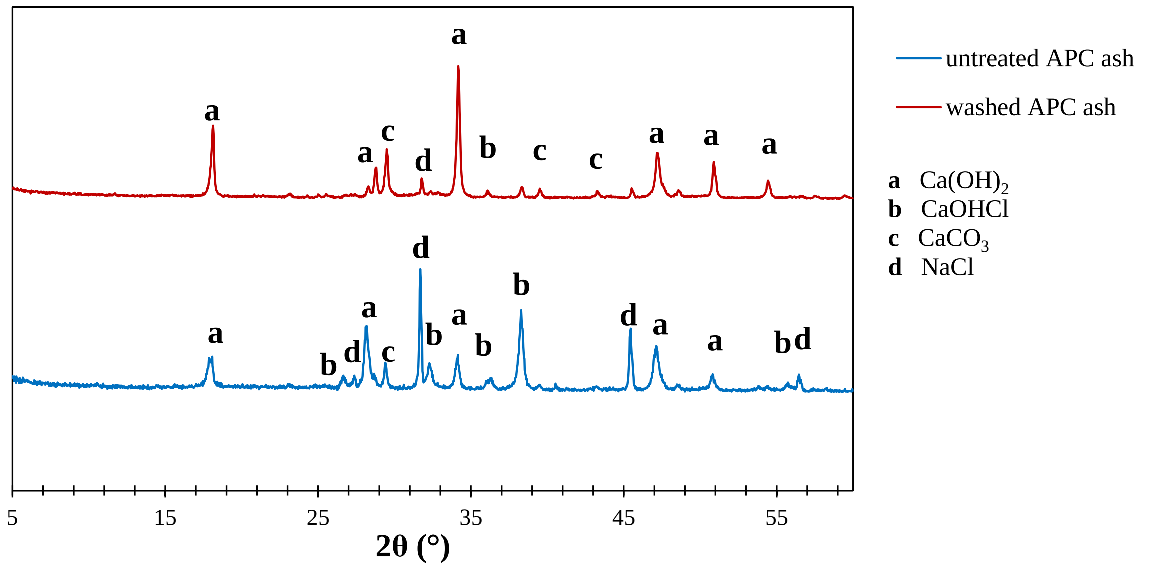

Figure 4.18: Comparison of the XRD of the APC residues used in the pilot-scale test before and after the washing pre-treatment.

Washing pre-treatment tests carried out in the regeneration/carbonation unit using this new sample of APC residues and applying a liquid to solid ratio of 5 l/kg allowed to estimate a weight loss of the material of around 40% wt. after the latter treatment. The acid neutralization capacity of the washed APC residues was also analysed and from these results (see Figure 4.19), assuming that the buffering plateau observed at pH=12 (i.e. 15 eq/kg) was only due to the calcium hydroxide content of the material, the total $Ca(OH)_2$ content of the washed ash was estimated (55.5% wt). This result combined with the weight loss observed after the washing treatment was used to estimate the amount of APC residues to use in the carbonation tests.

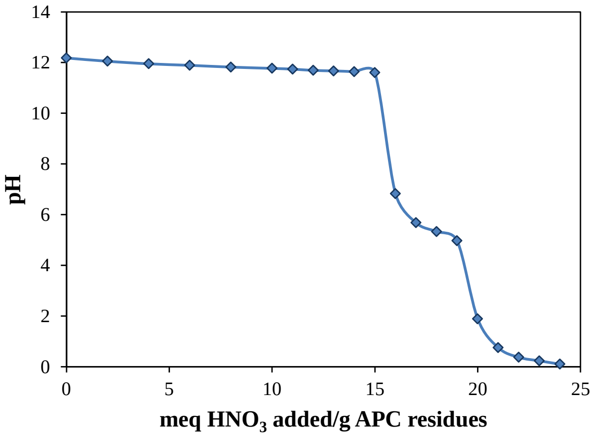

Figure 4.19: Acid neutralization capacity of the washed APC residues used in the pilot-scale tests.

4.4.3 Pilot-scale experiments procedures

Absorption tests procedure

Absorption tests were performed with load solutions at different KOH and NaOH concentrations, ranging from 2.35 to 3.8 eq/l and 2.8 and 3.8 eq/l respectively, since preliminary tests have shown that significant regeneration yields could be maintained only for K_2CO_3 or Na_2CO_3 concentrations lower than 4 eq/l. In fact, above this threshold, the L/S ratio was too low to allow for an effective mixing of the APC residues making the process unfeasible. This condition poses a constraint on the maximum NaOH or KOH concentration to be used in the absorption step.

Each test was started by flowing the landfill gas through the column. Once the inlet and outlet flow rates were stable, the absorption solution, stored in a tank, was fed to the column. The duration of each test, constrained by the liquid flow rate and the volume of the storage tank, was typically equal to 10 min. The spent solution was collected at the outlet of the column during steady-state operation, which was typically achieved after the first 2 min of operation. For the entire duration of the test, temperature, pressure, flow rate and composition of the inflow and outflow gas were continuously measured and recorded. The collected spent absorption solution was analysed by titration with HNO_3 to determine its carbonate content and then used in the regeneration phase, as described below. In order to verify the feasibility of recycling the regenerated solution in the absorption step, absorption tests were also carried out using the solutions obtained from the regeneration step. As the concentration of the regenerated solution was always lower than in the one of the load solution, the KOH or NaOH concentration of the latter was achieved by a proper makeup with a more concentrated raw alkali solution.

Regeneration procedure

As mentioned before, the process is made up by three consecutive steps (washing pre-treatment, regeneration, final washing), carried out in the same reaction tank. In the first step, distilled water and APC residues were mixed using a 5:1 L/S ratio and kept in the tank for about 15 min at ambient temperature. After this step, the slurry was filtered, allowing to produce a solid cake at the bottom of the reactor, while the filtered wastewater was collected in the liquid collection tank and, from there, discharged. In the second step, the spent solution from the absorber was added to the cake obtained from the previous step and, then, mixing was started again, allowing to re-suspend the residues in slurry phase in order to start the regeneration reaction. This phase, performed at a maximum temperature of 55°C for a reaction time of around 90 min, was followed by a second filtration step in order to recover the regenerated solution, that, after a proper makeup addition, can be reused as load solution in the absorption column. The carbonated cake remaining at the bottom of the reactor after the second filtration step was washed with distilled water (L/S = 5 l/kg, t = 15 min) and, after a third filtration step, recovered at the bottom of the reactor while the filtered wastewater was also collected and discharged.

At the end of each step, the solid cake formed upon filtration was weighted and a sample was taken to determine its humidity, calcite content and leaching behaviour. In particular, the amount of $CaCO_3$ contained in each solid sample after oven drying at 105 °C, was measured employing a Dietrich–Frühling calcimeter, by determining the volume of evolved gas after treatment with a 1.12 kg/l HCl solution. To assess the release of metals, metalloids and soluble salts at the natural pH of the solid samples, the leaching compliance test (EN 12457-2) which employs a L/S ratio of 10 l/kg was carried out. The concentrations of metals and metalloids were measured by ICP-OES analysis, employing an Agilent 710-ES instrument, whereas the leachate content of chloride was measured by titration with a $AgNO_3$ solution. The obtained concentrations were compared with the current EU landfill acceptance criteria (Council Decision 2003/33/EC).

The liquid collected at the end of each test was also weighted and samples were collected to analyse its composition. In particular, the samples of the solution collected after the regeneration phase were titrated with a HNO_3 solution in order to assess the extent of regeneration quantifying the amount of different species in solution based on its buffering capacity at specific pH ranges, i.e. hydroxides ($12 < pH < 14$), carbonates ($8 < pH < 11$) and bicarbonates ($5 < pH < 7$), adopting the procedure already described for lab-scale tests in section 4.2.2. The amount of residues to use in each test was estimated from the volume and composition of the spent solution to be regenerated and from the calcium hydroxide content of the washed APC residues (see paragraph 4.4.2) in order to achieve a 1.2 molar ratio between $Ca(OH)_2$ and K_2CO_3 or Na_2CO_3, selected on the basis of the results of the preliminary tests (see section 4.2.5). The weight loss occurring during the washing pre-treatment (around 40%) was also accounted for.

4.4.4 Results: AwR tests with raw alkali solutions

In this section the results of AwR pilot-scale tests obtained at using two types of raw alkali reagent (KOH or NaOH) at different concentrations in the absorption solution are reported and discussed.

CO_2 separation in the absorption stage

The conditions tested and the results obtained in the absorption tests carried out employing raw KOH solutions with concentrations ranging from 2.3 to 3.8 eq/l are presented in Table 4.4 (tests 1A-3A) while the data resulting for absorption tests carried out with raw NaOH solutions with concentrations ranging from 2.8 to 3.9 eq/l (test 7A-9A) are reported in Table 4.5.

Table 4.4: Main inputs and outputs of the absorption tests carried out with KOH solutions.

Test number		***1A***	***2A***	***3A***	***4A***	***5A***	***6A***
Type of test		*1st run*	*1 st run*	*1 st run*	*2nd run*	*2nd run*	*2nd run*
Inlet gas	flow rate (Nm^3/h)	19.8	20.3	19.8	19.4	19.9	20.5
	temperature (°C)	12.4	16.3	15.5	7.9	10.3	11.7
	CH_4 (% vol.)	56.3	55.1	54.8	56.5	56.8	55.1
	CO_2 (% vol.)	42.7	43.5	41.3	43.5	41.7	41.8
Inlet solution	flow rate (l/h)	60.0	60.0	60.0	60.0	60.0	60.0
	temperature (°C)	30.4	27.9	31.4	26.1	31.9	28.1
	KOH (eq/l)	2.33	2.80	3.80	2.45	3.80	2.37
	K_2CO_3 (eq/l)	0.00	0.00	0.00	0.10	0.30	0.06
Outlet gas	flow rate (l/h)	17.0	18.3	16.7	16.6	16.3	17.9
	temperature (°C)	19.6	17.3	18.4	17.3	23.3	21.4
	CH_4 (% vol.)	60.6	63.4	66.5	62.7	67.3	61.6
	CO_2 (% vol.)	37.1	35.3	32.5	37.3	33.1	35.7
Outlet solution	flow rate (L h^{-1})	60.0	60.0	60.0	60.0	60.0	60.0
	temperature (°C)	27.8	27.2	36.3	31.3	37.6	32.5
	KOH (eq/l)	0.00	0.00	0.20	0.00	0.20	0.00
	K_2CO_3 (eq/l)	2.33	2.82	3.60	2.55	3.96	1.20
CO_2 removal efficiency (%)		25.2	26.7	33.6	26.6	35.1	25.6

Table 4.5: Main inputs and outputs of the absorption tests carried out with NaOH solutions.

Test number		***7A***	***8A***	***9A***	***10A***	***11A***
Type of test		*1st run*	*1 st run*	*1 st run*	*2nd run*	*3rd run*
Inlet gas	flow rate (Nm^3/h)	20.0	19.8	19.9	19.4	19.9
	temperature (°C)	9.2	15.6	8.8	16	9.8
	CH_4 (% vol.)	56.3	55.5	56.9	56.1	55.8
	CO_2 (% vol.)	43.1	41.8	42.9	42.2	42.0
Inlet solution	flow rate (l/h)	60.0	60.0	60.0	60.0	60.0
	temperature (°C)	28.2	28.2	26.8	35.7	34.7
	NaOH (eq/l)	2.8	3.2	3.85	3.71	3.6
	Na_2CO_3 (eq/l)	0	0	0	0.34	0.15
Outlet gas	flow rate (l/h)	17.2	17.7	16.6	15.2	16.3
	temperature (°C)	14.7	18.4	17.9	19.8	18.9
	CH_4 (% vol.)	61.8	63.8	65.5	63.3	64.0
	CO_2 (% vol.)	35.3	33.7	33.8	34.4	33.3
Outlet solution	flow rate (L h^{-1})	60.0	60.0	60.0	60.0	60.0
	temperature (°C)	29.2	25.7	32.1	33.5	39.2
	NaOH (eq/l)	0	0	0.15	0.35	0.5
	Na_2CO_3 (eq/l)	2.8	3.2	3.77	3.71	3.4
CO_2 removal efficiency (%)		29.7	28.2	34.2	36.2	35.0

As may be observed in Table 4.4 and Table 4.5, the inlet landfill gas and the outlet gas stream presented a quite constant volumetric composition for all tests carried out either with KOH or NaOH solutions. In particular, the inlet gas presented 41-43% CO_2 and 54-57% CH_4 volumetric concentration while the outlet gas stream exhibited a CO_2 concentration ranging from 32 to 37% and a CH_4 content between 60 and 67%. The CO_2 concentration of the outlet gas showed to decrease for increasing concentrations of both KOH and NaOH in the load solution. On the basis of the inlet and outlet gas flow rates and of the respective CO_2 concentrations, the CO_2 removal efficiency values were estimated. As observed in Table 4.4 and Table 4.5, CO_2 removal efficiencies varied from 25.2% for 2.3 eq/l solutions to 33.6% for 3.8 eq/l KOH solutions while in case of tests carried out with NaOH solutions this parameter ranged between 29.7% for 2.8 eq/l solutions to 34.2% for 3.8 eq/l NaOH solutions. The increase of CO_2 removal with higher KOH/NaOH concentrations in the load solution was confirmed by the composition of the spent solutions, which showed a higher K_2CO_3 or Na_2CO_3 content for increasing alkali concentrations in the inlet stream. Actually, comparing the concentrations of KOH and

K_2CO_3 measured in the inlet and outlet solutions, it can be observed that an almost complete conversion of OH^- to CO_3^{2-} was obtained in all of the performed tests, as can be observed also for tests carried out with NaOH solutions. In Figure 4.20, the results obtained from absorption tests carried out using KOH and NaOH solutions at two different concentration values are compared. As can be noted in Figure 4.20 (a), the CO_2 removal efficiency obtained using the same concentration values in the load solutions were quite similar. Also the CH_4 concentrations resulting for the two types of reagents in the outlet gas were quite comparable at the same concentration value, see Figure 4.20 (b), with maximum contents of around 66% retrieved for the 3.8 eq/l solutions. As may be noted, the CH_4 concentration values obtained in the outlet gas do not meet the requirements for biomethane composition (> 96%). It is worth pointing out that, as previously mentioned, the absorption column was originally designed within a previous Life+ project to achieve the target CH_4 concentration for upgraded biogas using a much higher KOH or NaOH concentration than the ones tested in this work (Lombardi et al., 2008). Hence, in order to achieve a significant CO_2 removal with the same apparatus using KOH or NaOH solutions with maximum concentrations of 4 eq/l, a single absorption step would not be sufficient and instead a multistage procedure, using two or more in-series columns, would be required. The feasibility of obtaining a 90% CO_2 removal efficiency employing a 3.8 eq/l NaOH solution was demonstrated in the same experimental device by carrying out the absorption reaction in three subsequent stages (Baciocchi et al., 2013a).

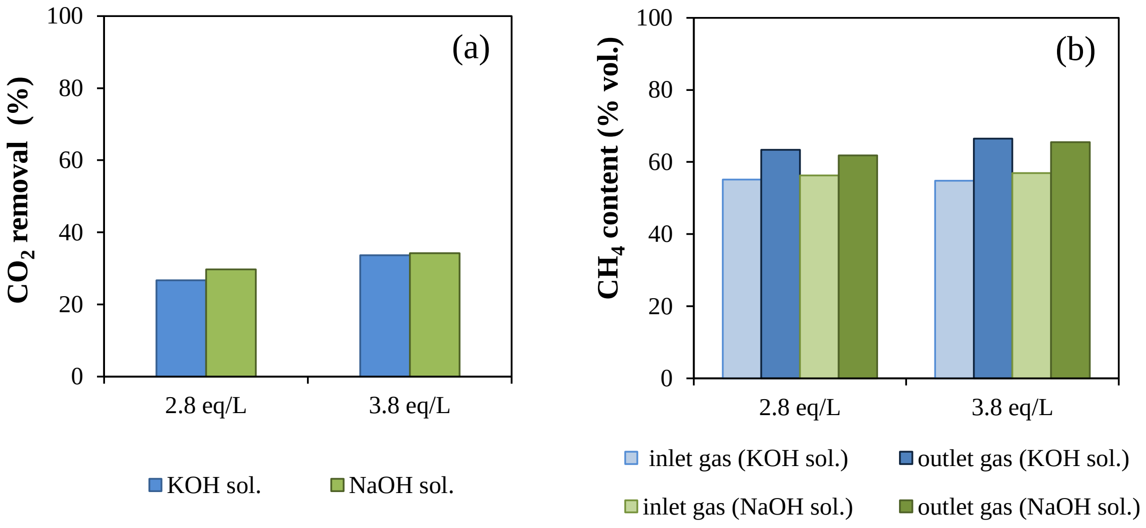

Figure 4.20: (a) CO_2 removal and (b) CH_4 concentration in the inlet and outlet gas as a function of the type and concentration of alkali reagent.

Alkali regeneration and CO_2 storage in the regeneration stage

Data on the main properties of the inflows and outflows resulting from each stage of the regeneration process (washing pre-treatment, regeneration reaction and final washing) applied to treat the spent solutions produced from KOH absorption tests discussed above are exhibited in Table 4.6 (test runs 1R-3R); the data resulting for the tests performed to treat spent NaOH absorption solutions are instead shown in Table 4.7 (test runs 6R-8R).

Table 4.6: Main inputs and outputs of each step of the regeneration process carried out to treat the spent solutions produced by the KOH absorption tests (see Table 4.4).

Test number		***1R***	***2R***	***3R***	***4R***	***5R***
Type of test		*1st run*	*1st run*	*1st run*	*2nd run*	*1st run*
Washing pre-treatment						
APC residues (kg)		2.55	3.09	4.55	3.88	1.43
Washing water (l)		12.76	15.43	22.73	19.42	---
Solid Product	dry weight (kg)	1.65	1.68	2.88	2.69	---
	absorbed water (l)	1.20	1.83	2.34	2.37	---
	$CaCO_3$ (% wt.)	39.0	35.8	32.0	23.5	---
Wastewater (l)		11.59	13.10	20.18	16.66	---
Regeneration reaction						
Spent solution	volume (l)	7.56	7.83	8.26	7.15	7.59
	K_2CO_3 (eq/l)	2.33	2.82	3.60	3.96	2.35
	KOH (eq/l)	0.00	0.00	0.20	0.20	0.00
Regenerated solution	volume (L)	7.09	8.52	7.37	5.68	5.55
	K_2CO_3 (eq/l)	0.17	0.20	0.34	0.47	0.10
	KOH (eq/l)	1.50	1.60	2.13	2.25	1.45
Regeneration yield η_R (%)		60.37	61.73	52.67	45.11	45.14
Solid Product	dry weight (kg)	1.95	2.24	3.37	3.60	1.78
	absorbed solution (l)	1.70	1.78	3.06	3.27	1.67
	$CaCO_3$ (% wt.)	72.3	75.0	65.6	55.1	65.5
Final washing						
Washing water (l)		7.83	n.m.	15.66	n.m.	7.31
Solid Product	dry weight (kg)	1.56	1.72	2.81	n.m.	1.46
	absorbed water (l)	1.61	1.75	2.81	n.m.	1.80
	$CaCO_3$ (% wt.)	83.0	85.0	79.8	n.m.	79.8
Wastewater (l)		7.63	9.81	15.71	n.m.	6.70

n.m.: non measured

Table 4.7: Main inputs and outputs of each step of the regeneration process carried out to treat the spent solutions produced by the NaOH absorption tests (see Table 4.5).

Test number		***6R***	***7R***	***8R***	***9R***
Type of test		*1^{st} run*	*1^{st} run*	*1^{st} run*	*2^{nd} run*
Washing pre-treatment					
APC residues (kg)		2.97	4.18	4.03	3.71
Washing water (l)		14.86	20.92	20.16	18.55
Solid Product	dry weight (kg)	1.91	2.49	2.29	2.23
	absorbed water (l)	2.20	2.16	2.23	2.4
	$CaCO_3$ (% wt.)	19.0	21.0	21.5	22.5
Wastewater (L)		13.03	18.6	17.92	15.97
Regeneration reaction					
Spent solution	volume (l)	7.33	9.03	7.43	7.02
	Na_2CO_3 (eq/l)	2.8	3.2	3.77	3.71
	NaOH (eq/l)	0	0	0.15	0.35
Regenerated solution	volume (l)	7.02	7.14	6.92	5.35
	Na_2CO_3 (eq/l)	0.08	0.1	0.46	0.43
	NaOH (eq/l)	1.75	2.07	2.00	2.37
Regeneration yield η_R (%)		59.89	51.15	49.42	48.67
Solid Product	dry weight (kg)	2.34	3.15	2.88	3.72
	absorbed solution (l)	2.27	2.56	2.21	2.72
	$CaCO_3$ (% wt.)	70.2	58.6	59.0	60.6
Final washing					
Washing water (l)		10.27	14.68	11.48	n.m
Solid Product	dry weight (kg)	2.03	2.73	2.37	n.m
	absorbed water (l)	2.29	2.99	2.56	n.m
	$CaCO_3$ (% wt.)	76.0	66.0	84.6	n.m
Wastewater (l)		9.39	14.60	11.26	n.m

n.m.: non measured

Specifically, Table 4.6 and Table 4.7 report the amounts of reagents (APC residues, spent solution and washing water) and products (solid product, regenerated solution and wastewater) associated to each treatment stage. In addition, the data necessary to estimate the performance of this process in terms of both the regeneration of the alkali solution for the absorption stage and of the amount of CO_2 permanently stored in the solid product are presented.

As shown in Table 4.6 and Table 4.7, the amount of residues used to treat around 8 l of spent solution in each test ranged between 2.6 and 4.6 kg, while the total amount of process water required for the two washing treatments was of 20-38 l, depending on the concentration of the spent solution. The outputs of the treatment consisted in the regenerated solution (7-8.5 l), wastewater (15-23 l in total) and the solid product from the final washing step (1.5-2.8 kg dry weight with a 50% humidity), since the solid products obtained in the previous steps were fed as inputs to the following steps. Moreover, Table 4.6 and Table 4.7 report the parameters needed to evaluate the performance of the second stage of the AwR process, i.e. the KOH or NaOH concentration of the regenerated solution and the $CaCO_3$ content of the solid product from each treatment step. The regenerated solution showed to contain mainly potassium or sodium hydroxide, with a concentration between 1.5 and 2.1 eq/l for KOH and 1.75 and 2.1 eq/l for NaOH, increasing as expected for higher K_2CO_3 or Na_2CO_3 concentrations of the treated spent solution (see Table 4.6 and Table 4.7). These results proved in quite good agreement with those obtained from lab-scale tests reported in section 4.3 for which for example a KOH concentration of 1.7 eq/l was attained treating a spent solution containing 2.35 eq/l K_2CO_3. The fact that a significantly lower KOH or NaOH concentration was achieved upon regeneration compared to that of the original load solution in both lab and pilot-scale tests could be mainly attributed to the dilution effect caused by the use of humid residues.

The overall yield of the regeneration process (η_R) was calculated as shown in Eq. (4.4), in which $[OH^-]_{REG}$ and $[CO_3^{--}]_{SPENT}$ indicate the concentration expressed in terms of eq/l of hydroxide in the spent solution and carbonate in the regenerated one respectively, while V_{REG} and V_{SPENT} represent the volumes of the corresponding solutions.

$$\eta_R = \frac{\left[OH^-\right]_{REG} V_{REG}}{\left[CO_3^{--}\right]_{SPENT} V_{SPENT}} 100 \tag{4.4}$$

As shown in Table 4.6, the regeneration yield resulting for the treatment of the spent solutions produced by first run KOH absorption tests varied between 53 and 62%, proving higher for the experiments carried out with less concentrated solutions. A similar decreasing trend of η_R for increasing concentrations of the load solution to regenerate was also found for the tests carried out with NaOH. Comparing the η_R values resulting for the two types of alkali reagents at the same concentration value, see Figure 4.21(a), it can be noted that the yields achieved were quite comparable.

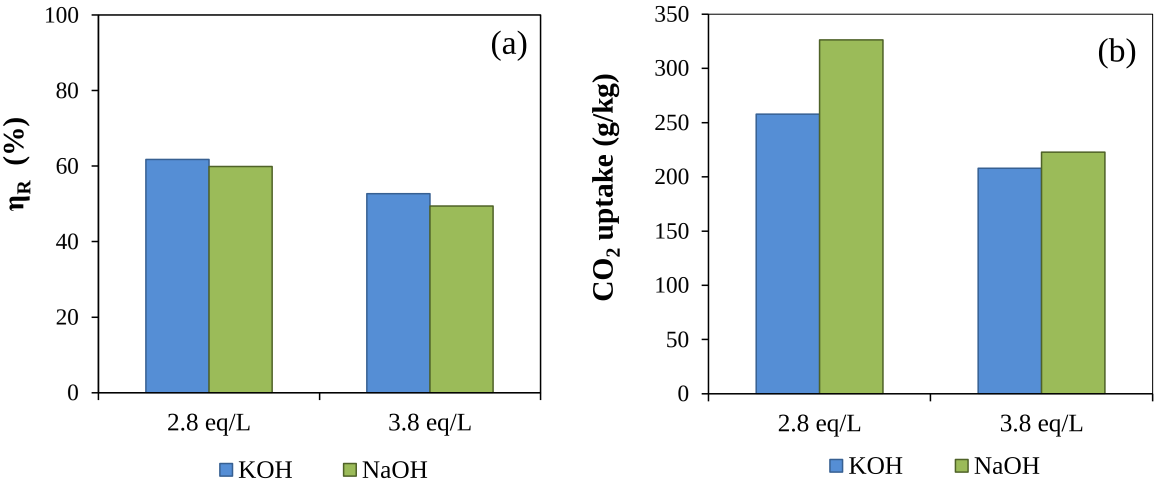

Figure 4.21: Comparison of (a) the overall regeneration efficiency of the process and (b) the CO2 uptake obtained for KOH and NaOH absorption solutions.

Since in the absorption stage a 100% conversion of hydroxide to carbonate phases was found for most of the performed tests, η_R may be considered as a direct indication of the efficiency of regeneration of the load solution for the absorption stage and hence of the amount of make-up of raw alkaline reagent required to re-establish its initial concentration. As can be noted in Table 4.6 and Table 4.7, the obtained η_R values are mainly correlated to the decrease observed between the carbonate concentration in the spent solution and the hydroxyl concentration obtained in the regenerated one. In fact, the ratio between the volume of the regenerated solution and that of the spent one ranged between 0.8 and 1, suggesting that the volume of the recovered regenerated solution played a secondary role in affecting the performance of the process. Instead, significant differences can be noted between the concentration values resulting for the spent and regenerated solution. For example for test 6R, 1.75 eq/l of NaOH were obtained in the regenerated solution, i.e. 40% lower than expected on the basis of the initial composition of the solution (2.8 eq/l of Na_2CO_3). This reduction is due on the one hand to the dilution of the spent solution caused by the water contained in the solid product after the washing pre-treatment and on the other hand to the chemical composition of the residues used in the process. In order to discriminate between the effects contributing to the decrease in concentration observed in the performed tests, Figure 4.22(a) and (b) reports the experimental and theoretical concentrations related to the regeneration process carried out with KOH and NaOH solution respectively.

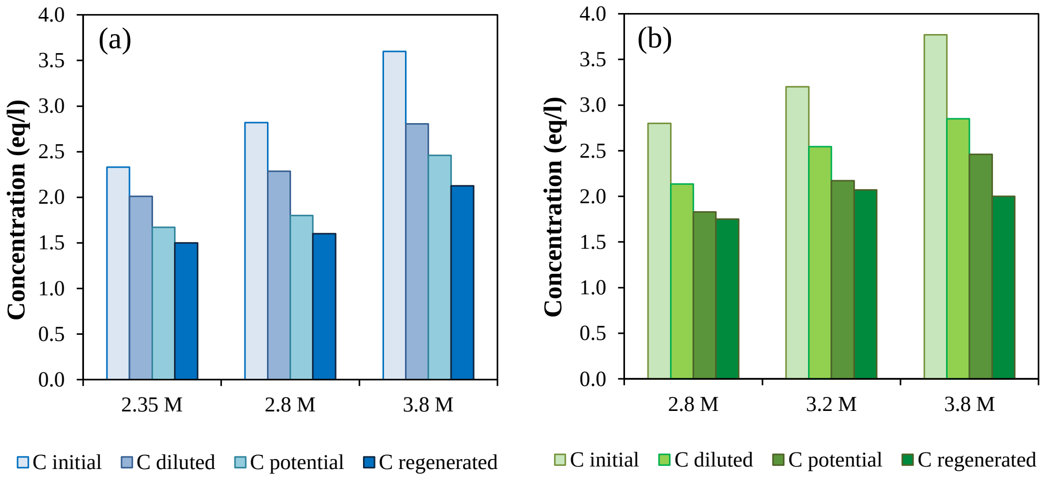

Figure 4.22: Trend of the main concentrations related to the regeneration process for (a) KOH or (b) NaOH solutions.

In particular, the initial K_2CO_3 or Na_2CO_3 concentration in the spent solution ($C_{INITIAL}$), the concentration resulting from its dilution due to the residues washing pre-treatment ($C_{DILUTED}$), the maximum potassium or sodium hydroxide concentration that could be achieved based on the buffering capacity of the regenerated solution ($C_{POTENTIAL}$) and the effective KOH or NaOH concentration measured in the regenerated solution ($C_{REGENERATED}$) are reported. As can be noted, the main decrease in concentration can be explained with the dilution effect resulting from the washing pre-treatment, since the solid product obtained after this step contained typically around 2 l of water which is quite significant considering that the volume of the treated spent solution was generally of around 7-9 l. However, based on the measurement of the total buffering capacity of the regenerated solution ($C_{POTENTIAL}$), the maximum amount of obtainable KOH or NaOH showed to be lower than $C_{DILUTED}$. This effect may be most probably related to the high soluble salts content of the residues and in particular of CaOHCl, which, even after the washing pre-treatment, may reduce the buffering capacity of the solution, as explained in paragraph 4.2.5.

As for the $CaCO_3$ content of the solid product, it ranged between: 32-39% wt. after the washing pre-treatment step, 66-72% wt. after regeneration and 80-85% wt. after final washing for tests carried out with KOH solutions while when sodium hydroxide solutions were used the $CaCO_3$ content of the solid product ranged between: 19-21% wt. after the washing pre-treatment step, 58-70% wt. after regeneration and 66-85% wt. after final washing. The increase in the calcite content of the solid product after the regeneration step was clearly due to the reaction of $Ca(OH)_2$ contained in the washed APC residues with

K_2CO_3 or Na_2CO_3 dissolved in the spent solution; the increase resulting after the final washing treatment was instead ascribed to the dissolution of soluble phases from the solid material which caused its enrichment in sparely soluble phases such as $CaCO_3$. This explanation was supported by the fact that the weight of the solid material showed to decrease after each washing treatment, whereas to increase after the regeneration reaction (see Table 4.6 and Table 4.7) and also by the mineralogical composition of the samples obtained after each treatment stage. The calcite content of the solid products of the regeneration step resulted very similar to those determined in the lab-scale experiments, e.g. 72.3% compared to 73.5% to treat a spent solution containing 2.35 eq/l K_2CO_3.

Based on the difference between the calcite content of the solid product before and after the regeneration reaction and on the dry weight of the solid product of this treatment step the amount of CO_2 removed from the solution was calculated. The values resulting for tests 1R, 2R and 3R carried out with KOH solutions (290, 363 and 391 g CO_2) proved very similar to those estimated on the basis of the variation of the K_2CO_3 concentration in the solution after the regeneration reaction and of its total volume, i.e. 285, 387 and 399 g CO_2, respectively. In tests performed with a NaOH solutions (tests 6R, 7R and 8R) instead a larger difference can be observed between CO_2 removed from the solution estimated based on the variation in the calcite content of the solid product and the one calculated on the basis of the variation of the K_2CO_3 concentration in the solution (i.e. 367, 458 and 413 g CO_2 against 528, 522 and 475 g CO_2 respectively).

Finally the amount of CO_2 stored in the solid product after the regeneration reaction (CO_2 uptake) expressed as g CO_2/kg dry material, was calculated from the difference between the weight % calcite contents of the products of the regeneration ($CaCO_{3\ REG}$) and washing pre-treatment ($CaCO_{3\ WASH}$) steps and reported in terms of the final dry solid mass of the regeneration product (see Eq. (4.5)).

$$CO_{2uptake} = \frac{(CaCO_{3REG} - CaCO_{3WASH}) \cdot 44/100}{100 - (CaCO_3)_{REG} \cdot 44/100} 1000 \qquad \textbf{(4.5)}$$

Namely the CO_2 uptakes determined for the solid products resulting from the tests carried out to regenerate 2.8 and 3.8 eq/l solutions ranged between 210 and 330 g CO_2/kg, see Figure 4.21(b). These values prove similar if not higher to those reported for lab-scale tests carried out on APC residues applying the wet carbonation route, i.e. contacting the humidified residues at a low L/S with 100% CO_2 at specific operating conditions (Fernández-Bertos et al., 2004; Baciocchi et al., 2009). As can be noted, the CO_2 uptake showed to decrease for increasing concentrations of the treated solution for both types of alkali reagent, as a consequence of the reduction in efficiency of the carbonation reaction associated to the use of a higher amount of residues. The CO_2 uptake achieved in the regeneration of NaOH solutions resulted slightly higher than that obtained treating KOH solutions, in particular for the 2.8 eq/l solution (i.e. 330 versus 260 g CO_2/kg). This result is probably related more to the variability in the initial $CaCO_3$ content of the washing pre-treatment product (in average 36% for KOH and 21% for NaOH tests) than to a higher yield of the carbonation reaction in the presence of NaOH solutions; the calcite content of the solid product of the regeneration reaction proved in fact similar if not higher for KOH compared to NaOH tests (e.g. 75% versus 70% for 2.8 eq/l solutions).

Leaching behaviour of the solid product

Figure 4.23 reports the main results of the leaching tests carried out on the solid products of the regeneration and final washing treatments using two reactants types (KOH or NaOH) and concentration (2.8 or 3.8 eq/l) in the absorption solution to regenerate. Specifically, in each graph the concentrations of the most critical elements are exhibited along with the relative acceptance criteria for inert, non-hazardous and hazardous waste landfills. In addition, in order to compare the results obtained by the tested treatments with the initial leaching behaviour of the residues, in the same graphs the results of the leaching tests carried out on the untreated APC residues are also shown. As can be noted, the leachate of the APC residues used in this process, characterized by a pH of 12, presented concentrations of chlorides and Pb that proved higher than the limits for hazardous waste disposal, as well as significant contents of Zn, Cr, Cu, Mo and Sb, all higher than the limits for inert waste landfilling.

Upon the regeneration reaction, the solid product presented an increased pH value compared to the untreated residues, i.e. 13 and 13.3 for the tests carried out for KOH solutions (Figure 4.23(a) and (b)) and 12.9 for the ones performed for NaOH solutions (Figure 4.23(c) and (d)), owing to the partial sorption of the regenerated solution onto the solid material.

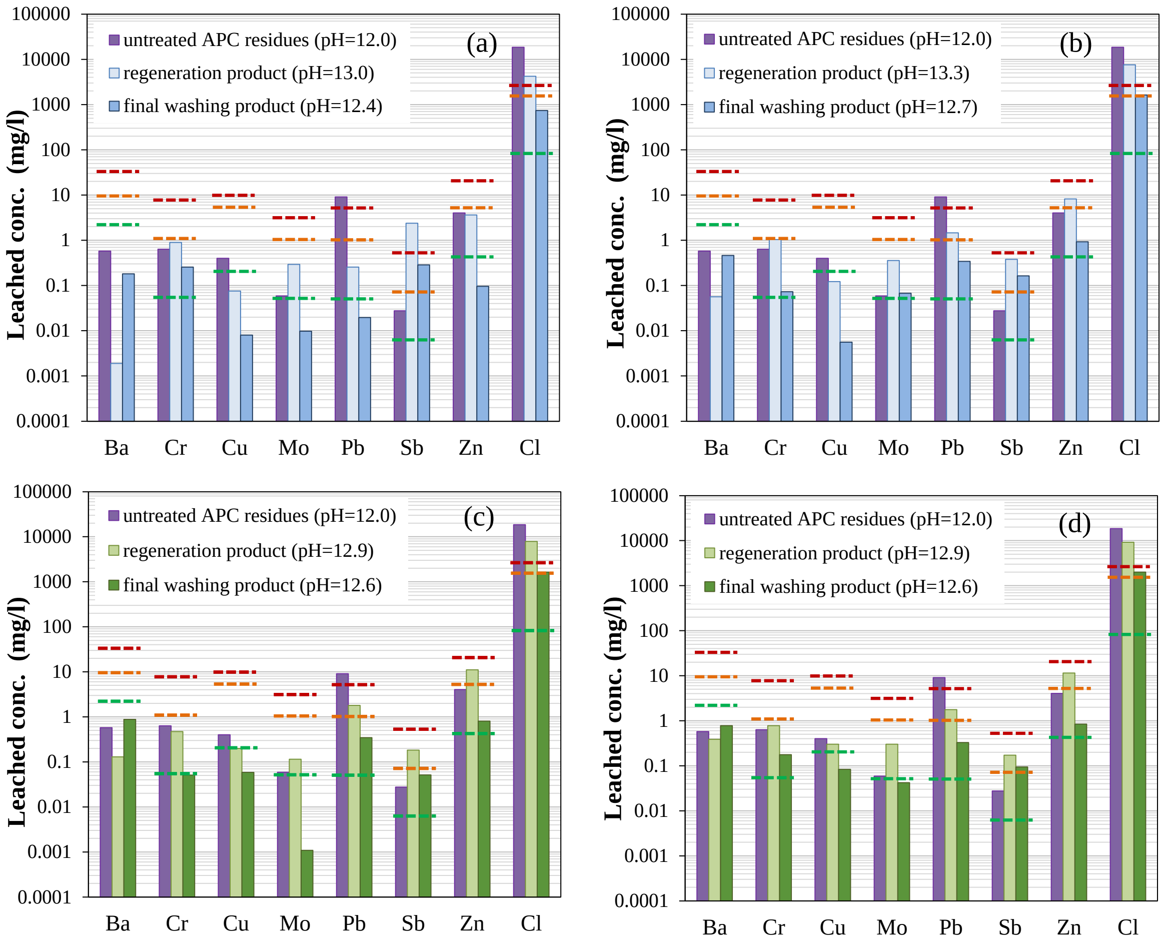

Figure 4.23: Leachate concentrations of the solid products of regeneration tests for: (a) 2.8 eq/l KOH, (b) 3.8 eq/l KOH, (c) 2.8 eq/l NaOH, (d) 3.8 eq/l NaOH absorption solutions in comparison to untreated residues and the acceptance criteria for inert (green line), non-hazardous (orange line) and hazardous (red line) waste landfills.

Regarding leachate concentrations, in general, a decrease in the release of Ba, Cu, Pb and Cl, whereas a higher mobility for Cr, Mo, Sb and Zn was observed in comparison to the untreated residues. These results are in good agreement with the findings of the lab-scale tests and can be mainly correlated to different effects caused by the applied treatments. Specifically, the decrease observed for chlorides may be related to the decrease in total concentration resulting mainly from the washing pre-treatment but also from the regeneration reaction (carried out in slurry phase at a temperature of around 50 °C). The reduction in mobility of Cu and Pb may be also related to a decrease in total concentration upon the washing pre-treatment and regeneration reaction, however it may be due also to the precipitation of Cu or Pb carbonates, that was indicated as likely from the results of geochemical modelling of the leachate concentrations of carbonated APC residues (Baciocchi et al., 2009). As for the results found for Zn leaching, which is generally reported to decrease upon carbonation (see e.g. Fernández-Bertos et al., 2004), the observed increase may be related to the higher pH of the solid product compared to that of the untreated residues. Finally, the increase in mobility resulting for oxyanion forming elements such as Cr, Sb and Mo, may be associated to the dissolution, as a consequence of the carbonation reaction, of phases controlling the solubility of these elements (Van Gerven et al., 2005; Cornelis et al., 2006; Baciocchi et al., 2009; Hyks et al., 2009). As for the influence of the type and concentration of alkaline reagent on the environmental behaviour of the solid product, a more noteworthy variation with the concentration of the solution to regenerate can be noted for the KOH solutions (see Figure 4.23(a) and (b)) than the NaOH ones (see Figure 4.23(c) and (d)), probably in relation to the larger difference in pH resulting in the first case. Finally, comparing the results obtained for the two types of reagents, it may be observed that the solid product collected in the KOH regeneration tests presented a lower leaching concentration of Cu, Cl, Pb and Zn, while instead the solid product of the NaOH regeneration reaction showed a lower mobility of Sb; however, in all of the tested conditions one or more of the acceptance criteria for hazardous or non-hazardous waste disposal (e.g. Cl, Zn, Sb and Cu) were not met.

After the final washing treatment, the pH of the solid product showed to decrease, see Figure 4.23(a)-(d). A pH value of 12.6 was obtained for all of the tested conditions, except for the test carried out to regenerate the 2.8 eq/l KOH solution, for which a slightly lower (12.4) value was achieved (see Figure 4.23(a)). The leaching behaviour of the samples collected in tests carried out with KOH solutions after the final washing treatment showed a general improvement compared to the carbonated samples with all concentrations lower than the limits for hazardous waste disposal; however, significant differences can be noted depending on the type of solution and its initial concentration. In particular, for KOH, only the solid product obtained from the test carried out to treat the 2.33 eq/l solution was found to comply to the limits for non-hazardous waste disposal, while for increasing concentrations of the alkali solution the limit values for Sb (test 2.8 eq/l) and Sb and Cl (test 3.8 eq/l) were exceeded, see Figure 4.23(a) and (b) respectively. For the experiments with NaOH solutions, chloride leachate concentrations showed to slightly exceed the limit for non-hazardous waste disposal for all of the tested conditions, while in the test with the highest concentration (3.8 eq/l) also Sb resulted above the limit for non-hazardous waste disposal. This is an important aspect to consider in the evaluation of the techno-economical and environmental feasibility of the proposed AwR process, since it may condition the management options for the solid product.

4.4.5 Results: AwR tests with regenerated alkali solutions

In this section the results obtained using regenerated KOH or NaOH solutions (second run tests) instead of raw ones are reported and discussed in comparison to those obtained for raw solutions of a similar composition

CO_2 separation in the absorption stage

In the perspective of coupling the absorption and regeneration steps, it is fundamental to investigate if the yield of CO_2 separation in the absorption stage may be affected by the use of regenerated alkali solutions instead of the raw ones. For this reason several regenerated solutions obtained from first run tests were fed again to the absorption column for a further run, after a proper reagent make-up to re-establish the initial KOH or NaOH concentration. In particular the data resulting for the second run test carried out with 2.33 and 3.8 eq/l KOH solutions are reported in Table 4.4 (tests 4A-5A) and in Table 4.5 the second and third run test carried out for a 3.8 eq/l NaOH solution (tests 10A-11A) are presented. As can be noted in Table 4.4 and Table 4.5, the comparison with the results previously commented for first run tests suggests that no remarkable differences can be observed both for the KOH and NaOH solutions. The only noteworthy variation that can be noted is that the inlet solutions presented a non negligible concentration of carbonates due to the slightly lower carbonate to hydroxyl conversion achieved in the regeneration stage. Consequently, the outlet solutions presented a higher K_2CO_3 or Na_2CO_3 concentration compared to the ones resulting from the second run tests. Hence, it may be expected that the carbonate concentration of the solution will consistently increase during multiple AwR runs.

As for the CO_2 removal efficiency, actually the values estimated from the results of the second run tests proved slightly higher than the first run ones, e.g. 35.1% compared to 33.6% for the 3.8 eq/l KOH solution and 36.2% instead of 34.2% for the 3.8 eq/l NaOH solution, (see Table 4.4 and Table 4.5). However, this outcome was probably due more to a variation in the inflow and outflow gas composition and flow rate than to an actual enhancement of the CO_2 absorption process.

The comparison between the yield of first and second run absorption tests carried out for 3.8 eq/l KOH and NaOH solutions reported in Figure 4.24, confirms that no appreciable differences were found neither in terms of CO_2 removal (see Figure 4.24(a)) nor in terms of the CH_4 concentration of the outlet gas (see Figure 4.24(b)). This infers the overall qualitative equivalence between raw and regenerated solutions concerning the yield of the absorption stage, although the effect of multiple AwR cycles should be investigated to definitively confirm this finding.

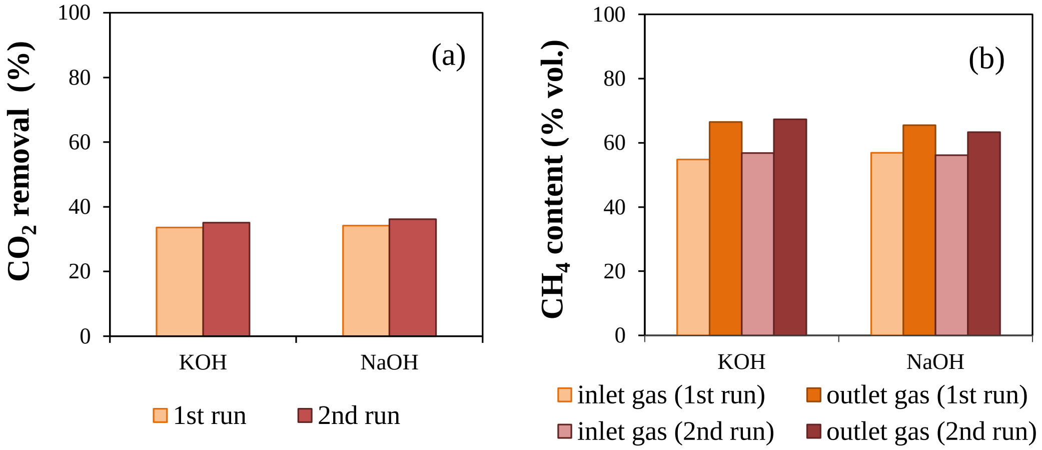

Figure 4.24: (a) CO_2 removal and (b) CH_4 concentration in the inlet and outlet gas for 3.8 eq/l KOH and NaOH raw (1st run) and regenerated (2nd run) solutions.

<u>Alkali regeneration and CO_2 storage in the regeneration stage</u>

In Table 4.6 the main inputs and outputs resulting from the regeneration experiment carried out to treat the spent solution generated from absorption test 5A, indicated as test run 4R, are reported; the data resulting for the second run regeneration test (test 9R) carried out for a 3.8 eq/l NaOH solution (test 10A) are reported in Table 4.7. It was decided to specifically analyse the performance of the regeneration step for the more concentrated solutions, since the first run tests carried out on these solutions with both types of reagents proved to yield the lowest overall regeneration efficiencies and CO_2 uptakes. In addition, in order to assess the feasibility of reducing the total amount of process water to employ in the regeneration process, the wastewater produced in the final washing treatment step of the tests performed for first run 3.8 eq/l KOH and NaOH solutions was used for the washing pre-treatment step of the respective second run tests. The comparison of the overall regeneration efficiency resulting for 1^{st} and 2^{nd} run KOH or NaOH 3.8 eq/l absorption solutions is reported in Figure 4.25(a). As can be noted, a decrease in the performance of the regeneration stage was observed only for KOH solutions (i.e. 52.7 versus 45.1%), while for NaOH tests the overall regeneration remained at a value around 49%.

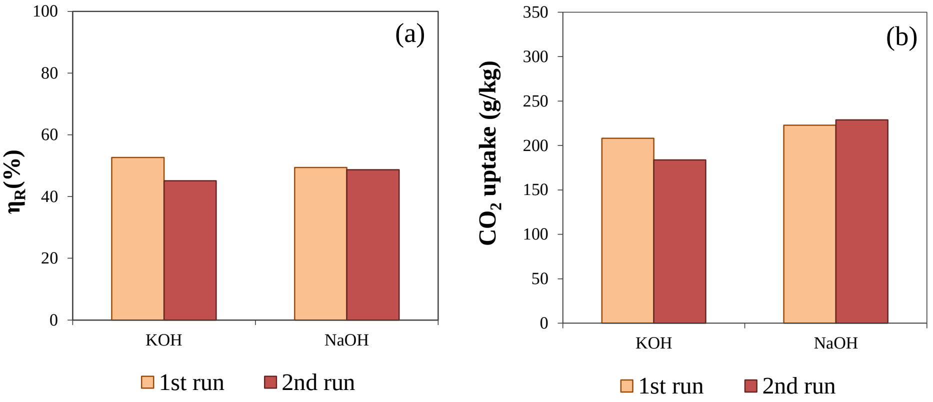

Figure 4.25: Comparison of (a) the overall regeneration efficiency of the process and (b) the CO2 uptake obtained for 1st run and 2nd run KOH and NaOH 3.8 eq/l solutions.

The results obtained for KOH may be mainly ascribed to the lower volume of recovered regenerated solution compared to the treated spent one (i.e. 79% compared to 89%) but also to the slightly lower K_2CO_3 to KOH conversion achieved in the solution (83% instead of 86%). This second factor can be also correlated to the lower calcite content of the solid product (55.1 versus 65.6% wt.). In fact, even though also in the 2nd run tests carried out with NaOH solutions the ratio between the volume of recovered solution and the treated one decreased compared to that found for the 1st run tests, the conversion of Na_2CO_3 to NaOH in the solution increased. This latter result was related to the use in the pre-treatment step of the wastewater generated from the final washing of the solid product of the first run test, which hence contained a certain amount of NaOH. It is not clear why the same behaviour was not found for the tests carried out using KOH solutions, hence further testing is required to clarify this issue. The results obtained for the 1st and 2nd run tests in terms of the CO_2 uptake of the solid product collected after the regeneration stage, reported in Figure 4.25(b), proved to be in good agreement with the trend of the extent of regeneration determined for the spent KOH and NaOH solutions; in the first case in fact in the 2nd run test a lower CO_2 uptake was found (i.e. 184 versus 208 g CO_2/kg), while in the latter case a slightly higher value was retrieved for the 2nd run test (i.e. 229 versus 223 g CO_2/kg).

Leaching behaviour of the solid product

Regarding the leaching behaviour of the solid products obtained treating regenerated solutions, the eluate concentrations of samples collected after the regeneration of 1st and 2nd run 3.8 eq/l KOH and NaOH spent solutions are reported and compared in Figure 4.26 (a) and (b), respectively.

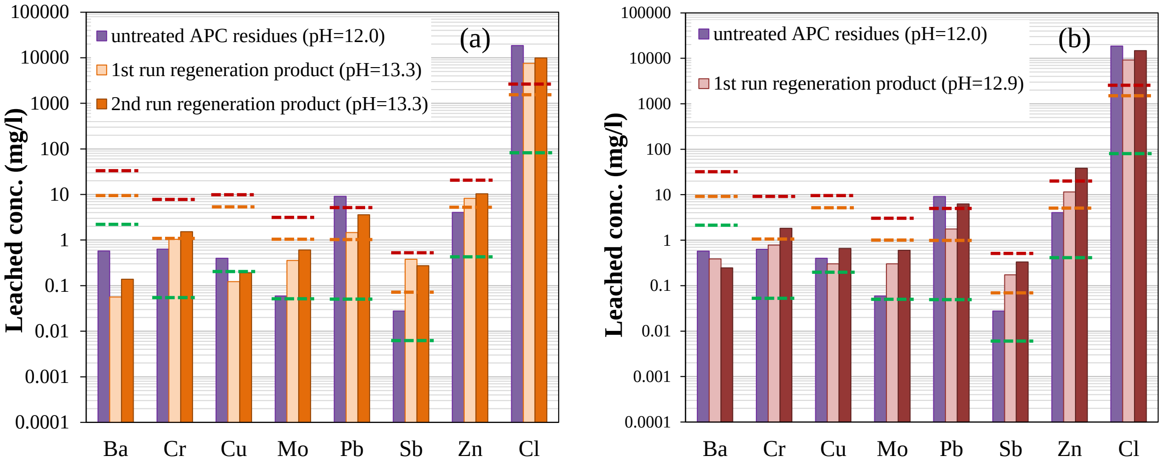

Figure 4.26: Leachate concentrations of the solid products of regeneration tests for 1st run and 2nd run 3.8 eq/l: (a) KOH, (b) NaOH absorption solutions in comparison to untreated residues and the acceptance criteria for inert (green line), non-hazardous (orange line) and hazardous (red line) waste landfills.

The pH of the leachates of 1st and 2nd run tests performed using the same type of solution resulted quite similar (i.e. 13.3-13.4 for KOH and 12.9 for NaOH absorption solutions). However, in both cases the solid product obtained after the regeneration stage in the 2nd run tests presented leachate concentrations generally higher than the ones obtained in the 1st run tests, as a result of the use of both pre-treatment water and spent solutions with a certain content of the same elements, having been already in contact with the solid material. In particular, the leaching concentrations of the most critical elements appeared to be higher in the eluates of the tests carried out with NaOH solutions. Anyhow, considering the acceptance criteria for waste landfilling, the environmental behaviour of the solid products obtained in the 2nd run tests may be classified as similar to that of the solids collected after the 1st runs, showing to require the final washing treatment prior to disposal. The effects of the final washing treatment on the product of 2nd run regeneration tests were not specifically tested, however it may be expected that similar results to those found for the 1st run tests could be achieved.

4.4.6 Results: AwR tests without the washing pre-treatment step

In this paragraph the differences resulting between AwR tests performed on washed residues and these carried out directly employing APC residues without the washing pre-treatment are presented.

CO_2 separation in the absorption stage

As already pointed out in Paragraph 4.4.4, in the regeneration stage of the AwR process a significant amount of process water is required. Since the final washing treatment step proved to be necessary in order to obtain an improvement of the leaching behaviour of the solid product compared to the untreated residues, the possibility of avoiding the washing-pre-treatment step was also evaluated. To this aim an AwR test was carried out using a 2.33 eq/l KOH load absorption solution without the washing pre-treatment step and the resulting regenerated solution was employed in a second run absorption test (test run 6A) to evaluate if the efficiency of the absorption reaction could be affected. As shown in Table 4.4, no considerable differences were observed in terms of process efficiency, since the CO_2 removal yield achieved (25.6%) was comparable to the values found in the 1st and 2nd run absorption tests carried out employing a 2.4 KOH eq/l solution (i.e. 25.2 and 26.6%). Coherently, also the CH_4 concentration measured in the outlet gas resulting from these tests were quite similar (around 61.5% vol).

Alkali regeneration and CO_2 storage in the regeneration stage

The main data attaining to the regeneration test carried out without the washing pre-treatment step (test run 5R) are reported in Table 4.6. As can be observed comparing the results obtained in this test to those achieved for the regeneration of a KOH solution with a similar composition (test 1R), the regeneration yield proved to decrease considerably without the washing pre-treatment step, passing from 60.4 to 45.1%. This result may be related to the significantly lower volume of regenerated solution obtained (5.6 compared to 7.1 l) which was due to the fact that in the tests performed with washed residues the material presented an initial humidity of around 45% wt. In addition, despite the fact that without the washing pre-treatment the spent solution was not diluted, the KOH concentration in the regenerated solution proved anyhow slightly lower than that resulting for test 1R (1.45 compared to 1.5 eq/l). This finding confirms the results of the lab-scale tests for which a high concentration of soluble salts in the residues showed to hinder the extent of regeneration (see paragraph 4.2.5). Furthermore, a lower yield of the carbonation reaction without the washing pre-treatment was also indicated by the calcite content of the solid product of the regeneration reaction which was lower compared to that resulting for test 1R (65.5 versus 72.3%). However, the net CO_2 uptake proved to be higher without the washing pre-treatment (324.5 versus 214.5 g CO_2/kg), since the calcite content of the untreated residues was much lower compared to that of the washed ones (13 versus 39% wt.) owing to the dissolution of soluble phases but possibly also to partial carbonation of the material already occurring in the washing step.

Leaching behaviour of the solid product

Regarding the leaching behaviour of the solid product collected after the regeneration and final washing steps in the test performed without the washing pre-treatment, the leachate concentrations of the most critical contaminants are reported in comparison to those resulting for test 1R in Figure 4.27(a) and (b), respectively.

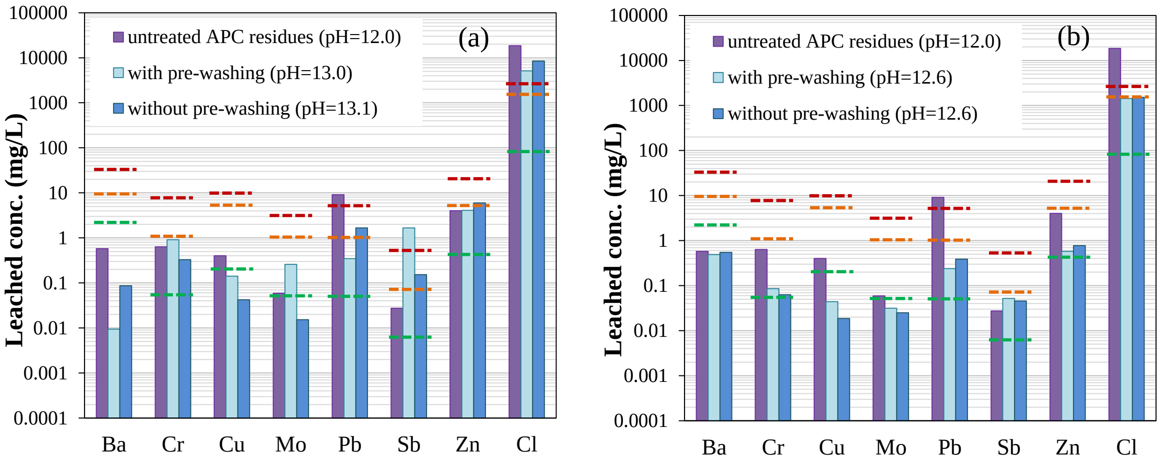

Figure 4.27: Leachate concentrations of the solid products of regeneration tests for 2.3 KOH eq/l absorption solutions: (a) after regeneration, (b) after final washing in comparison to untreated residues and the acceptance criteria for inert (green line), non-hazardous (orange line) and hazardous (red line) waste landfills.

As can be noted in Figure 4.27(a), the solid product obtained after regeneration in the experiment carried out without the washing pre-treatment presented a similar pH (around 13) but a higher leachate concentration of Ba, Pb, Zn and Cl compared to the test performed applying the washing pre-treatment. As for the previous experiments, this solid product presented eluate concentrations higher than the limits for disposal in hazardous waste landfills, in particular for Pb and Cl, indicating the need of the final washing treatment. As shown in Figure 4.27(b), upon final washing, the leaching behaviour of the solid products obtained from both types of tests showed to significantly improve, allowing theoretically to declassify the residues from hazardous to non hazardous waste.

4.5 Conclusions

In this chapter the possibility of applying carbonation of industrial residues as a technique to permanently storing the CO_2 separated from a biogas upgrading process was assessed. In particular an innovative absorption with regeneration (AwR) process was developed in the framework of the UPGAS-LOWCO2 Life+ project in which the carbonation of industrial residues was applied in order to regenerate the spent solution produced from an absorption column used to capture the carbon dioxide contained in a landfill biogas. This treatment allows also to permanently store the separated CO_2 in a solid and thermodynamically stable form while in the upgrading treatment commonly applied carbon dioxide is generally release in to the atmosphere due to its biogenic origin. Furthermore a third advantage obtained in this process is the improvement of the environmental behaviour of the industrial residues used to regenerate the spent solution.

Therefore, firstly the feasibility of regenerating the spent alkaline solution obtained from the absorption column was demonstrated by means of specific tests carried out with calcium hydroxide. Afterwards, several lab-scale tests on different suitable industrial residues were performed in order to select the material that allowed to obtain the highest yield of regeneration of a spent KOH absorption solution. Namely, three different types of residues were considered, i.e. the APC residues from a hospital waste incinerator, the finest size fraction of the bottom ash disposed of at the landfill where the pilot-scale plant is located and the AOD slag produced in an electric arc furnace steel manufacturing plant. Within these material the APC residues, due to their chemical, physical and mineralogical composition, showed the highest KOH regeneration capacity and were then selected to be used in the following phases of the project. A series of tests were hence performed at lab-scale in order to identify the optimal operating conditions to apply in the process in order to maximize the alkaline solution regeneration and the CO_2 uptake. In order to improve the yield of regeneration of the KOH solution, a washing pre-treatment of the APC residues with distilled water proved to be necessary so to remove the high soluble salts content (in particular chlorides) of these materials that showed to hinder the regeneration reaction. In the selected operating conditions (i.e. $R=1.2$ eq Ca_R/eq K_2CO_3, 55 °C) tests performed on washed APC residues allowed to reach in 1 hour a 90% KOH regeneration efficiency and a 30% CO_2 uptake. In addition, the series of investigated treatments (pre-washing, carbonation and second washing) showed also to significantly affect the leaching of the critical components for this type of residues, Cl, Pb and Zn in particular. Namely the final solid product showed to comply with the acceptance criteria for non hazardous landfills, indicating that the proposed process can also improve the environmental behaviour of this type of industrial residues.

Before the final design of the pilot scale carbonation reactor, several lab scale experiments were carried out in order to test the feasibility of reducing the volume of water required for the two washing treatments. Furthermore, tests were also performed using samples of the spent KOH and NaOH solutions produced by the existing pilot scale absorption column in order to confirm the process performance already obtained in the previous lab scale tests. These activities allowed to define the operating conditions to adopt in each stage of the regeneration process as well as to size and design the pilot-scale plant. In particular the lab-scale regeneration tests performed with spent absorption solution samples showed that a regeneration efficiency of 75-78% in the solution coupled with a CO_2 uptake of 45-46% in the solid material could be achieved both using KOH and NaOH solutions. In addition the leaching behaviour of the final solid product confirmed to be significantly improved compared to that of the untreated APC residues. On the basis of these results the design of the pilot plant was carried out and the regeneration unit was built and installed in the landfill in the end of 2011.

In the last phase of the project the performance of the absorption with regeneration process developed in the framework of the UPGAS-LOWCO2 Life+ project was evaluated performing integrated pilot-scale tests carried out in the two specifically designed units. In particular, the influence of the composition (type of alkali reagent and concentration) of the solution employed for the absorption reaction was assessed in terms of the CO_2 removal efficiency achieved in the absorption stage, the regeneration efficiency and CO_2 uptake resulting in the regeneration stage and the leaching behaviour of the solid product. As may have been expected, the performance achieved employing either type of alkali reagent (KOH or NaOH) at similar concentration values resulted basically equivalent with regard to the efficiency of CO_2 separation from the biogas and also to the volume and composition of the regenerated solution and to the environmental properties of the solid product. Instead, the concentration of the alkali reagent in the load absorption solution showed to significantly affect the yield of both stages of the AwR process. Specifically, the CO_2 removal efficiency in the absorption stage showed to be enhanced (going from 25 to 35%) for an increase of the initial concentration of the alkali reagent, whereas the yield of hydroxyl regeneration in the solution and of CO_2 uptake in the solid product proved to be lower for higher initial KOH or NaOH concentrations in the load solution (passing from 50 to 60% and from 208 to 326 gCO_2/kg, respectively). In addition, also the leaching behaviour of the solid product showed to worsen for higher concentrations of the alkali hydroxide phase to regenerate, indicating that only for the lowest concentration value tested (2.33 eq/l) the solid product could be declassified as non-hazardous waste. Hence, based only on these results the optimal concentration value that may allow to maximize the performance of the AwR process with reference to all of the targeted goals cannot be easily identified. Therefore, other evaluations such as economical and life cycle assessments are being performed in order to establish the conditions that may result in the highest benefits in terms of environmental and economical sustainability. Since, for example, from a preliminary economical evaluation the cost of NaOH appears to be approximately 50% lower than that of KOH, and the experimental results showed the equivalence in the overall performance of these two reagents, it appears reasonable to select the former for the AwR process. One of the most critical issues for the feasibility of the AwR process appears to be the volume and composition of the regenerated solution that can be recovered and reused in the absorption stage.

Based on the results of this study, it can be observed that for most of the tested conditions the extent of the regeneration reaction was almost complete, indicating that in order to increase the overall regeneration efficiency, a further optimization of the operating conditions under which the regeneration reaction is carried out would not be beneficial. Hence, process modifications aimed at reducing the dilution effect or increasing the recovery of the regenerated solution, as well as the selection of a different type of industrial residues characterized by a high content of calcium (hydr)oxides, such as cement kiln dust and some types of steel slag, could be attempted. Furthermore it as to be noted that the weak point of the process is represented by the high amount of wastewater produced. As for the possibility of reducing the use of process water, both of the washing treatments appeared to be necessary when using APC residues, the first one to increase the regeneration efficiency and the second one to improve the leaching behaviour of the solid product. However, an optimization in terms of water consumption appeared to be feasible and even beneficial employing the wastewater resulting from the final washing step for the pre-treatment of the residues, since it may allow to recover part of the KOH or NaOH contained in the solid product of the regeneration reaction. The reuse of the waste water in the process could be optimized in order to minimize the need of fresh water and obtained as a final by-product a concentrated brine solution that could be directly disposed of in evaporation ponds. Alternatively this by-product may be treated in specific processes, such as the Solval one, in order to obtain NaCl that may be used as a primary material for sodium carbonate production.

5 ENERGY AND MATERIAL REQUIREMENTS OF A DIRECT CARBONATION PROCESS

Adapted from:

Zingaretti, D., Costa, G., Baciocchi, R., 2013a. Assessment of the energy requirements for CO_2 storage by carbonation of industrial residues. Part 1: Definition of the process layout, Energy Procedia (in press);

Zingaretti D, Costa G, Baciocchi R, 2013b. Assessment of the energy requirements for CO_2 storage by carbonation of industrial residues: Mass and Energy balance (submitted to International Journal of Greenhouse Gas Control).

5.1 Introduction

In the last decades various studies investigated at laboratory scale the feasibility of using carbonation of minerals or industrial residue as a technique to store the anthropogenic carbon dioxide emissions. However pilot and full scale applications of this process are currently missing, except for a pilot scale installation developed by Reddy et al. (2011). One of the key factors for assessing the feasibility of the investigated accelerated carbonation processes for implementation at industrial scale is represented by the associated materials and energy requirements. Recently, several studies have focused on the evaluation of the energy penalties related to mineral carbonation (O'Connor et al., 2005, Huijgen et al., 2006a, Kelly et al., 2011 and Kirchofer et al., 2012). However the energy requirements estimated in these works differ considerably from one study to the other also when the evaluation was based on the same experimental data, probably as a consequence of the differences in the assumptions made. Besides, most of the studies available in literature made reference to the slurry phase carbonation route, whereas the wet route was not considered. The aim of the study presented in this chapter was to develop a specific model that can allow to assess the material and energy requirements for the storage of the CO_2 emissions of a natural gas-fired power plant by direct carbonation of different types of minerals and industrial residues using either the slurry phase or the wet route. After a short discussion of the state of the art on the evaluation of the energy requirements of accelerated carbonation (see paragraph 5.2), the layouts developed for both process routes are presented in paragraph 5.3. Then, for each unit operation included in the two layouts, the assumptions and equations used for performing the mass and energy balance are clearly stated (see paragraph 5.4). On this basis, the influence of the characteristics of the materials (i.e. main mineralogy and particles size) and of the operating conditions (i.e. temperature, CO_2 pressure and liquid to solid ratio) on the energy and materials requirements of the investigated carbonation routes are analysed (see Paragraph 5.5 and 5.6). Finally, the results obtained in this study for a type of industrial residues are compared to those obtained in previous works for the same material and operating conditions, with the aim of clarifying the reasons behind the difference in the estimates of the energy requirements reported in the literature (see Paragraph 5.7).

5.2 State of the art

So far, only a few studies have attempted to evaluate the energy penalties associated to direct carbonation of minerals and alkaline industrial residues (O’Connor et al., 2005, Huijgen et al., 2006a, Kelly et al., 2011 and Kirchofer et al., 2012).

The Albany Research Centre (ARC) presented a preliminary study aimed at developing an ex-situ aqueous process to convert magnesium silicate-rich ultramafic rocks and minerals, such as olivine, wollastonite and serpentine, to magnesium carbonates by using gaseous CO_2 in an aqueous solution (O’Connor et al., 2005). In this study seven kinds of ultramafic minerals were analysed considering various pre-treatment options and operating conditions for the carbonation reaction and based on the results of lab-scale tests, the feasibility of the process was investigated. At the optimal operating conditions using olivine (L/S = 2.33 kg/kg, t=120 min, T=185 °C, p_{CO2}=150 bar and d<37 µm) the authors determined an energy requirement of 352 MW for the storage of 100% of the CO_2 emissions from a 1.3 GW coal-fired electric generation plant characterized by a heat release of around 10 GJ/tCO_2 emitted. The energy demand of this process using olivine, expressed in terms of CO_2 emissions, was estimated to be around 28% of the total amount of carbon dioxide sequestered, that corresponds to an energy requirement of 2.66 GJ/t CO_2 (O’Connor et al., 2005).

Huijgen and co-workers evaluated the energetic performance of CO_2 sequestration by aqueous carbonation of Ca-silicates ores and industrial residues (Huijgen et al., 2006a). Specifically they considered data obtained from carbonation experiments carried out at lab-scale using both a wollastonite and steel slag feedstock and on this basis they assumed a mineral carbonation process layout, thus determining the CO_2 sequestration efficiency at various operating conditions. The minimum energy penalty in terms of CO_2 emissions determined for wollastonite and steel slag was 16% and 17% respectively (at L/S=5 kg/kg, t= 15 min, T= 473 K, p_{CO2}=2 MPa, particle size lower than 38 µm) making reference to a power plant characterized by a heat release of 18 GJ/tCO_2 emitted. For L/S = 2 kg/kg higher energy penalties resulted for wollastonite and in particular for steel slag (i.e. 25% and 31% respectively). The grinding of the feedstock and the compression of the carbon dioxide were identified as the main energy-consuming process steps. In addition, a sensitivity analysis has shown that further grinding (particularly for wollastonite) or reducing the CO_2 partial pressure (in the case of steel slag) can potentially improve the process efficiency (Huijgen et al., 2006a).

Kelly et al. performed a preliminary energy balance for three CO_2 mineralization pathways at industrial scale, i.e. industrial caustics, naturally occurring minerals and industrial wastes (Kelly et al., 2011). The basis for this evaluation is a theoretical 1 GW coal-fired power plant emitting 8×10^6 t CO_2/y, (i.e. a heat release of around 10 GJ/tCO_2 emitted) which is captured by one of the considered mineral carbonation pathways. The estimation of the energy penalties for the carbonation of olivine and wollastonite was performed on the basis of previous works (O'Connor et al., 2005, Huijgen et al., 2006a) taking also into account the requirements for mining and CO_2 separation. The resulting energy penalties ranged between 55-69% for olivine and were over 100% for wollastonite (Kelly et al., 2011). Regarding the industrial residues Kelly et al. concluded that the energy penalty associated with CO_2 mineralization of iron slag proposed by Huijgen et al., (2006a) is greater than 100%, making this process unlikely to be feasible. However the CO_2 mineralization process with fly ash described by Reddy et al. (2011), carried out in a fluidized bed contacting coal fly ash with flue gas for 1.5-2 h at 60°C, was indicated to present a much lower energy penalty (9 to 22%). The latter result may be mainly related to the avoidance of CO_2 capture and compression and mechanical pre-treatment of the fly ash.

Recently Kirchofer et al. (2012) estimated the energy and material requirements of different aqueous carbonation processes using both natural silicate minerals (i.e. olivine and serpentine) and industrial by products, such as cement kiln dust (Huntzinger et al., 2009), coal fly ash (Back et al., 2008) and steel making slag (Huijgen et al., 2006a), in order to compare their environmental performance by Life Cycle Analysis (LCA). The minimum energy penalty expressed in terms of percent CO_2 emitted per CO_2 sequestered, considering natural gas as energy source, was obtained for cement kiln dust at ambient temperature and pressure conditions, resulting equal to 14%, while the results obtained for the other considered materials were 25% for olivine, 75% for serpentine, 34% for steel slag and 45% for fly ash. Furthermore, within the range of operating conditions considered, heating provided the most relevant contribution, followed by mixing and grinding. It should be noted that in this study the energy requirements for CO_2 capture were not considered while those related to mining and transportation of reactants and products were accounted for. Regarding the carbonation of minerals, in this study the energy penalties were estimated on the basis of the experimental results obtained in dissolution tests, assuming that all the dissolved cations react with CO_2 in the precipitation stage. This may explain the observed differences in the considered operating conditions and resulting energy requirement compared to the previously mentioned studies. As for the carbonation of residues, it is worth mentioning that the same process scheme was applied for all of the tested materials regardless of the applied L/S ratio.

As can be noted, the energy penalties evaluated in these works differ considerably from one study to the other, even considering the different power plant types used as reference, also when the evaluation was based on the same experimental data, probably as a consequence of the differences in the assumptions made and in the selected process layout. Besides, most of the studies available in literature made reference to the slurry phase carbonation route, whereas the wet route was not considered.

5.3 Process layout

Two different carbonation process routes were taken into account in this study, i.e. the slurry phase and the wet route; the corresponding process layouts are reported in Figure 5.1 and Figure 5.2 respectively.

In the slurry phase route (see Figure 5.1), the alkaline materials, after being ground to a specific particle size (unit A), are mixed with water at a given liquid-to-solid ratio (unit B); the resulting slurry is pumped (unit C) to the heat exchanger (unit D) where it is heated to 30 K below the reactor temperature, and then is fed to the carbonation reactor (unit F) after flowing through a heater (unit E) required to achieve the desired reaction temperature. The CO_2 is pressurized in a multiple stage compressor (unit G) to reach the desired pressure and fed to the reactor in which the carbonation reactions take place. The heat of the slurry leaving the carbonation reactor is recovered in unit D; after cooling, the slurry is separated (unit H), producing a solid product and a liquid stream that could be in principle recycled to unit B, although this option was not considered in this work. It is worth noting that the process layout considered for the slurry phase route is similar to the one proposed by O’Connor et al. (2005) and Huijgen et al. (2006a).

The process layout considered for the wet route (see Figure 5.2) is comprised of a lower number of unit operations and the energy consumption is mainly associated to CO_2 compression (unit G), size reduction of the residues (unit A) and the operation of the carbonation reactor (unit K), envisioned for this application as a rotary drum.

Furthermore in order to evaluate the energy requirements of wet carbonation of industrial residues using a syngas with 40% CO_2 instead of pure carbon dioxide, in some evaluations the capture of CO_2 was also taken into account in this process layout.

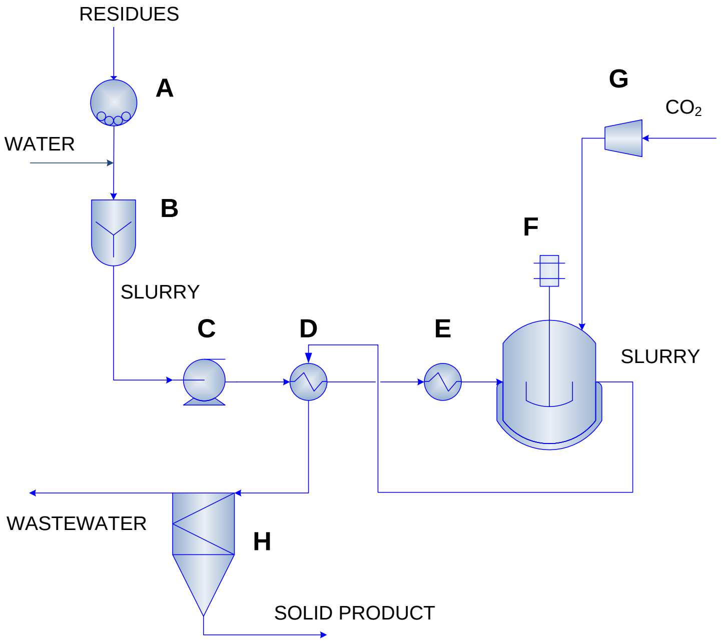

Figure 5.1: Carbonation process layout considered for the slurry phase route.

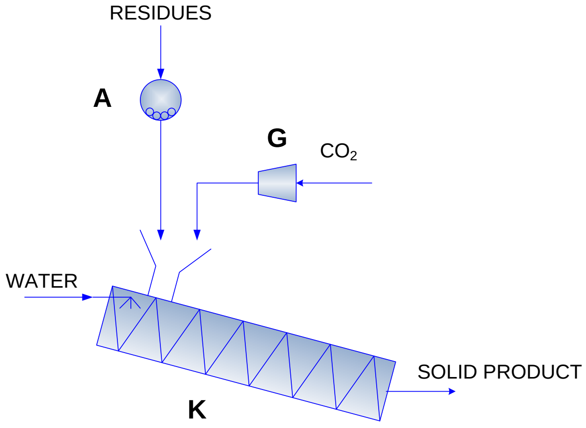

Figure 5.2: Carbonation process layout considered for the wet route.

5.4 Mass and energy balance

The material balance for the direct carbonation process were performed making reference to the two process layouts described above. The total energy requirement of the process was estimated adding the specific energy requirements associated to each unit considered in the process layout and taking into account the conversion efficiency of electrical energy into mechanical energy for each unit and considering a 35% efficiency of conversion of thermal energy into electrical energy. The energy requirements were expressed per ton of CO_2 sequestered (MJ/tCO_2).

5.4.1 Carbonation of minerals and industrial residues

The energy consumption associated to the carbonation process applying the slurry phase or the wet route was evaluated considering the results of carbonation tests performed at lab scale and already published in the literature (O'Connor et al., 2005; Baciocchi et al., 2009; 2010b, 2011b, 2012b and Huijgen et al., 2005). For each carbonation test considered in this study, the type of mineral or residue and its initial particle size (d_0), the particle size of the material treated in the carbonation reactor (d_1), the reaction temperature, the CO_2 pressure, the liquid to solid (L/S) ratio and the experiment duration are taken into account. The operating conditions considered for tests carried out on minerals are reported in Table 5.1. As can be noted, the carbonation experiments considered for minerals were performed at a temperature of 373-473 K, CO_2 pressure of 0.5-15 MPa and a liquid to solid ratio of 2.3-10 l/kg.

The minerals considered in the present study for evaluating the energy requirements of the carbonation process are the wollastonite sample tested by Huijgen et al. (2005) (called WOLL2) and three minerals tested by O'Connor et al., 2005 i.e. the olivine collected from the Twin Sisters deposit in NW Washington (OLIV), the serpentine resource in the State Line district along the Maryland-Pennsylvania border (SERP) and the wollastonite collected from Willsboro NY (WOLL1). The initial chemical composition considered for each mineral is reported in Table 5.2.

Table 5.1: Slurry Phase Carbonation operating conditions for minerals ([1] O'Connor et al., 2005, [2] Huijgen et al., 2005, M=mechanical pre-treatment, H=thermal pre-treatment).

ID	**Mineral**	**Pre Treatment**	**d_1**	**d_0**	**T**	**P_{CO2}**	**L/S**	**Time**	**R_{CO2}**	**R_x**	**R_{eff}**	**Ref**
	--		mm	mm	K	Mpa	l/kg	h	t_{RES}/t_{CO2}	--	t_{RES}/t_{CO2}	
M1	OLIV1	--	20	0.037	458	15	2.3	2	1.80	0.65	2.77	[1]
M2	OLIV1	--	20	0.075	458	15	5.7	1	1.80	0.16	11.25	[1]
M3	OLIV1	--	20	0.038	458	15	5.7	1	1.80	0.61	2.95	[1]
M4	OLIV1	M	20	0.037	458	15	5.7	1	1.80	0.81	2.22	[1]
M5	SERP1	H	20	0.038	428	15	5.7	1	2.10	0.92	2.28	[1]
M6	SERP1	H	20	0.037	428	15	5.7	1	2.10	0.82	2.56	[1]
M7	WOLL1	M	20	0.037	473	4	5.7	1	2.80	0.82	3.41	[1]
M8	WOLL1	--	20	0.038	458	4	5.7	1	2.80	0.43	6.51	[1]
M9	WOLL2	--	20	0.038	373	2	5.0	0.25	3.13	0.35	9.00	[2]
M10	WOLL2	--	20	0.038	423	2	5.0	0.25	3.13	0.64	4.88	[2]
M11	WOLL2	--	20	0.038	473	2	5.0	0.25	3.13	0.73	4.26	[2]
M12	WOLL2	--	20	0.106	423	2	3.0	0.25	3.13	0.35	8.90	[2]
M13	WOLL2	--	20	0.106	423	2	5.0	0.25	3.13	0.36	8.62	[2]
M14	WOLL2	--	20	0.106	423	2	10.0	0.25	3.13	0.37	8.43	[2]
M15	WOLL2	--	20	0.500	473	2	5.0	0.25	3.13	0.24	13.29	[2]
M16	WOLL2	--	20	0.106	373	0.5	5.0	0.25	3.13	0.16	19.00	[2]
M17	WOLL2	--	20	0.106	373	1	5.0	0.25	3.13	0.24	13.29	[2]
M18	WOLL2	--	20	0.106	373	2	5.0	0.25	3.13	0.24	13.29	[2]
M19	WOLL2	--	20	0.106	373	4	5.0	0.25	3.13	0.27	11.50	[2]
M20	WOLL2	--	20	0.106	473	0.5	5.0	0.25	3.13	0.15	21.22	[2]
M21	WOLL2	--	20	0.106	473	1	5.0	0.25	3.13	0.33	9.53	[2]
M22	WOLL2	--	20	0.106	473	2	5.0	0.25	3.13	0.42	7.40	[2]
M23	WOLL2	--	20	0.106	473	4	5.0	0.25	3.13	0.47	6.69	[2]

Table 5.2: Initial chemical composition of the considered minerals.

	OLIV1	SERP1	WOLL 1	WOLL 2
Mg_2SiO_4	88.7%	---	---	---
Fe_2SiO_4	11.3%	---	---	---
$CaSiO_3$	---	---	100%	84.3%
SiO_2	---	---	---	13.9%
$Mg_3Si_2O_5(OH)_4$	---	95.4%	---	---
Fe_2O_3	---	4.5%	---	---
$CaCO_3$	---	---	---	1.8%

Table 5.3 and Table 5.4, instead, report the operating conditions taken into account for the slurry phase and the wet route tests carried out on industrial residues. As can be noted for the slurry phase route experiments carried out at T=323-473 K, p_{CO2}=0.1-2 MPa and L/S=2-10 l/kg were considered while for the wet route, the operating conditions considered were T=303-323 K, p_{CO2}=0.1-1 MPa and L/S=0.02-0.4 l/kg. Furthermore Table 5.5 reports the operating conditions of the wet carbonation experiments carried out with industrial residues using a gas mixture, that simulate the typical composition of a syngas, instead of pure CO_2 (already discussed in Chapter 3) used for assessing the energy requirements of the process.

Regarding alkaline industrial residues, nine different materials were considered in the present study, i.e. two types of Air Pollution Control residues (APC) collected from the baghouse section of a hospital waste incineration plant (Baciocchi et al., 2009) and seven types of steel making slags.

Table 5.3: Slurry Phase Carbonation operating conditions for industrial residues ([1] Baciocchi et al., 2011b, [2] Baciocchi et al., 2012b and [3] Huijgen et al., 2005).

ID	**Residue**	**d_0**	**d_1**	**T**	**P_{CO2}**	**L/S**	**Time**	**R_{CO2}**	**R_x**	**R_{EFF}**	**Ref**
	--	mm	mm	K	Mpa	l/kg	h	t_{RES}/t_{CO2}	--	t_{RES}/t_{CO2}	
S1	EAF	1.19	0.15	373	1.0	10	1	2.314	0.116	20.000	[1]
S2	EAF	1.19	0.15	323	1.0	10	1	2.314	0.162	14.286	[1]
S3	EAF	1.19	0.15	423	1.0	10	1	2.314	0.093	25.000	[1]
S4	EAF	1.19	0.15	323	1.9	10	1	2.314	0.093	25.000	[1]
S5	EAF	1.19	0.15	373	1.0	5	0.5	2.314	0.486	4.762	[2]
S6	EAF	1.19	0.15	373	1.0	5	1	2.314	0.440	5.263	[2]
S7	BOF1	20	0.052	373	0.1	10	0.5	4.645	0.533	8.709	[3]
S8	BOF1	20	0.052	373	0.9	10	0.5	4.645	0.580	8.009	[3]
S9	BOF1	20	0.052	373	2.0	5	0.5	4.645	0.633	7.333	[3]
S10	BOF1	20	0.052	373	2.0	2	0.5	4.645	0.664	7.000	[3]
S11	BOF1	20	0.052	373	1.9	10	0.5	4.645	0.598	7.772	[3]
S12	BOF1	20	0.052	373	2.0	10	0.5	4.645	0.568	8.174	[3]
S13	BOF1	20	0.052	323	1.9	10	0.5	4.645	0.545	8.524	[3]
S14	BOF1	20	0.052	423	1.9	10	0.5	4.645	0.756	6.143	[3]
S15	BOF1	20	0.023	473	2.0	5	0.25	4.645	0.664	7.000	[3]
S16	BOF2	1.19	0.15	373	1.0	5	1	2.764	0.663	4.167	[2]
S17	BOF2	1.19	0.15	373	1.0	5	0.5	2.764	0.497	5.556	[2]
S18	BOF3	1.19	0.15	373	1.0	5	1	2.933	0.733	4.000	[2]
S19	BOF3	1.19	0.15	373	1.0	5	0.5	2.933	0.748	3.922	[2]

Table 5.4: Wet Carbonation operating conditions for industrial residues ([1] Baciocchi et al., 2010b, [2] Baciocchi et al., 2012b and [3] Baciocchi et al., 2009).

ID	Residue	d_0	d_1	T	P_{CO2}	L/S	Time	R_{CO2}	R_x	R_{EFF}	Ref
	--	mm	mm	K	Mpa	l/kg	h	t_{RES}/t_{CO2}	--	t_{RES}/t_{CO2}	
W1	AOD	0.15	0.15	323	0.1	0.4	1	1.992	0.421	4.735	[1]
W2	AOD	0.15	0.15	323	0.3	0.4	1	1.992	0.401	4.965	[1]
W3	AOD	0.15	0.15	323	1	0.4	1	1.992	0.427	4.662	[1]
W4	EAF	1.19	0.15	323	0.1	0.4	1	2.314	0.209	11.099	[1]
W5	EAF	1.19	0.15	323	0.3	0.4	1	2.314	0.345	6.716	[1]
W6	EAF	1.19	0.15	323	1	0.4	1	2.314	0.334	6.920	[1]
W7	EAF	1.19	0.15	323	1	0.3	0.5	2.314	0.289	8.000	[1]
W8	BOF2	1.19	0.15	323	1	0.3	1	2.764	0.332	8.333	[2]
W9	BOF2	1.19	0.15	323	1	0.3	1	2.764	0.263	10.526	[2]
W10	BOF3	1.19	0.15	323	1	0.3	1	2.933	0.293	10.000	[2]
W11	BOF3	1.19	0.15	323	1	0.3	0.5	2.933	0.249	11.765	[2]
W12	APC1	0.075	0.075	303	0.3	0.02	1	3.218	0.257	12.500	[3]
W13	APC1	0.075	0.075	303	0.3	0.1	1	3.218	0.682	4.717	[3]
W14	APC1	0.075	0.075	303	0.3	0.2	1	3.218	0.692	4.651	[3]
W15	APC1	0.075	0.075	303	0.3	0.4	1	3.218	0.724	4.444	[3]
W16	APC1	0.075	0.075	303	0.3	0.6	1	3.218	0.673	4.785	[3]
W17	APC1	0.075	0.075	313	0.3	0.02	1	3.218	0.676	4.762	[3]
W18	APC1	0.075	0.075	323	0.3	0.02	1	3.218	0.772	4.167	[3]
W19	APC1	0.075	0.075	303	1	0.02	1	3.218	0.225	14.286	[3]
W20	APC1	0.075	0.075	303	0.1	0.02	1	3.218	0.241	13.333	[3]

Specifically, the types of steel making slag considered were: the basic oxygen furnace steel slags (BOF1) tested in carbonation experiments by Huijgen et al.(2005), four kinds of basic oxygen furnace slags (BOF2, BOF3, BOF4 and BOF5) collected from an integrated steel manufacturing plant site in Italy (Baciocchi et al., 2012b), electric arc furnace slags (EAF) and ladle slags produced at the outlet of argon oxygen decarburization and desulfurization units (AOD) in a stainless steel making plant (Baciocchi et al., 2010b, 2011b). The main chemical composition of AOD, EAF, BOF2, BOF3, BOF4, BOF5, APC1 and APC2 (see Table 5.6) was estimated on the basis of the results obtained by elemental composition measurements, XRD analysis, acid neutralization capacity measurements and calcimetry analysis reported in Baciocchi et al.(2009, 2010b, 2011b, 2012b), whereas the composition reported by Huijgen et al.(2006a) was considered for BOF1.

Table 5.5: Wet Carbonation operating conditions for industrial residues using a gas mixture with 40% CO_2.

ID	**Residue**	**d_1**	**d_0**	**T**	**P_{CO2}**	**L/S**	**Time**	**R_{CO2}**	**R_x**	**R_{eff}**	**Ref**
	--	mm	mm	K	Mpa	l/kg	h	$t_{RESIDUE}/ton_{CO2}$	--	$t_{RESIDUE}/ton_{CO2}$	
W21	AOD	0.15	0.15	323	0.28	0.4	1	1.992	0.431	4.621	--
W22	AOD	0.15	0.15	323	0.04	0.4	1	1.992	0.127	15.649	--
W23	AOD	0.15	0.15	323	0.16	0.4	1	1.992	0.362	5.504	--
W24	AOD	0.15	0.15	293	0.28	0.4	1	1.992	0.349	5.701	--
W25	AOD	0.15	0.15	303	0.28	0.4	1	1.992	0.428	4.658	--
W26	BOF4	1.19	0.125	323.15	0.04	0.3	1	2.253	0.181	12.422	--
W27	BOF4	1.19	0.125	323.15	0.2	0.3	1	2.253	0.233	9.671	--
W28	BOF4	1.19	0.125	323.15	0.4	0.3	1	2.253	0.227	9.940	--
W29	BOF5	1.19	0.125	323.15	0.28	0.3	1	2.296	0.139	16.556	--
W30	BOF5	1.19	0.125	323.15	0.04	0.3	1	2.296	0.099	23.202	--
W31	BOF5	1.19	0.125	323.15	0.16	0.3	1	2.296	0.110	20.833	--
W32	BOF5	1.19	0.125	293.15	0.28	0.3	1	2.296	0.080	28.818	--
W33	BOF5	1.19	0.125	303.15	0.28	0.3	1	2.296	0.106	21.645	--
W34	APC2	0.075	0.075	323.15	0.28	0.2	1	3.747	0.693	5.405	--
W35	APC2	0.075	0.075	323.15	0.04	0.2	1	3.747	0.358	10.460	--
W36	APC2	0.075	0.075	323.15	0.16	0.2	1	3.747	0.724	5.179	--
W37	APC2	0.075	0.075	293.15	0.28	0.2	1	3.747	0.564	6.640	--
W38	APC2	0.075	0.075	303.15	0.28	0.2	1	3.747	0.657	5.701	--

Table 5.6: Initial chemical composition of the considered residues.

	AOD	EAF	APC1	APC2	BOF1	BOF2	BOF3	BOF4	BOF5
Ca_2SiO_4	92.6%	75.5%	---	---	---	19.8%	17.2%	30.9%	12.1%
$CaSiO_3$	---	---	---	---	56.8%	---	---	---	---
Ca_3SiO_5	---	---	---	---	---	26.3%	---	---	32.1
SiO_2	---	2.9%	---	---	---	---	---	---	---
$Ca(OH)_2$	---	---	40.0%	24.4%	---	6.5%	28.0%	26.6%	17.1%
CaOHCl	---	---	30.6%	51.0%	---	---	---	---	---
$Mg(OH)_2$	---	---	---	---	---	---	11.5%	17.0%	---
MgO	2.7%	4.20%	---	---	---	6.4%	---	---	7.9%
$CaCO_3$	4.6%	3.60%	19.1%	10.8%	7.7%	0.9%	8.4%	5.9%	4.0%
Fe_3O_4	0.1%	4.60%	---	---	---	---	34.9%	19.6%	22.1
CaF_2	0.05%	0.03%	---	---	---	---	---	---	---
FeO	---	---	---	---	35.5%	37.6%	---	---	---
NaCl	---	---	10.3%	13.8%	---	---	---	---	---
Cr_2O_3	0.06%	5.1%	---	---	---	---	---	---	---
Al_2O_3	---	4.0%	---	---	---	2.4%	---	---	---
MnO	---	---	---	---	---	---	---	---	4.6%

In order to estimate the chemical composition and the physical properties of the final product obtained after carbonation, it was assumed that in the carbonation reactor one or more of the reactions reported in Eq. (5.1)-(5.10) take place, depending on the composition of the treated materials.

$$Ca_2SiO_4 + 2\ CO_2 \rightarrow 2\ CaCO_3 + SiO_2 \tag{5.1}$$

$$CaSiO_3 + CO_2 \rightarrow CaCO_3 + SiO_2 \tag{5.2}$$

$$Ca_3SiO_5 + 3\ CO_2 \rightarrow 3\ CaCO_3 + SiO_2 \tag{5.3}$$

$$Ca(OH)_2 + CO_2 \rightarrow CaCO_3 + H_2O \tag{5.4}$$

$$2\ CaOHCl + CO_2 \rightarrow CaCO_3 + CaCl_2 + H_2O \tag{5.5}$$

$$Mg(OH)_2 + 2\ CO_2 + CaO \rightarrow MgCa(CO_3)_2 + H_2O \tag{5.6}$$

$$MgO + 2\ CO_2 + CaO \rightarrow MgCa(CO_3)_2 \tag{5.7}$$

$$Mg_2SiO_4 + 2CO_2 \rightarrow 2MgCO_3 + SiO_2 \tag{5.8}$$

$$Fe_2SiO_4 + 2CO_2 \rightarrow 2FeCO_3 + SiO_2 \tag{5.9}$$

$$Mg_3Si_2O_5(OH)_4 + 3CO_2 \rightarrow 3MgCO_3 + 2SiO_2 + 2H_2O \tag{5.10}$$

In order to estimate the energy requirement associated to the size reduction unit (S.R.U.) the values of the work index (W_i) to be used for each material were taken from Perry and Green (1987). In particular for olivine and serpentine the W_i value was set as 14 kWh/t, calculated as a mean value between the working indexes of sandstone and silica sand while for wollastonite, according to Huijgen et al.(2006a), W_i was estimated starting from the value reported for limestone and silica sand (i.e. 14.04 kWh/t). For the considered residues instead W_i was assumed to be equal to 12.16 kWh/t for the seven types of steel slags while for the APC residues the work index value reported for cement raw material was used (i.e. 10.57 kWh/t).

For some experiments performed by O’Connor et al.(2005), a mechanical (case M4 and M7) or thermal pre-treatment (case M5 and M6) of the mineral was considered. The energy requirements associated to these pre-treatment were estimated in accordance with the evaluation performed by O’Connor et al.(2005) on the energy consumption associated to each pre-treatment methodology. Namely, for the thermal treatment an energy consumption of 326 kWh/t for heating the feedstock to 630 °C was assumed while for the mechanical treatment the duty associated to a ultrafine grinding of the minerals performed using a scalable stirred-media detritor (SMD) mill estimated as described in the next paragraph for the tertiary grinding was considered.

Based on the mass flow rate of CO_2 to store (i.e. m_{CO2}), the amount of alkaline material to feed in the process at each carbonation condition was determined. The mass ratio of minerals or residues necessary to convert a unit mass of CO_2 into the solid carbonate phase (R_{CO2}) was estimated according to O’Connor et al.(2005). Furthermore, the reactivity of the material at the operating conditions of the carbonation process was expressed by R_X that indicates the extent of conversion of the calcium or magnesium (hydr)oxides or silicate phases to the corresponding carbonates (O’Connor et al., 2005). Based on R_{CO2} and R_X, the effective amount of alkaline materials to be used for each set of operating conditions (R_{EFF}) was estimated. The values of R_{CO2}, R_X and R_{EFF} estimated for each carbonation condition applied to minerals are reported in Table 5.1 while the values estimated for the carbonation of residues are presented in Table 5.3, Table 5.4 and Table 5.5. As it can be noticed, within the tested materials the Twin Sister olivine (OLIV) for the minerals and the AOD slags and the EAF slags for the residues presented the lowest R_{CO2} values (i.e. around 1.8 t minerals/t CO_2 and around 2 and 2.31 t residues/t CO_2 respectively) indicating the higher reactivity of these materials within those considered in the present study. However, the effective amount of alkaline material to be used in each case per unit of stored CO_2 (R_{EFF}) proved to change significantly depending on the specific operating conditions applied.

5.4.2 Mass and energy balance

Size reduction

Following the approach of O’Connor et al. (2005) and Hangx et al. (2009), the different crushing and grinding steps needed to reach the desired final particle size were considered. Firstly, in order to achieve a particle size of 50 mm, a primary crushing step with an associated energy requirement of around 2.0 kWh/t of material based on data from the U.S. Bureau of Mining (O’Connor et al., 2005) was assumed. After this step a second grinding step was considered and the associated energy requirement was determined based on the amount of minerals or industrial residues to be treated (R_{EFF}) and on the grinding work estimated applying Bond’s equation reported in Eq. (5.11) (Perry and Green, 1987), in which d_0 is the original particle size of the material, d_1 is the imaginary sieve size through which 80% wt. of the feedstock pass and W_i is the standard Bond's work index of the alkaline material.

$$W = 10\ W_i \left(\frac{1}{\sqrt{d_1}} - \frac{1}{\sqrt{d_0}} \right) \tag{5.11}$$

In the case of a final grain size (d_1) lower than 70 µm, an empirical multiplying factor was applied to Bond's equation as suggested by Perry and Green (1987) leading to the relationship reported in Eq. (5.12).

$$W = 10\ W_i \left(\frac{1}{\sqrt{d_1}} - \frac{1}{\sqrt{d_0}} \right) \cdot \frac{10.3 + d_1}{1.145 \cdot d_1} \tag{5.12}$$

Finally, in order to achieve a final particle size lower than 37 µm, a tertiary grinding step was included and an associated energy requirement of 150 kWh/t of material was taken into account according to the direct measurements carried out on minerals by O'Connor et al. (2005). Based on the values of d_0 and d_1 of the considered materials, in this study the energy requirements associated to the size reduction unit (S.R.U.) was estimated considering all the three stages in case of minerals while for the residues this term was mainly estimated considering the formulation of Bond's equation reported in Eq. (5.11).

Liquid-solid mixing

The energy required for mixing the minerals or residues with water was estimated applying Eq. (5.13), where V is the total volume of water and material to be mixed, µ the dynamic viscosity and G the average velocity gradient.

$$E_{MIX} = \frac{V \cdot \mu \cdot G^2}{m_{CO2}} \tag{5.13}$$

In particular, by setting the dimensions of one mixing unit and considering the total volume to be mixed in each carbonation test, the required number of units was estimated together with the overall energy requirement associated to this unit operation. The value of the average velocity gradient for the mixer (unit B) and the carbonation reactor (unit F) was chosen considering a typical rapid mixing operation (i.e. $G=500\ s^{-1}$) while for the liquid-solid separation step applied downstream of the carbonation reactor (unit G) a value typical for flocculation processes was selected (i.e. G=60 s^{-1}).

Slurry Pumping

The energy required to pump the slurry was estimated multiplying the slurry flow rate for the total dynamic head applied in each carbonation condition considering the final pressure required in the carbonation reactor and the friction head of the pipeline. Specifically, as already done by Huijgen et al. (2006a), the total pressure to be reached by the slurry pump was estimated considering the partial CO_2 pressure and the water vapour pressure reported in the literature for the specific temperature applied in each carbonation condition.

Heating

In the slurry phase route the heat required for reaching the reaction temperature was assumed to be provided in two steps by means of a heat exchanger (unit D) and a heater (unit E). Specifically, in the heat exchanger it was assumed to heat the inlet slurry from 293 K to 30 K below the final carbonation temperature and to cool the outlet of the carbonation reactor down to 313 K. The supplementary heat required to reach the final carbonation temperature was assumed to be provided in unit E.

The overall energy requirement associated to the heating of the slurry was estimated considering the energy required to achieve the final carbonation temperature, the energy recovered in the heat exchanger by cooling the outlet stream from the carbonation reactor, the heat of reaction of the carbonation process and the heat loss from the carbonation reactor. Namely, the energy required for heating the slurry to the desired temperature was calculated by Eq. (5.14), where m and C_P are the mass flow rate and the specific heat capacity of the slurry, respectively, and ΔT is the difference between the inlet and the outlet temperature.

$$E_{HEAT} = \frac{m \cdot C_P \cdot \Delta T}{m_{CO2}} \tag{5.14}$$

The same equation was also used to calculate the energy recovered by cooling the outlet stream from the carbonation reactor in the heat exchanger. The specific heat capacity of the slurry to be heated or cooled was estimated considering the chemical composition of the solid product before and after the carbonation reaction (estimated as described in section

5.4.1), the amount of water fed and the dependence of the specific heat capacity on temperature, according to the equations reported in Table 5.7. The heat released by the carbonation reactions taken into account in our process (Eq. (5.1)-(5.10)) was estimated on the basis of the enthalpy of reaction calculated at the specific operating conditions applied and considering the Peng-Robinson's state equation for carbon dioxide. The heat losses from the carbonation reactor walls to ambient air were estimated assuming the stainless steel reactor to be insulated with a glass wool layer and considering natural convection on the exterior ambient-air side and conduction on the inner side.

Table 5.7: Heat capacity equations (J/mol K) used to estimate the C_P of the residues (for the references [a] Robie et al., 1978, [b] Allal et al., 1997, [c] Schmetterer and Masset, 2012 and [d] Robie et al., 1984).

Phase	Heat capacity equation	Ref
Ca_2SiO_4	$c_p^0 = 2.4871 \cdot 10^2 - 8.3145 \cdot 10^{-4}\ T - 2.0521 \cdot 10^3\ T^{-0.5} - 9.0774 \cdot 10^4\ T^{-2}$	[a]
MgO	$c_p^0 = 65.211 - 1.2699 \cdot 10^{-3} T - 387.24\ T^{-0.5} - 4.6185 \cdot 10^5\ T^{-2}$	[a]
$CaCO_3$	$c_p^0 = 99.715 + 2.6920 \cdot 10^{-2} T - 2.1576 \cdot 10^6\ T^{-2}$	[a]
Fe_3O_4	$c_p^0 = -3.5580 \cdot 10^3 + 3.3473 \cdot 10^2 T^{0.5} - 9.3090\ T + 2.5388 \cdot 10^{-3}\ T^2 + 1.4273 \cdot 10^5\ T^{-1}$	[a]
CaF_2	$c_p^0 = -24.692 + 5.8095 \cdot 10^{-2}\ T + 1.8706 \cdot 10^3\ T^{-0.5} - 2.8774 \cdot 10^6\ T^{-2}$	[a]
SiO_2	$c_p^0 = 2.3306 - 7.7765 \cdot 10^{-2} T + 1.9237 \cdot 10^{-5}\ T^2 - 3.3753 \cdot 10^3\ T^{-0.5} + 2.6036 \cdot 10^6\ T^{-2}$	[a]
$Ca(OH)_2$	$c_p^0 = 1.8667 \cdot 10^2 - 2.1911 \cdot 10^{-2}\ T - 1.5998 \cdot 10^3\ T^{-0.5}$	[a]
$Mg(OH)_2$	$c_p^0 = 1.0222 \cdot 10^2 + 1.5107 \cdot 10^{-2}\ T - 2.6172 \cdot 10^6\ T^{-2}$	[a]
$CaSiO_3$	$c_p^0 = 1.1125 \cdot 10^2 + 1.4373 \cdot 10^{-2} T + 16.936 \cdot\ T^{-0.5} - 2.7779 \cdot 10^6\ T^{-2}$	[a]
FeO	$c_p^0 = 67.352 + 3.7580 \cdot 10^{-3} T - 3.8167 \cdot 10^2\ T^{-0.5} + 3.1570 \cdot 10^5\ T^{-2}$	[a]
NaCl	$c_p^0 = 45.151 + 1.7974 \cdot 10^{-2}\ T$	[a]
CaOHCl	$c_p^0 = 18.181 + 8.345 \cdot 10^{-3}\ T + 0.216 \cdot 10^6\ T^{-2} + 0.166 \cdot 10^{-6}\ T^2$	[b]
Ca_3SiO_5	$c_p^0 = 161.317 + 0.14234\ T - 5.9152256 \cdot 10^{-5} T^2 - 2390270\ T^{-2}$	[c]
Cr_2O_3	$c_p^0 = 1.1902 \cdot 10^2 + 9.4964 \cdot 10^{-3} T - 3.4045\ T^{-0.5} - 1.4419 \cdot 10^6\ T^{-2}$	[a]
MnO	$c_p^0 = 59.749 + 3.6 \cdot 10^{-3} T - 2.8265 \cdot 10^2\ T^{-0.5} - 3.1362 \cdot 10^4\ T^{-2}$	[a]
Al_2O_3	$c_p^0 = 1.5736 \cdot 10^2 + 7.1899 \cdot 10^{-4} T - 9.8804 \cdot 10^2\ T^{-0.5} - 1.8969 \cdot 10^6\ T^{-2}$	[a]
$CaCl_2$	$c_p^0 = 76.846 + 6.6490 \cdot 10^{-6}\ T^2 - 1.2847 \cdot 10^6\ T^{-3}$	[a]
$MgCa(CO_3)_2$	$c_p^0 = 5.4788 \cdot 10^2 - 0.16759\ T + 7.7076 \cdot 10^{-5} T^2 - 6.5479 \cdot 10^3\ T^{-0.5}$	[a]
Mg_2SiO_4	$c_p^0 = 2.2798 \cdot 10^2 + 3.4139 \cdot 10^{-3} T - 1.7446 \cdot 10^3\ T^{-0.5} - 8.9397 \cdot 10^5\ T^{-2}$	[a]
Fe_2SiO_4	$c_p^0 = 1.7276 \cdot 10^2 - 3.4055 \cdot 10^{-3} T + 2.2411 \cdot 10^{-5}\ T^2 - 3.6299 \cdot 10^6\ T^{-2}$	[a]
$Mg_3SiO_5(OH)_4$	$c_p^0 = 8.9960 \cdot 10^2 - 0.14476\ T - 1.0932 \cdot 10^4\ T^{-0.5} + 4.4999 \cdot 10^6\ T^{-2}$	[a]
$MgCO_3$	$c_p^0 = 81.119 + 5.2254 \cdot 10^{-2}\ T - 1.8320 \cdot 10^6\ T^{-2}$	[a]
Fe_2O_3	$c_p^0 = -838.61 + 86.525\ T^{0.5} - 2.3434\ T + 6.0519 \cdot 10^{-4}\ T^2 + 2.7821 \cdot 10^4\ T^{-1}$	[a]
$FeCO_3$	$c_p^0 = 257.38 - 0.04620\ T - 3081.9 T^{-0.5} + 1.523 \cdot 10^6\ T^{-2}$	[d]
H_2O	$c_p^0 = 75.19$	[a]

For the wet carbonation route, instead, the overall energy requirement associated to the heating of the reactants was estimated considering only the energy required to reach the final carbonation temperature according to Eq. (5.14). In this case, in fact, the recovery of the energy produced by the exothermic carbonation reaction was neglected since it was considered to be difficultly recoverable due to the fact that, differently from the slurry phase process, the outlet stream from the carbonation reactor is basically made up by a solid material.

<u>CO_2 Compression</u>

The energy requirement associated to CO_2 compression was estimated assuming to use a multiple stage compressor to increase the carbon dioxide pressure from 0.1 to 7.38 MPa and a boosting pump to compress CO_2 to higher pressure, as reported by McCollum and Ogden (2006). Specifically, it was assumed to use a 5 stage compressor, with the energy requirement for each stage ($E_{STAGE,i}$) estimated applying Eq. (5.15), where Z_s is the average CO_2 compressibility for each stage, R the gas constant, T_{in} the CO_2 temperature at the compressor inlet, M the molecular weight of CO_2, η_{is} the isentropic efficiency of compressor, k_s the average ratio of the specific heats of CO_2 for each individual stage and CR the compression ratio of each stage.

$$E_{STAGE,i} = \left(\frac{Z_s \cdot R \cdot T_{in}}{M \cdot \eta_{is}} \right) \cdot \left(\frac{k_s}{k_s - 1} \right) \cdot \left[\left(CR \right)^{\frac{k_s - 1}{k_s}} - 1 \right] \tag{5.15}$$

The energy requirement associated to the boosting pump, instead, was calculated according to Eq. (5.16), where P_{fin} and P_{in} are the final and initial CO_2 pressure respectively and ρ is the density of CO_2 during pumping.

$$E_{BOOST.PUMP} = \frac{\left(P_{fin} - P_{in} \right)}{\rho} \tag{5.16}$$

The values of the coefficients to be used for both the compressor and the boosting pump were chosen according to McCollum and Ogden (2006).

<u>Operation of the wet carbonation reactor</u>

In order to estimate the energy consumption associated to the rotation of the drums used as carbonation reactors in the wet route, the energy requirement of one drum was first estimated considering the resistive torque due to kinetic friction and the constant angular velocity of the drum. The total energy consumption for this unit operation was then estimated calculating the number of drums required in each condition by setting the size of the drum and the volume of alkaline material to be fed in each unit.

<u>CO_2 capture</u>

The energy consumption associated to the capture of carbon dioxide from the flue gas was estimated according to the IPCC report (2005). In particular a duty of 4000 MJ/t CO_2 was considered, i.e. 20% of the energy produced from the power plant considered in the study. In the rest of this chapter the contribution of the CO_2 capture to the total energy requirement of the process is shown only for the results reported in paragraph 5.6.4 for comparison with the results obtained using a syngas, since in the other cases this duty is constant for all the tested carbonation conditions.

5.5 Results: Carbonation of minerals

5.5.1 Slurry phase Route

Figure 5.3 reports the effect of the particle size on the energy requirements estimated for the slurry phase carbonation of Twin Sisters olivine (OLIV).

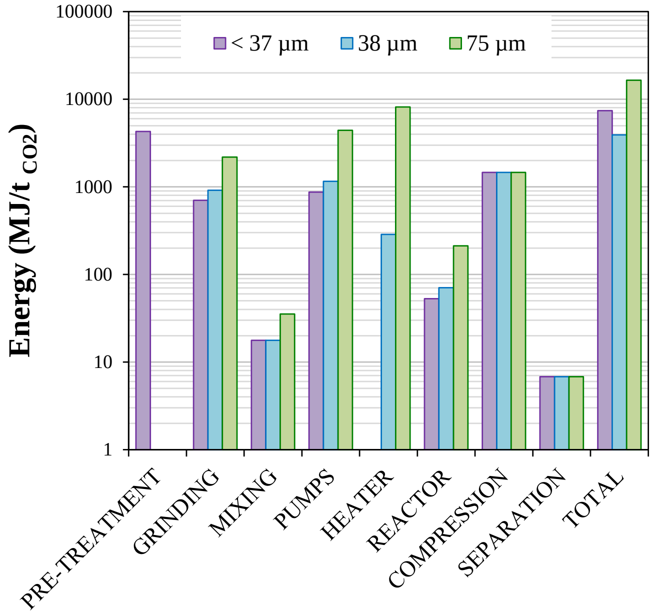

Figure 5.3: Effect of the particle size $d_1$on the energy requirement estimated for carbonation of OLIV.

As can be seen decreasing the particle size of the mineral from 75 to 38 µm the total energy requirement of the process also decrease from 16500 to 3900 MJ/t CO_2. This effect can be mainly correlated to the increase in the reactivity of the material for the lower particle size that hence entails a lower amount of material to treat in the process, i.e. 2.95 t mineral/t CO_2 instead of 11.25 t mineral/t CO_2 (see Table 5.1). However when a mechanical pre-treatment of the mineral is applied to reach a particle size lower than 37 µm, the total energy requirement of the process increases to around 7400 MJ/t CO_2 since although in this case a lower amount of mineral is required (2.22 t mineral/t CO_2) the use of a ultrafine grinding step entails an additional energy duty of around 4200 MJ/t CO_2.

In Figure 5.4 instead the effect of (a) CO_2 pressure, (b) liquid to solid ratio, (c) temperature and (d) particle size on the energy requirements estimated for the slurry phase carbonation of WOLL2 are reported.

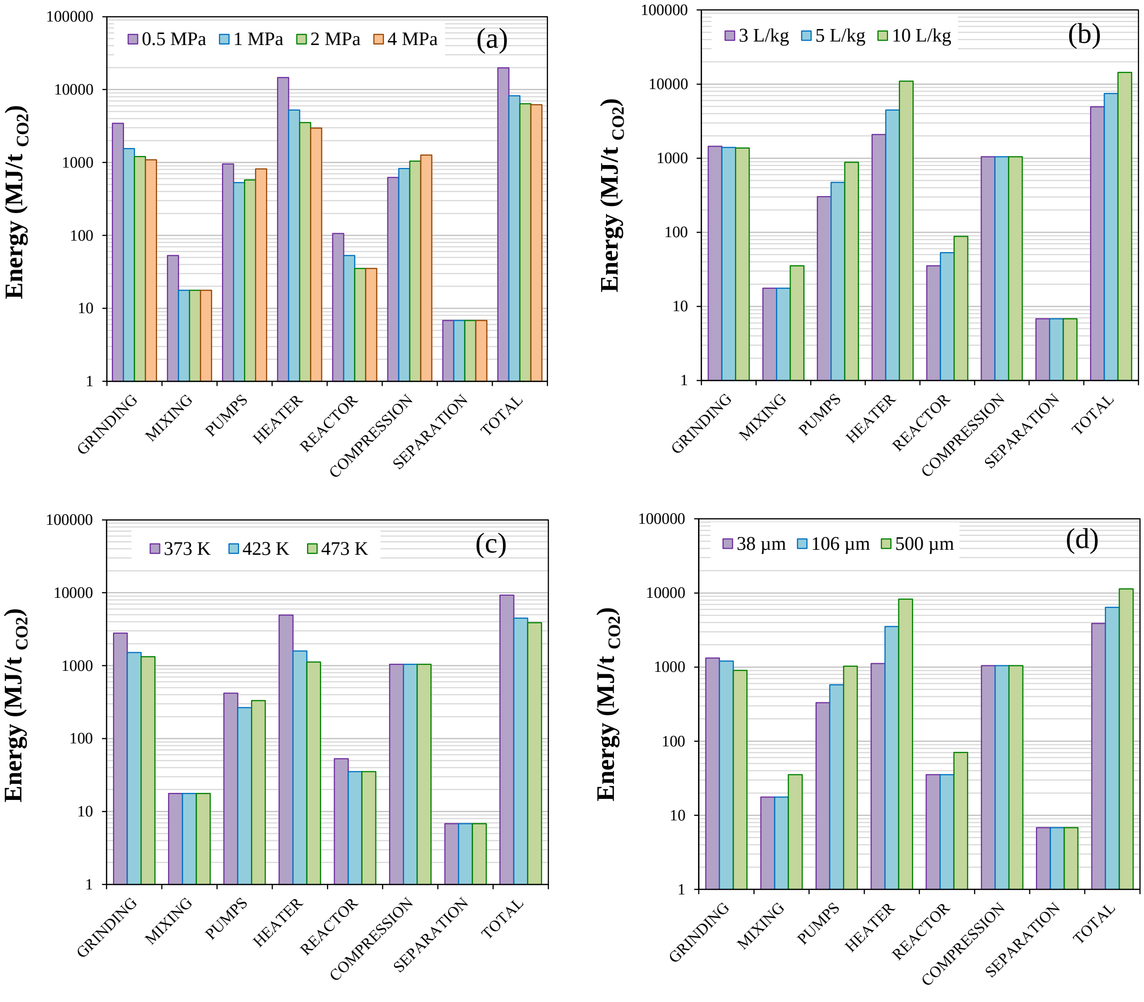

Figure 5.4: Effect of (a) temperature, (b) L/S ratio, (c) particle size and (d) CO_2 pressure on the energy requirement estimated for carbonation of WOLL2.

As can be seen from Figure 5.4 (a) an increase in the applied CO_2 pressure from 0.5 to 4 MPa proved to diminish the total energy requirement of the process due to a higher reactivity of the material that entails a lower amount of minerals to treat (i.e. 6.7 instead of 21.5 t mineral/t CO_2); although the energy associated to the pumping and compression slightly increase with higher pressures, the energy requirements associated to the other unit operations proved to be constant or lower. This trend is more evident for a pressure increase from 0.5 to 1 MPa where the total energy requirement of the process decreases from 19800 to 8200 MJ/t CO_2. Regarding the effect of the liquid to solid ratio (see Figure 5.4 (b)), an higher energy requirement of the process is expected for higher L/S values, i.e. 5000 against 14400 MJ/t CO_2 going from 3 to 10 l/kg. This trend is strictly related to the increase in the amount of water that has to be treated that entails higher duties for the heater, the pumps and the carbonation reactor while the reactivity of the minerals remains almost constant (8.4 instead of 8.9 t mineral/t CO_2). Besides, as expected, increasing the reaction temperature from 373 to 473 K (see Figure 5.4(c)) the reactivity of the mineral was improved and a lower total energy requirement of the process is obtained (around 3900 instead of 9200 MJ/t CO_2) due to the reduction in the amount of material to treat in process (4.26 instead of 9 t mineral/t CO_2). Finally, Figure 5.4(d) confirms that, as already observed for the Twin Sisters Olivine (OLIV), a reduction in the particle size of the material proved to increase the reactivity of the minerals and hence reduce the total energy requirement of the process.

5.5.2 Lowest energy requirements for each type of mineral

In Figure 5.5 the lowest energy requirements estimated for each considered mineral in a slurry phase carbonation process are reported, highlighting the contribution of the main unit operations; the term "other" includes the energy requirements associated to the mixing of the slurry, the carbonation reactor and the clarifier. The main contributions to the total energy requirements of the process are represented by minerals grinding and thermal pre-treatment, gas compression and slurry heating. The total energy requirement estimated for a slurry phase carbonation process applied to minerals ranges from around 2900 to 7900 MJ/t CO_2 with the lowest duty obtained for the Twin Sisters olivine tested by O’Connor et al. (2005). This material in fact presented a good reactivity in the tested condition and a low amount of mineral (i.e. 2.77 t mineral/t CO_2) has to be treated in the process so that the reaction enthalpy is sufficient to provide the heat necessary for reaching the desired temperature. In the carbonation case M5, although a low amount of mineral has to be processed, a total energy requirement of about 6400 MJ/t $CO_2$was estimated since to activate the serpentine a thermal pre-treatment was required, with an extra duty of around 2700 MJ/t CO_2. Furthermore from Figure 5.5 one can observe that the results obtained for the two type of wollastonite differ significantly mainly due to the fact that although the WOLL2 present a lower amount of $CaSiO_3$ compare to WOLL1 (84.3 against 100%) the reactivity of the former mineral in the tested condition proved to be significantly higher and, hence, a lower amount of minerals has to be processed in the carbonation case M11 compared to M8 (4.26 t mineral/t CO_2 instead of 6.51 t mineral/t CO_2).

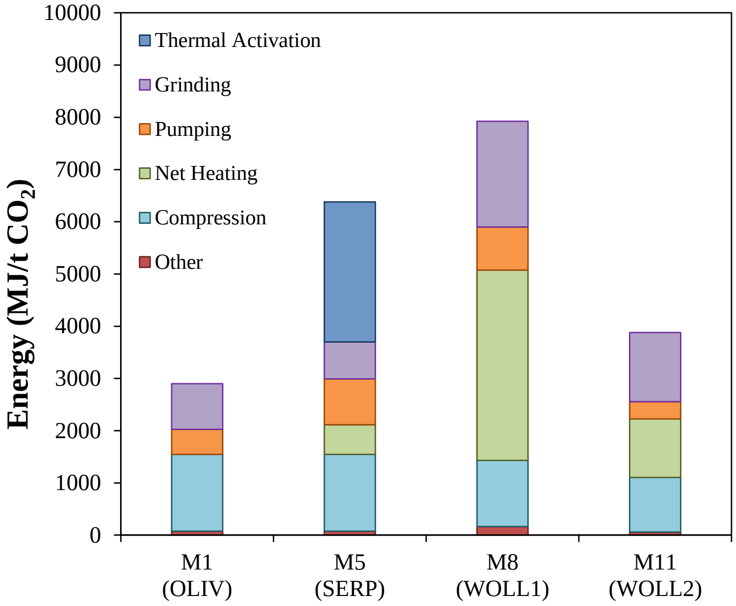

Figure 5.5: Comparison of the lowest energy requirement of a slurry phase carbonation process carried out using different minerals.

5.6 Results: Carbonation of industrial residues

5.6.1 Slurry phase Route

Figure 5.6 reports the effect of CO_2 pressure (a), liquid to solid ratio (b) and temperature (c) on the energy requirements estimated for the slurry phase carbonation of BOF1 slags. In most of the analysed conditions, heating resulted by far the most energy intensive operation, followed by size reduction. As shown in Figure 5.6 (a), a slight decrease in the total energy requirement of the process (from 13834 to 13503 MJ/t CO_2 stored) was observed, when the carbon dioxide pressure was increased from 0.1 to 1.9 MPa, notwithstanding the increased energy duty resulting for the pump and compressor units. This behaviour results from the slight decrease of the effective amount of residues required per ton of CO_2 (from 8.71 to 7.77 t residues/t of CO_2), see Table 1. As reported in Figure 5.6 (b), an increase of the liquid to solid ratio from 2 to 10 l/kg led to a significant increase of the total energy requirement of the process (from around 2750 to 14300 MJ/t CO_2 stored); this trend can be correlated to the increase of the water flow rate that has to be processed, which leads to a higher energy requirement for the heater and the pumps, despite the slight increase of the residues reactivity.

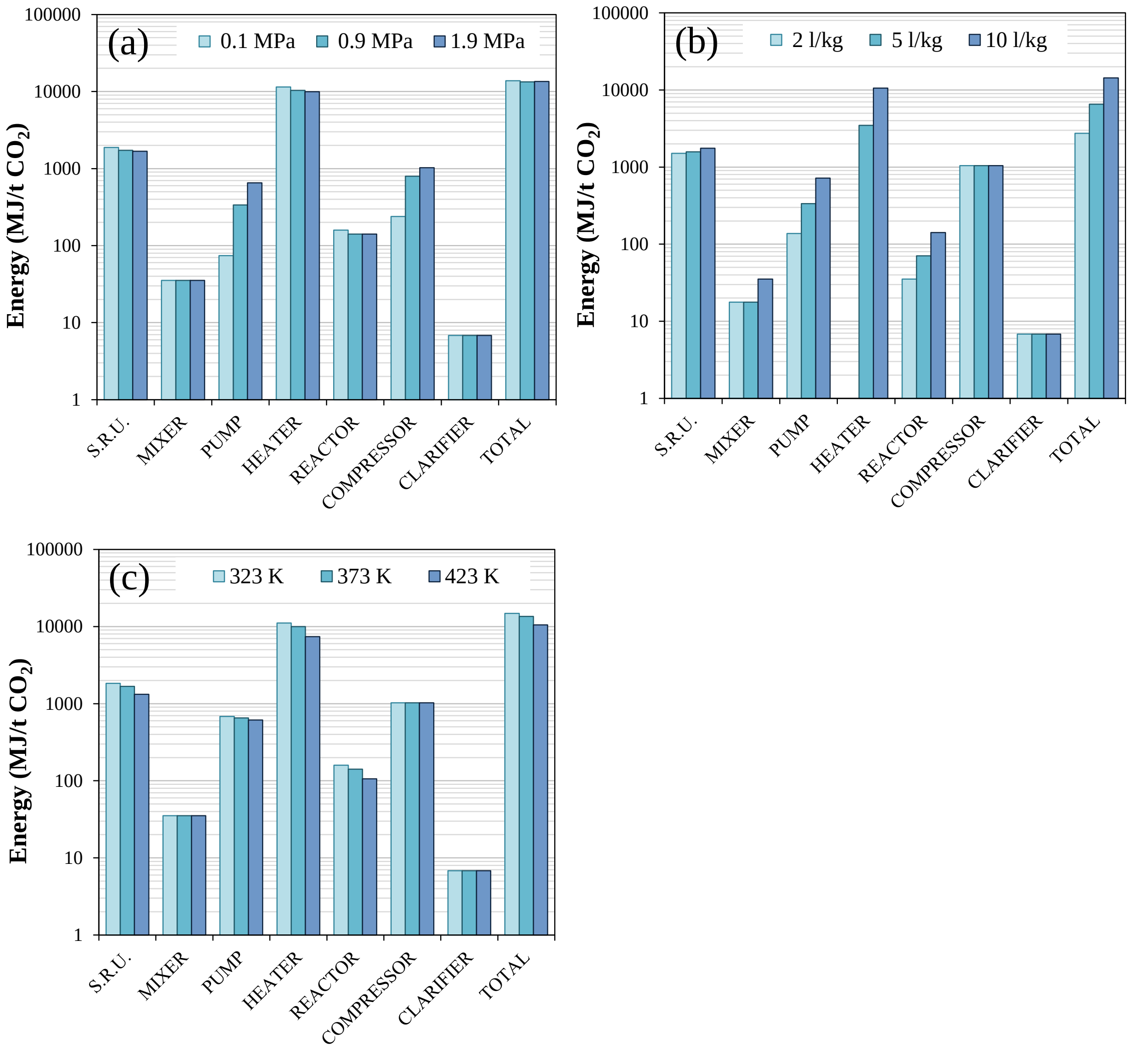

Figure 5.6: Effect of CO_2 pressure, liquid to solid ratio and temperature on the energy requirement estimated for slurry phase carbonation of BOF1 slags. (a) L/S= 10 l/kg, T=373 K, t= 30 minutes; (b) p_{CO2}= 2 MPa, t= T=373 K, 30 minutes; (c) p_{CO2}= 2 MPa, L/S=10 l/kg, t= 30 minutes.

Actually, it may be noted that for the a L/S of 2 l/kg the second heating stage is not required since the heat released by the reaction is sufficient to achieve the reaction temperature. In Figure 5.6 (c) it can be observed that increasing the operating temperature, the energy requirement of the process showed to decrease from 14800 to 10500 MJ/t CO_2, as the material proved to be more reactive at a higher temperature with a consequent reduction of the amount of residues required to store CO_2 from 8.52 to 6.14 t residues/t CO_2.

Figure 5.7 reports the comparison of the energy requirements associated to a slurry phase carbonation process carried out at 373 K and a L/S of 5 l/kg using three different types of BOF slags. The total energy requirement estimated for the BOF1 slags proved to be higher than the ones obtained for BOF2 and BOF3 (6531 MJ/t CO_2 compared to 1517 and 1306 MJ/t CO_2 respectively). This trend can be explained considering that BOF1 presented a higher initial particle size (d_0) and a lower d_1 value compared to the other two types of residues, thus entailing a higher duty associated to the size reduction operation. Furthermore, since the steel slags tested by Huijgen et al. (2005) were characterized by a lower amount of reactive phases, a higher amount of BOF1 slags was required per ton of CO_2 stored, thus involving higher energy requirements for heating and pumping the materials.

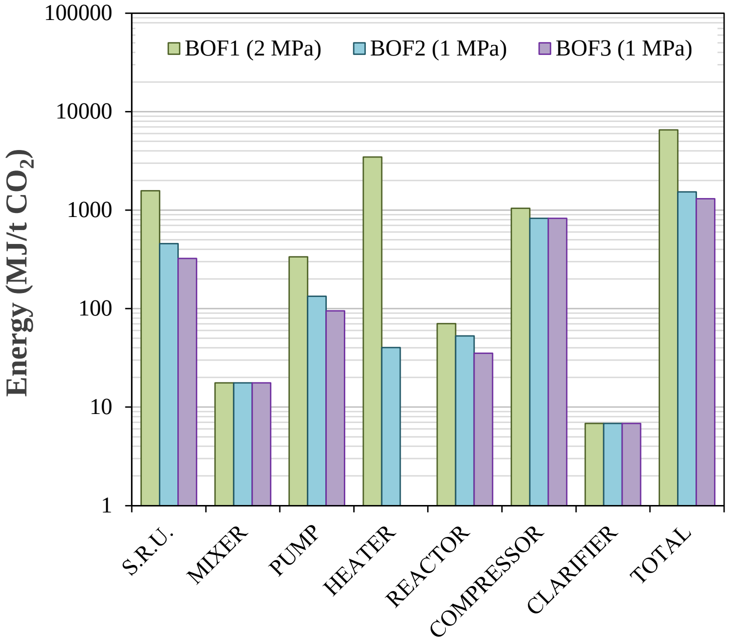

Figure 5.7: Comparison of the energy requirement of a slurry phase carbonation process carried out using different industrial residues (L/S= 5 l/kg; T= 373 K, t= 30 minutes).

5.6.2 Wet Route

Figure 5.8 reports the energy requirement associated to a wet carbonation process carried out applying different carbon dioxide pressures and using three types of industrial residues, i.e. AOD slags (Figure 5.8 (a)), EAF slags (Figure 5.8 (b)) and APC1 residues (Figure 5.8 (c)). At increasing CO_2 pressure, a moderate rise in the total energy requirement of the process is observed for the AOD slags and APC1 residues. This can be explained considering that the amount of residues fed to the process for the three carbonation conditions (see Table 5.4) is almost the same since the reactivity of these material proved not to be significantly affected by the increase in the carbon dioxide pressure and only different duties for the CO_2 compressor can be observed.

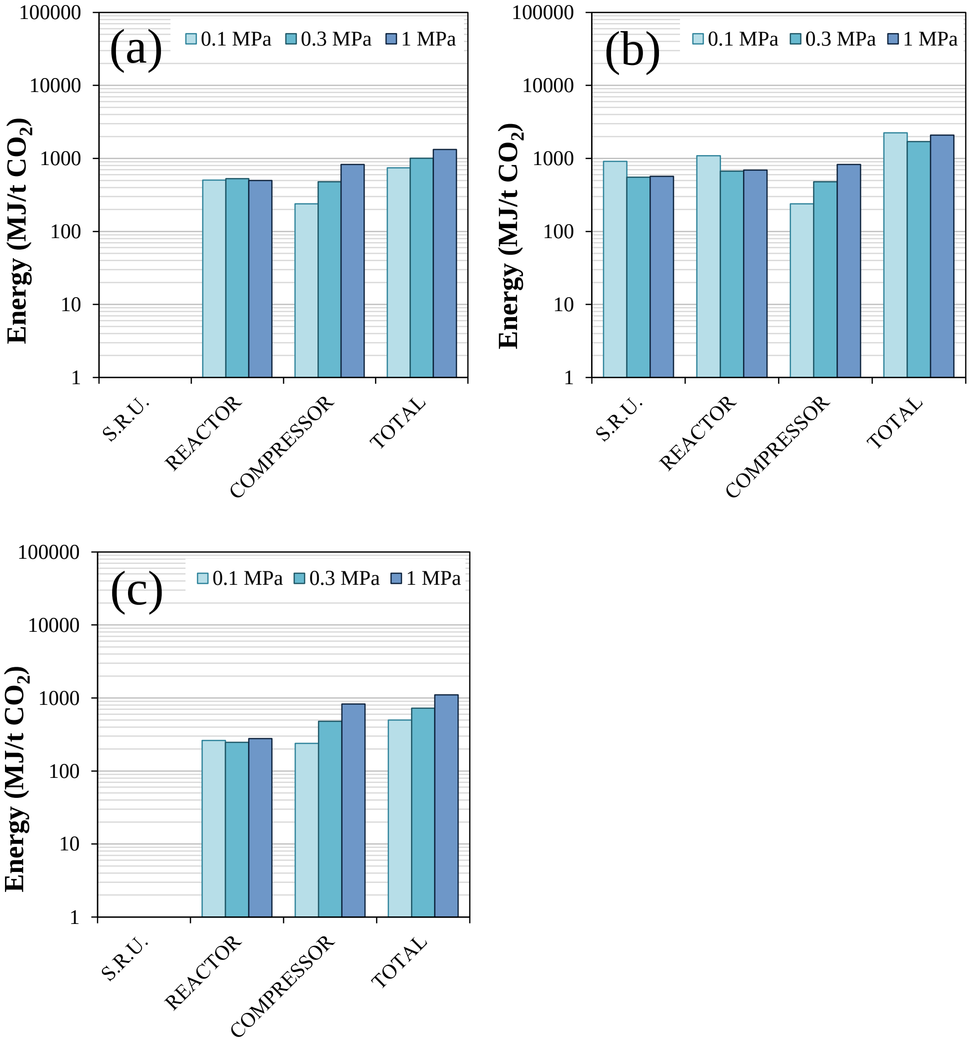

Figure 5.8: Effect of the CO_2 pressure on the energy requirement estimated for wet carbonation of different residues: (a) AOD slags, L/S= 0.4 l/kg, T= 323 K, t=1 hour; (b) EAF slags, L/S= 0.4 l/kg, T= 323 K, t=1 hour; (c) APC1 residues, L/S= 0.02 l/kg, T= 303 K, t=1 hour.

The reactivity of the EAF slags, instead, seems to be influenced by the applied carbon dioxide pressure, since at increasing CO_2 pressure a lower amount of residues is required (i.e. around 7 t residues/t CO_2 at p_{CO2}= 1 MPa compared to 11 t residues /t CO_2 needed at 0.1 MPa). This difference in the amount of material to process entails higher duties associated to the size reduction unit and the carbonation reactor and, hence, an apparently surprisingly higher total energy requirement of the process when a CO_2 pressure of 0.1 MPa is applied. The energy requirements obtained for different types of residues applying the wet carbonation route at the same operating conditions are shown in Figure 5.9. The EAF slags present the highest total energy requirement due to the higher duty of the carbonation reactor and of the size reduction unit. As far as the requirement of the carbonation reactor is concerned, it must be observed that the APC1 residues and the AOD slags proved to be more reactive than the EAF slags, requiring to process a lower amount of residues (i.e. 4.9 and 4.4 t residues/t CO_2 for AOD slags and APC1 residues respectively against 6.7 t residues/t CO_2 for EAF slags). Furthermore, for the AOD slags and the APC1 residues, differently from the EAF slags, a size reduction unit is not required since these materials are characterized by an initial particle diameter directly suitable for the carbonation process.

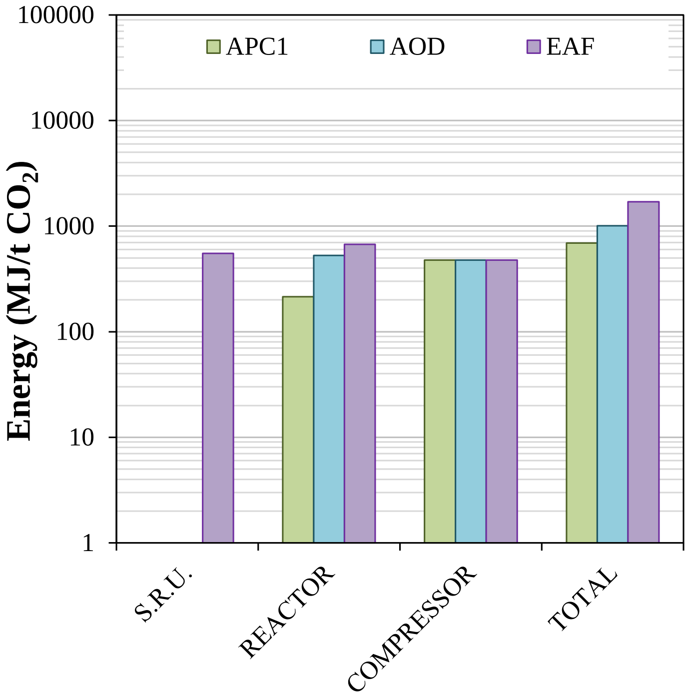

Figure 5.9: Comparison of the energy requirement of a wet carbonation process carried out using different industrial residues (p_{CO2}= 0.3 MPa, T= 323.15 K, L/S=0.4 l/kg; t= 1 hour).

5.6.3 Lowest energy requirements for each type of residue and route

Figure 5.10 shows the lowest energy requirements estimated for each considered residue applying the slurry phase (a) or the wet route process (b), highlighting the contribution of the main unit operations relevant for each route; for the slurry phase route the term "other" includes the energy requirements associated to the mixing of the slurry, the carbonation reactor and the clarifier, while for the wet route it includes the energy required to operate the rotary drum carbonation reactor.

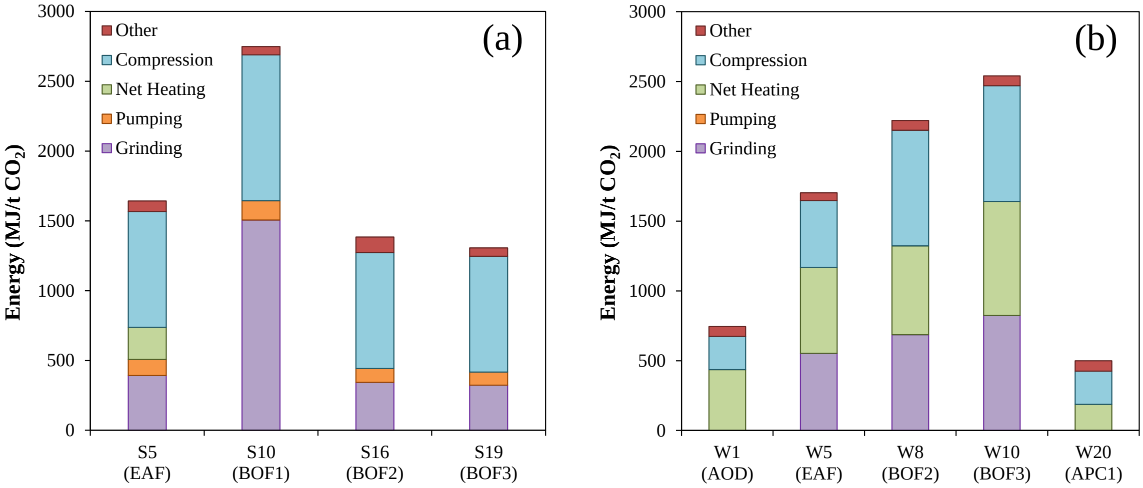

Figure 5.10: Comparison of the lowest energy requirement estimated for each type of residues considered applying the slurry phase (a) or the wet carbonation route (b). For the specific operating conditions see Table 5.3 and Table 5.4.

As shown in Figure 5.10 (a), the main contributions to the total energy requirements of the slurry phase carbonation process are associated to the size reduction of the residues and carbon dioxide compression. The total energy requirement resulting for this route ranged between 1300 and 2750 MJ/t CO_2, with the highest duty associated to the carbonation of BOF1 slags (case S10); these residues, in fact, presented a higher initial particle size (20 mm) and, hence, a higher energy duty associated to grinding, namely 1500 MJ/t against the 350-400 MJ/t estimated for EAF slags (case S5), BOF2 slags (case S16) and BOF3 slags (case S19). Based on our estimates, in most of the cases considered in Figure 5.10 (a), the energy required for heating the slurry could be totally recovered from the reaction enthalpy, except for case S5, corresponding to EAF slags. This type of residues, in fact, presented a lower reactivity at the tested operating conditions compared to the other types of residues, thus requiring a higher amount of residues and water to be processed and hence a higher energy input for heating the slurry. The minimum energy requirement obtained for the wet carbonation route, shown in Figure 5.10 (b), was observed to range between 500 and 2540 MJ/t CO_2 with the lowest values obtained for the AOD slags and the APC1 residues, i.e. 744 and 500 MJ/t CO_2, respectively. These results can be explained considering that these two types of residues presented an initial particle size already suitable for carbonation, allowing to neglect the energy requirements associated to the grinding step. In addition, for AOD slag and APC1 residues a higher reactivity with CO_2 was found also at mild operating conditions (i.e. 323 K and 0.1 MPa for AOD slag and 303 K and 0.1 MPa for APC1 residues), hence compression and heating requirements also resulted lower. Comparing the results obtained for the same type of residues (i.e. EAF, BOF2 and BOF3) in the two routes one can observe that the energy requirements estimated in the slurry phase route are generally equal or lower than the ones obtained for the wet route. These results can be explained considering that these materials demonstrated a higher reactivity (R_X) for the conditions applied in the slurry phase route. Furthermore, for all the considered wet carbonation conditions (see Figure 5.10 (b)) more than 30% of the total energy requirement was found to be associated to the heating of the residues and water. This result was obtained assuming to neglect the recovery of the heat generated by the exothermic carbonation reaction. This assumption was made since, differently from the slurry phase route where the carbonation reaction takes place in the same medium to be heated, the heat transfer efficiency in the wet route can be hardly predicted and exploited. This choice may penalize the wet route compared to the slurry phase one since if the heat recovery were taken into account, as for the slurry phase route, the energy required for heating the residues in the wet route could be reduced or even avoided.

5.6.4 Energy requirements for carbonation using 40% CO_2 gas mixture

Figure 5.11 reports the comparison of the energy requirements estimated for the wet carbonation of APC2 (at 323 K, 0.2 l/kg), BOF5(at 323 K, 0.3 l/kg) and AOD slag (at 323 K, 0.4 l/kg) using either pure CO_2 at 0.3 MPa or a N_2/CO_2 gas mixture at 40% CO_2 concentration (i.e. closely resembling the CO_2 concentration typically found in syngas or biogas) at p_{CO2} of 0.28 MPa. Differently from the results reported in previous paragraphs, in this case the energy penalty associated to CO_2 capture, evaluated as described in paragraph 5.4.2, was also considered in the energy requirements associated to the carbonation using pure CO_2. As can be noted, the energy requirements estimated for the main units of the wet route process proved to be almost constant for the AOD slag and the APC2 residues since the reactivity of these materials showed to be only slightly influenced by the gas composition. For the BOF5, instead, although the applied partial pressure of CO_2 was basically the same in both experiments (0.28 against 0.3 MPa) the reactivity of the material proved to decrease significantly when the N_2/CO_2 gas mixture was used as a result of the higher amount of residues (16.5 instead of 10.7 t residues/t CO_2) and the higher energy requirements for the SRU and the carbonation reactor.

However, it is worth pointing out that for all the three tested residues the total energy requirement estimated for a wet carbonation process carried out with syngas is anyhow lower than the energy penalty required only for capturing carbon dioxide in a process that use pure CO_2. Although this aspect has to be investigated in more details carrying out experiments with other residues and testing also the performance in the slurry phase route, it represent an important finding in order to reduce the energy penalties associated to the carbonation process in view of pilot or full scale applications of the process.

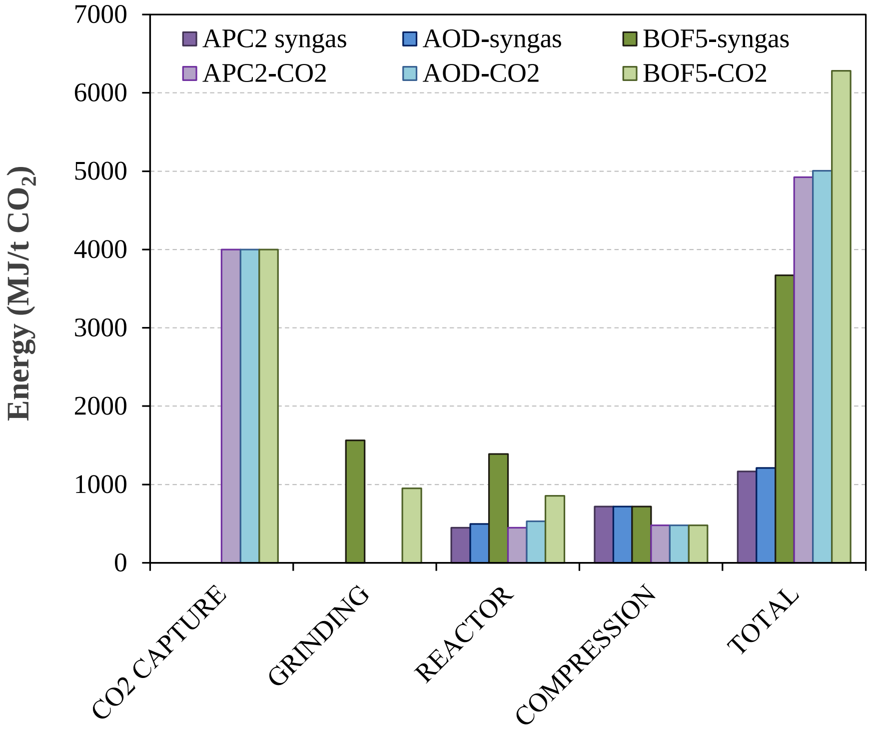

Figure 5.11: Comparison of the energy requirement estimated for wet carbonation of three types of industrial residues using pure CO2 or a syngas (pCO2= 0.3 MPa for pure CO2 and 0.28 MPa for syngas, 323 K).

5.7 Comparison with previous studies

The total energy requirements of the slurry phase carbonation process estimated following the approach outlined in this work are compared in Figure 5.12 with those reported for the same type of residues and operating conditions in previous studies (Huijgen et al., 2006a, Kelly et al., 2011 and Kirchofer et al., 2012) with the aim of clarifying the reasons behind the differences in the estimates. It was decided to compare the results obtained by different authors for the BOF1 since all the evaluations available in literature on the energy requirements of carbonation of alkaline materials except the one reported by O'Connor et al. (2005) have assess the material and energy balance for this specific residue and, hence, it could be easier to compare the assumptions made and the obtained results. In particular, in Figure 5.12 (a) the energy requirements estimated following the approach presented in this study for carbonation of BOF1 (at 473 K, d_1<38 µm, p_{CO2}=2 MPa, L/S=5 l/kg, t=15 minutes) are reported together with the results of Huijgen et al. (2006) and Kelly et al. (2011). In Figure 5.12 (b), instead, the energy penalties estimated in the present work and the results reported by Kirchofer et al. (2012) for carbonation of BOF1 (at 373 K, d_1<100 µm, p_{CO2}=0.1 MPa, L/S=10 l/kg, t=30 minutes) are compared. For completeness and further discussion, Figure 5.12 (a) and (b) also report the energy requirements estimated following the approach outlined in this work, but assuming to neglect the recovery of the heat of the outlet stream from the carbonation reactor.

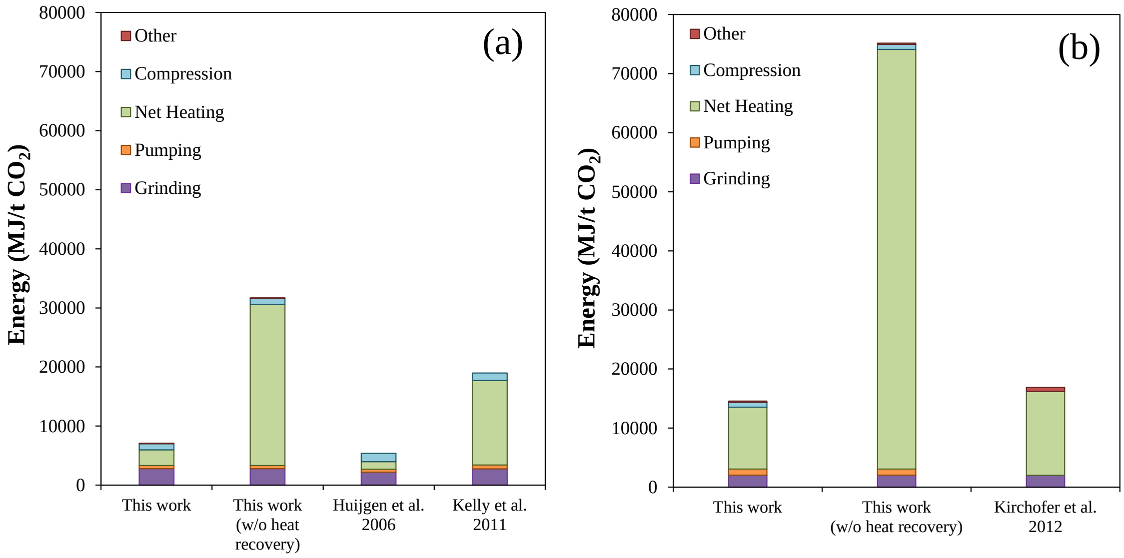

Figure 5.12: Comparison of the energy requirement estimated applying the present approach and the ones reported in previous studies for the same types of residues and operating conditions: (a) BOF1, L/S= 5 l/kg, p_{CO2}= 2 MPa, T= 473 K, t= 15 minutes, (b) BOF1, L/S= 10 l/kg, p_{CO2}= 0.1 MPa, T= 373 K, t= 30 minutes.

As shown in Figure 5.12 (a) and Figure 5.12 (b), for all of the compared studies the unit operations that mainly influence the total energy requirement of the slurry phase carbonation process are material grinding and heating, followed by CO_2 compression and slurry pumping. However, remarkable differences can be noted between the results obtained in these studies, which can be substantially ascribed to the different energy requirements estimated for the heating of the reagents (residues and water). As can be seen, the results obtained in this work considering to include the heat recovery term proved to be in good agreement with those reported by Huijgen et al. (2006) (see Figure 5.12 (a)). The layout and assumptions considered in these two studies, in fact, are quite similar and the difference that can be noted is mainly ascribed to the different assumption made for the energy balance of the heat exchanger (unit D in Figure 5.1). Namely, in the present work it was assumed to use this unit to heat the inlet slurry from 293 K to 30 K below the final carbonation temperature while Huijgen and co-workers opted for heating to 20 K below the carbonation temperature. A more relevant difference, instead, can be observed between the energy requirements estimated in this work and the ones reported by Kelly et al. (2011). Although the operating conditions considered in the latter study were not clearly specified, considering the carbonation extent assumed by the authors to assess the energy requirement of the process (i.e. 67%), it can be reasonably argued that Kelly and co-workers estimated the energy balance making reference to the carbonation experiment S15 performed by Huijgen et al. (2006) (see Table 1). Although Kelly et al. (2011) did not specifically clarify if they accounted for the recovery of the heat of the outlet stream from the carbonation reactor in the evaluations carried out for industrial residues, the energy requirement estimated by Kelly et al. (2011) reported in Figure 5.12 (a), results intermediate between the values calculated in this study assuming to neglect or to consider heat recovery. If heat recovery is taken into account, as done in this work and in the assessment carried out by Huijgen et al. (2006) (see Figure 5.12 (a)), the total energy requirement of the process would in fact considerably decrease from around 19000 MJ/t CO_2 estimated by Kelly to 7100 MJ/t CO_2. This seems to suggest that the high energy requirement for steel slags carbonation reported by Kelly et al (2011), which led these authors to conclude that the process is likely unfeasible, is affected by the assumption of neglecting any possibility of heat recovery. Finally, in Figure 5.12 (b) the comparison of the results obtained by Kirchofer et al. (2012) and the energy requirements estimated for the same operating conditions using the approach presented in this work is reported. Also in this case, the information included by Kirchofer et al. (2012) does not clarify whether the recovery of the heat of the outlet stream from the carbonation reactor was considered. Nevertheless, looking at Figure 5.12 (b), it can be noticed that the total energy requirement reported by Kirchofer et al. (2012) proved to be only slightly higher than the one estimated using the approach presented in this work, i.e. considering the heat recovery term. On the other hand, if the heat recovery term is neglected, the energy requirement associated to the process is shown to drastically increase from around 14600 to 75200 MJ/t CO_2. This observation leads to conclude that these authors have probably assumed to consider (at least partially) the heat recovery term. The comparative analysis discussed in this section highlights the importance of heat recovery in determining the energy requirements of the carbonation process. Besides the other hypothesis, the assumption made on this element of the energy balance of the carbonation process is therefore a key choice and should be clearly stated to avoid misunderstandings in the interpretation of results. Given the importance of this term on the global energy requirements, the effective possibility of recovering the excess heat should be clearly tested at least at pilot scale.

5.8 Conclusions

The energy requirements of a direct carbonation process carried out using various types of minerals and alkaline industrial residues applying both the slurry phase and wet routes at different operating conditions were assessed. The estimates were based on defined layouts and clearly stated assumptions and equations for the mass and energy balance of each unit operation, considering the results of lab scale carbonation tests already reported in the literature.

The main energy requirements were associated to the duties for grinding minerals or residues (when relevant) and for heating the alkaline material and the associated water to the carbonation reaction temperature. The main factors affecting the energy requirements were thus the physico-chemical properties of the material that influence the energy needed for grinding the minerals or residues and for heating the reagents, i.e. the initial particle size and chemical composition of the material. The initial size of the alkaline feedstock exerts a direct effect on the energy required per unit mass of material. The chemical composition of the minerals or residues and, in particular, their content of reactive phases affects the reactivity of the material and, hence, the amount of feedstock needed for storing a unit mass of CO_2, with a consequence on the total energy required for both grinding and heating. The latter term is clearly also affected by the liquid to solid ratio used, that determines the duty needed to heat the water associated to the residues.

The energy penalty resulting from associating the mineral carbonation process to energy production depends on the type of power plant considered. Making reference to a natural gas-fired power plant, assuming a heat release of 20 GJ per ton of CO_2 emitted, the lowest energy penalties estimated in this work for a direct carbonation process, without considering the energy penalty associated to the CO_2 capture stage, were shown to vary between 15-40% for the slurry phase carbonation of minerals while regarding industrial residues this term was within 7-14% for the slurry phase route and 3-13% for the wet one, depending on the type of material used. Clearly, making reference to a coal-fired power plant, assuming a heat release of 10 GJ per ton of CO_2 emitted, all energy penalties would double. Comparing the performances obtained using industrial residues instead of minerals it is possible to observe that, as expected, the lower total energy requirement of the process obtained for the residues are due to the less severe operating conditions applied, that entails lower energy requirements for heating and compression, and to the initial particle size of this waste material that often is already suitable for the process avoiding partially or totally the use of a size reduction unit.

The evaluation performed in this study were obtained making different assumptions on the heat recovery terms in the two considered carbonation route. In particular in the case of the slurry phase, it was assumed to recover both the heat of the exothermic carbonation reaction and the sensible heat of the outlet stream from the carbonation reactor; on the contrary, no heat recovery was assumed for the wet route. It is thus important to point out again that this choice may penalize the wet route compared to the slurry phase one since, if heat recovery were taken into account as for the slurry phase route, the energy required for heating the alkaline material in the wet route could be reduced or even avoided, leading to a basically negligible energy penalty of the whole process.

One of the main findings of this work is that in many cases the energy penalties associated to the carbonation of industrial residues are lower or, in the worst case, comparable to the ones expected for the capture step. This means that the carbonation process of most alkaline residues is likely feasible, but clearly ways for reducing the associated energy requirements should be investigated. Some papers have recently addressed the possibility of performing the carbonation of industrial residues directly using flue-gas or syngas. For this reason, based on the lab-scale carbonation tests carried out with syngas and discussed in Chapter 3, the total energy requirement of a wet carbonation process performed with three different types of industrial residues was evaluated. These estimate allowed to observed that although the reactivity of the material proved to be partially influenced by using syngas instead of pure CO_2, the total energy requirements of the process showed to be lower than these for capturing CO_2, leading to a possibly relevant reduction in the total energy penalty of the CCS chain.

Furthermore the energy requirements estimated in this work for slurry phase carbonation of steel slags were compared with those obtained in previous studies. The transparency in the assumptions and choices made in the development of the mass and energy balance allowed to identify the similarities and differences with previous works. The assumptions made on the inclusion of the heat recovery term turned out once again to greatly affect the total energy requirements.

6 CONCLUSIONS AND PERSPECTIVES

Despite a relevant number of publications and patents on accelerated carbonation of minerals and industrial residues have been issued in the last two decades, its application and deployment has been hindered so far by the relatively high energy and/or material requirements associated to the process. An assessment of the energy requirements of direct carbonation of minerals and alkaline industrial residues was performed in this work, using defined layouts and clearly stated assumptions and equations for the mass and energy balance of each unit operation, considering the results of lab scale carbonation tests already reported in the literature. Making reference to a natural gas-fired power plant, assuming a heat release of 20 GJ per ton of CO_2 emitted, the lowest energy penalties were shown to range between 15-40% for the slurry phase carbonation of minerals while regarding industrial residues this term was within 7-14% for the slurry phase route and 3-13% for the wet one, depending on the type of material used. Based on these results, the feasibility of the process proved to be strictly related to the possibility of recovering, even partially, the heat of the outlet stream from the carbonation reactor. Anyhow, the energy penalties of mineral carbonation, coupled with those associated to the capture step needed to obtain concentrated CO_2 for the carbonation process, would make the whole CCS chain poorly viable. Therefore, integration of capture and mineral carbonation or even better their lumping in a single step would allow to overcome this issue, greatly reducing the overall energy penalty.

The feasibility of integrating capture and carbonation of industrial residues has been investigated in the framework of the UPGAS-LOWCO2 Life+ project, developing the Absorption with Regeneration process (AwR). In this process the carbonation of APC residues was applied with the aim of regenerating the spent solution produced from an absorption unit used to capture the carbon dioxide contained in landfill biogas with an alkali solution. The pilot-scale tests performed in a unit specifically designed and built within this work, allowed to achieve a maximum KOH/NaOH regeneration efficiency between 50 and 60%, with an average CO_2 uptake in the obtained solid product around 200-250 g/kg. In addition, after a final washing of the solid product collected after regeneration, an improvement of the leaching of the critical components, Cl, Pb and Zn in particular, was observed and the final solid product showed to comply with the acceptance criteria for non hazardous landfills. Therefore, besides reducing the solvent make-up required for the absorption step, the proposed process showed different environmental benefits, including the permanent storage of the separated CO_2 in a solid and stable form and the improvement of the environmental behaviour of the industrial residues used to regenerate the spent solution.

The feasibility of lumping capture and mineral carbonation was investigated by performing direct aqueous carbonation of thermally activated serpentine using flue gas instead of pure CO_2. As far as the dissolution step is concerned, flow through tests, performed at 30-90°C under different CO_2 partial pressures using a N_2/CO_2 gas mixture with 10% CO_2, showed a fast Mg dissolution with extents up to 60% in two hours at 90°C. Given the promising results obtained in these tests, the carbonation potential of the thermally activated serpentine was tested at mild operating conditions ($T=30\text{-}90$ °C, $p_{CO2}=1$ bar) performing direct aqueous carbonation tests. In these experiments the measured extent of carbonation was found to be lower than 20%, suggesting that an indirect process with temperature and p_{CO2} swing could be more effective.

Finally, the possibility of lumping capture and carbonation of different alkaline industrial residues (i.e. APC residues, AOD and BOF slags) was assessed carrying out wet carbonation experiments using a gas mixture with the typical CO_2 content of a syngas (i.e. 40%). The APC residues and the AOD slags allowed to achieve around 60-70% carbonation extent, whereas only 44% was obtained for the BOF slags. As no remarkable difference was observed between the results obtained using pure CO_2 or the N_2/CO_2 gas mixture at the same CO_2 partial pressure, the use of CO_2 diluted sources, such as syngas, looks feasible although the performance achievable are significantly affected by the chemical-physical characteristics of the material used.

In conclusion, the results obtained in this work open some opportunities to reduce the overall energy penalty of the CCS chain based on storage by accelerated carbonation. As far as mineral carbonation is concerned, more efforts are still needed to develop an efficient reaction route allowing to get reasonably high carbonation yields using CO_2 diluted sources. Regarding alkaline residues, despite the experimental results seems to be promising in terms of extent of reaction at mild operating conditions, the requirements of suitable feedstocks may represent a bottleneck for the deployment of the process, considering the limited availability of these materials.

7 REFERENCES

Alexander G., Moroto-Valer M.M., Gafarova-Aksoy P.,2007. Evaluation of reaction variables in the dissolution of serpentine for mineral carbonation. Fuel 86, 273–281.

Allal K.M., Dolignier J.C., Martin G., 1997. Determination of thermodynamical data of calcium hydroxichloride. IFP Institut francais du Petrole Journal 52, 361–368.

Back M., Kuehn M., Stanjek H., Peiffer S., 2008. Reactivity of alkaline lignite fly ashes towards CO_2 in water. Environmental Science & Technology 42, 4520–4526.

Baciocchi R., Carnevale E., Costa G., Gavasci R., Lombardi L., Olivieri T., Zanchi L., Zingaretti D., 2013c. Performance of a biogas upgrading process based on alkali absorption with regeneration using APC residues (submitted to Waste Management).

Baciocchi R., Carnevale E., Costa G., Lombardi L., Olivieri T., Paradisi A., Zanchi L., Zingaretti D., 2013b. Pilot-scale investigation of an innovative process for biogas upgrading with CO_2 capture and storage. Energy Procedia (in press).

Baciocchi R., Carnevale E., Corti A., Costa G., Lombardi L., Olivieri T., Zanchi L., Zingaretti D., 2013a. Innovative process for biogas upgrading with CO_2 storage: results from pilot plant operation. Biomass & Bioenergy 53, 128-137.

Baciocchi R., Costa G., Di Gianfilippo M., Polettini A., Pomi R., Stramazzo A., 2012b. Evaluation of the CO_2 storage capacity of different types of steel slag subjected to accelerated carbonation. In: Proceedings of Crete 2012, 3rd International Conference on Industrial and Hazardous Waste Management, 12-14 September 2012, Chania, Crete, Greece.

Baciocchi R., Costa G., Gavasci R., Lombardi L., Zingaretti D., 2012a. Regeneration of a spent alkaline solution from a biogas upgrading unit by carbonation of APC residues. Chemical Engineering Journal 179, 63-71.

Baciocchi R., Costa G., Faraoni G., Lombardi L., Olivieri T., Zingaretti D., 2011c. Pilot-scale carbonation of APC residues for CO_2 storage and alkali regeneration downstream an absorption column for biogas upgrading. In: Proceedings of Sardinia 2011 Thirteenth International Waste Management and Landfill Symposium 3 - 7 October 2011 S. Margherita di Pula (Cagliari). Sardinia. Italy. ISBN 978-88-6265-000-7.

Baciocchi R., Costa G., Di Bartolomeo E., Polettini A., Pomi R., 2011b. Wet versus slurry carbonation of EAF steel slag. Greenhouse Gases: Science and Technology 1, 312–319.

Baciocchi R., Corti A., Costa G., Lombardi L., Zingaretti D., 2011a. Storage of carbon dioxide captured in a pilot-scale biogas upgrading plant by accelerated carbonation of industrial residues. Energy Procedia 4, 4985-4992.

Baciocchi R., Costa G., Lombardi L., Mostbauer P., Olivieri T., Zingaretti D., 2010c. Report A1.1 – Technical Report on activities of Action A1, Preliminary evaluations.

Baciocchi R., Costa G., Di Bartolomeo E., Polettini A., Pomi R., 2010b. Carbonation of stainless steel slag as a process for CO_2 storage and slag valorization. Waste and Biomass Valorization 1, 467-477.

Baciocchi R., Costa G., Lategano E., Marini C., Polettini A., Pomi R., Postorino P., Rocca S., 2010a. Accelerated carbonation of different size fractions of bottom ash from RDF incineration. Waste Management 30, 1310-1317.

Baciocchi R., Costa G., Di Bartolomeo E., Polettini A., Pomi R., 2009. The effects of accelerated carbonation on CO_2 uptake and metal release from incineration APC residues. Waste Management 29, 2994-3003.

Baciocchi R., Mazzotti M., Storti G., 2006. Process design and energy requirements for the capture of carbon dioxide from air. Chemical Engineering and Processing 45, 1047-1058.

Baldyga J., Henczka M., Sokolnicka K., 2011. Mineral carbonation accelerated by dicarboxylic acids as a disposal process of carbon dioxide. Chemical Engineering Research and Design 89, 1841-1854.

Blencoe J.G., Palmer D.A., Anovitz L.M., Beard J.S., 2004. Carbonation of calcium silicates for long-term CO_2 sequestration. Patent WO200409043.

Bobicki E.R., Liu Q., Xu Z., Zeng H., 2012. Carbon capture and storage using alkaline industrial wastes. Progress in Energy and Combustion Science 38, 302-320.

Bodénan F., Deniard P., 2003. Characterization of flue gas cleaning residues from European solid waste incinerators: assessment of various Ca-based sorbent processes. Chemosphere 51, 335–347.

Bonenfant D., Kharoune L., Sauvé S., Hausler R., Niquette P., Mimeault M. et al., 2008. CO_2 sequestration potential of steel slags at ambient pressure and temperature. Industrial & Engineering Chemistry Research 47, 7610-7616.

Butt D.P., Lackner C.H., Wendt C.H., Park Y.S., Bejamin A., Harradine D.M., Holesinger Y., Rising M., Nomura K.,1997. A method for permanent disposal of CO_2 in solid form. World Resource Review 9, 324–336.

Canterford J.H. and Tsambourakis G., 1984. Some observations on the properties of dypingite, $Mg_5(CO_3)(OH)_2{\bullet}5H_2O$, and related minerals. Mineralogical Magazine 48, 437-42.

Cornelis G., Johnson C.A., Van Gerven T., Vandecasteele C., 2008. Leaching mechanisms of oxyanionic metalloid and metal species in alkaline solid wastes: A review. Applied Geochemistry 23, 955-976.

Costa G., 2009. Accelerated carbonation of minerals and industrial residues for carbon dioxide storage. Doctoral Dissertation. University of Rome “Tor Vergata”.

Costa G., Baciocchi R., Polettini A., Pomi R., Hills C.D., Carey P.J., 2007. Current status and perspectives of accelerated carbonation processes on municipal waste combustion residues. Environmental Monitoring and Assessment 135, 55-75.

Council Decision 2003/33/EC, 1999. Criteria and procedures for the acceptance of waste at landfills, Official Journal of the European Communities L 11, 19/12/2002, 27–49.

Davies PJ, Bubela B., 1973. The transformation of nesquehonite into hydromagnesite. Chemical Geology 12, 289–300.

Dell RM, Weller SW., 1959. The thermal decompostion of nesquehonite $MgCO_3$ $3H_2O$ and magnesium ammonium carbonate $MgCO_3.(NH_4)_2CO_3$ $4H_2O$. Transactions of the Faraday Society 55, 2203–20.

Directive 2009/29/EC of the European Parliament and of the council of 23 April 2009 amending directive 2003/87/EC so as to improve and extend the greenhouse gas emission allowance trading scheme of the community

Directive 2009/28/EC of the European Parliament and of the council of 23 April 2009 on the promotion of the use of energy from renewable sources and amending and subsequently repealing Directives 2001/77/EC and 2003/30/EC

Directive 2003/87/EC of the European Parliament and of the council of 13 october 2003 establishing a scheme for greenhouse gas emission allowance trading within the community and amending council directive 96/61/EC

Eloneva S., Teir S., Salminen J., Fogelholm C.J., Zevenhoven R., 2008. Fixation of CO_2 by carbonating calcium derived from blast furnace slag. Energy 33, 1461-67.

Fernandez A.I., Chimenos J.M., Segarra M., Fernandez M.A., Espiell F., 2000. Procedure to obtain hydromagnesite from a MgO-containing residue. Kinetic study. Industrial & Engineering Chemistry Research 39, 3653-3658.

Fernández-Bertos M., Li X., Simons S.J.R., Hills C.D., Carey P.J., 2004. Investigation of accelerated carbonation for the stabilization of MSW incinerator ashes and the sequestration of CO_2. Green Chemistry 6, 428–436.

Giammar D.E., Bruant R.G., Peters C.A., 2005. Forsterite dissolution and magnesite precipitation at conditions relevant for deep saline aquifer storage and sequestration of carbon dioxide. Chemical Geology 217, 257–276.

Gunning P.J., Hills C.D., Carey P.J., 2010. Accelerated carbonation treatment of industrial wastes. Waste Management 30, 1081-1090.

Hänchen M, Prigiobbe V, Baciocchi R, Mazzotti M., 2008. Precipitation in the Mg-carbonate system–effects of temperature and CO_2 pressure. Chemical Engineering Science 63, 1012–28.

Hänchen M., Krevor S., Mazzotti M., Lackner K.S., 2007. Validation of a population balance model for olivine dissolution. Chemical Engineering Science 62, 6412-6422.

Hänchen M., Prigiobbe V., Storti G., Seward T.M., Mazzotti M., 2006. Dissolution kinetics of fosteritic olivine at 90-150 degrees C including effects of the presence of CO_2. Geochimica Et Cosmochimica Acta 70, 4403-4416.

Hangx S.J.T., Spiers C.J., 2009. Coastal spreading of olivine to control atmospheric CO_2 concentrations: A critical analysis of viability. International Journal of Greenhouse Gas Control 3, 757-767.

Hariharan S., Werner M., Zingaretti D., Baciocchi R., Mazzotti M., 2013b. Dissolution kinetics of thermally activated serpentine under flue gas atmosphere. In: Proceedings of Fourth International Conference on Accelerated Carbonation for Environmental and Materials Engineering (ACEME 2013), 9-12 April 2013 - Leuven, Belgium.

Hariharan S.B., Werner M., Zingaretti D., Baciocchi R., Mazzotti M., 2013a. Dissolution of activated serpentine for direct flue-gas mineralization. Energy Procedia (in press).

Huijgen W.J.J., Witkamp G.J., Comans R.N.J., 2006b. Mechanisms of aqueous wollastonite carbonation as a possible CO_2 sequestration process. Chemical Engineering Science 61, 4242–4251.

Huijgen W.J.J., Ruijg G.J., Comans R.N.J., Witkamp G.J., 2006a. Energy consumption and net CO_2 sequestration of aqueous mineral carbonation. Industrial & Engineering Chemistry Research 45, 9184-9194.

Huijgen W.J.J., Comans R.N.J., 2006. Carbonation of steel slag for CO_2 sequestration: leaching of products and reaction mechanisms. Environmental Science and Technology 40, 2790-2796.

Huijgen W.J.J., Witkamp G.J., Comans R.N.J, 2005. Mineral CO_2 sequestration by steel slag carbonation. Environmental Science and Technology 39, 9676-9682.

Huijgen W.J.J., Comans R.N.J., 2003. Carbon dioxide sequestration by mineral carbonation: literature review. Petten, NL: Energy Research Centre of the Netherlands.

Huntzinger D.N., Gierke J.S., Kawatra S.K., Eisele T.C., Sutter L.L., 2009. Carbon dioxide sequestration in Cement Kiln Dust through mineral carbonation. Environmental Science & Technology 43, 1986–92.

Hyks J., Astrup T., Christensen T.H., 2009. Long-term leaching from MSWI air pollution control residues: leaching characterization and modelling. Journal of Hazardous Materials 162, 80–91.

IAWG (International Ash Working Group: Chandler A.J., Eighmy T.T., Hartl´en O., Kosson D., Sawell S.E., van der Sloot H., Vehlow J.), 1997. Municipal Solid Waste Incinerator Residues, Studies in Environmental Science 67, Elsevier Science, Amsterdam.

IEA (International Energy Agency), 2010. CO_2 emissions from fuel combustion.

IEA (International Energy Agency), 2009. Cement Technology Roadmap - Carbon emissions reductions up to 2050

Iizuka A., Fujii M., Yamasaki A., Yanagisawa Y., 2004. Development of a new CO_2 sequestration process utilizing the carbonation of waste cement. Industrial & Engineering Chemistry Research 43, 7880-7887.

IPCC, 2005. IPCC special report on carbon dioxide capture and storage. Cambridge University Press, Cambridge, United Kingdom and New York, NY, USA.

Kelly K.E., Silcox G.D., Sarofim A.F., Pershing D.W., 2011. An evaluation of ex situ, industrial-scale, aqueous CO_2 mineralization. International Journal of Greenhouse Gas Control 5, 1587–1595.

Kirchofer A., Brandt A., Krevor S., Prigiobbe V., Wilcox J., 2012. Impact of alkalinity sources on the life-cycle energy efficiency of mineral carbonation technologies. Energy & Environmental Science 5, 8631-8641.

Kloprogge J.T., Martens W.N., Nothdurft L., Duong L.V., Webb G.E., 2003. Low temperature synthesis and characterization of nesquehonite. Journal of Materials Science Letters 22, 825–829.

Kodama S., Nishimoto T., Yamamoto N., Yogo K., Yamada K., 2008. Development of a new pH-swing CO_2 mineralization process with a recyclable reaction solution. Energy 33, 776-784.

Konno H., Nanri Y., Kitamura M., 2002. Crystallization of aragonite in the causticizing reaction. Powder Technology 123, 33-39.

Lackner K.S., 2003. Climate change: a guide to CO_2 sequestration. Science 300, 1677-1678.

Lackner K.S., 2002. Carbonate chemistry for sequestering fossil carbon. Annual review of energy and the environment 27, 193-232.

Lackner K.S., Wendt C.H., Butt D.P., Joyce E.L., Sharp D.H., 1995. Carbon dioxide disposal in carbonate minerals. Energy 20, 1153-1170.

Lekakh S.N., Rawlins C.H., Robertson D.G.C., Richards V.L., Peaslee K.D., 2008. Kinetics of aqueous leaching and carbonization of steelmaking slag. Metallurgical and Materials Transactions 39B, 125-34

Lombardi L., Corti A., Carnevale E., Baciocchi R., Zingaretti D., 2011a. Carbon dioxide removal and capture for landfill gas up-grading. Energy Procedia 4, 465-472;

Lombardi L., Corti A., Carnevale E., 2008. Carbon dioxide capture from landfill gas. In: Proceedings of the 2nd International Conference on Accelerated carbonation for Environmental and Materials Engineering (ACEME08), Rome, Italy, 2008.

Maroto-Valer M.M., Kuchta M.E., Zhang Y., Andrésen J.M., Fauth D.J., 2005. Activation of magnesium rich minerals as carbonation feedstock materials for CO_2 sequestration. Fuel Processing Technology 86,1627-45.

Maroto-Valer M.M., Zhang Y., Kuchta M.E., Andresen J.M., Fauth D.J., 2004. Process for sequestering carbon dioxide and sulfur oxide. Patent WO2004098740.

McCollum D.L., Ogden J.M., 2006. Techno-Economic models for carbon dioxide compression, transport and storage & correlations for estimating carbon dioxide density and viscosity. UC Davis: Institute of Transportation Studies (UCD).

McKelvy M.J., Chizmenshya A.V.G., Diefenbacher J., Bearat H., Wolf G., 2004. Exploration of the role of heat activation in enhancing serpentine carbon sequestration reactions. Environmental Science & Technology 38, 6897–903.

Ming D.W., Franklin W.T., 1985. Synthesis and characterization of lansfordite and nesquehonite. Soil Science Society of America Journal 49, 1303-1308.

O’Connor W.K., Dahlin D.C., Rush G.E., Gerdemann S.J., Penner L.R., Nilsen D.N., 2005. Aqueous mineral carbonation: mineral availability, pretreatment, reaction parametrics and process studies. Report DOE/ARC-TR-04-002. Albany Research Center.

O'Connor W.K. et al., 2000. CO_2 Storage in solid form: a study of direct mineral carbonation. In Proceedings of the 5th International Conference on Greenhouse Gas Technologies, Cairns, Australia.

Pan S.Y., Chang E.E., Chiang P.C., 2012. CO_2 capture by accelerated carbonation of alkaline wastes: a review on its principles and applications. Aerosol and Air Quality Research 12, 770-791.

Park A.H.A., Fan L.S., 2004. CO_2 mineral sequestration: physically activated dissolution of serpentine and pH swing process. Chemical Engineering Science, 59, 5241-5247.

Perry R.H., Green D.W., 1987. Perry's Chemical Engineers' Handbook. McGraw-Hill, New York.

Persson M., Jönsson O., Wellinger A., 2006. Biogas upgrading to vehicle fuel standards and grid injection. IEA Bioenergy. Available at < http://www.iea-biogas.net/_content/publications/publications.php> [accessed 10.02.2012].

Petrovich R., 1981b. Kinetics of dissolution of mechanically comminuted rock-forming oxides and silicates: 1. Deformation and dissolution of quartz under laboratory conditions. Geochimica Et Cosmochimica Acta 45, 1665-1674.

Petrovich R., 1981a. Kinetics of dissolution of mechanically comminuted rock-forming oxides and silicates in the laboratory and at the earths surface. Geochimica Et Cosmochimica Acta 45, 1675-1686.

Pokrovsky O.S., Schott J., 2000. Kinetics and mechanism of forsterite dissolution at 25 degrees C and pH from 1 to 12. Geochimica Et Cosmochimica Acta 64, 3313-3325.

Prigiobbe V., Costa G., Baciocchi R., Hanchen M., Mazzotti M., 2009. The effect of CO_2 and salinity on olivine dissolution kinetics at 120 degrees C. Chemical Engineering Science 64, 3510-3515.

Quina M.J., Santos R.C., Bordado J.C.M., Quinta Ferreira R.M., 2008. Characterization of air pollution control residues produced in a municipal solid waste incinerator in Portugal. Journal of Hazardous Materials 152, 853–869.

Reddy K.J., Kohn S., Weber H., Argyle M.D., Bhattacharyya P., Taylor D. et al., 2011 Simultaneous capture and mineralization of coal combustion flue gas carbon dioxide (CO_2). Energy Procedia 4, 1574-83.

Rendek E., Ducom G., Germain P., 2006. Carbon dioxide sequestration in municipal solid waste incinerator (MSWI) bottom ash. Journal of Hazardous Materials B128, 73-79.

Robie R.A., Hemingway B.S., Fisher J.R., 1978. Thermodynamic properties of minerals and related substances at 298.15 K and 1 bar (10^5 Pascal) pressure and at higher temperatures. United States Government Printing Office, Washington.

Robie R.A., Haselton H.T., Hemingway J, Hemingway J B.S., 1984. Heat capacities and entropies of rhodochrosite ($MnCO_3$) and siderite ($FeCO_3$) between 5 and 600 K. American Mineralogist 69, 349-357.

Ryckebosch E., Drouillon M., Vervaeren H., 2011. Techniques for transformation of biogas to biomethane. Biomass & Bioenergy 35, 1633-1645.

Sayles F.L., Fyfe W. S., 1973. Crystallization of magnesite from aqueous-solution. Geochimica et Cosmochimica Acta 37, 87– 99.

Schmetterer C., Masset P.J., 2012. Heat capacity of compounds in the $CaO\text{-}SiO_2$ System – A review. Journal of Phase Equilibria & Diffusion 33, 261-275.

Schott J., Berner R.A., Sjoberg E.L., 1981. Mechanism of pyroxene and pmphibole weathering: 1. Experimental studies of iron-free minerals. Geochimica Et Cosmochimica Acta 45, 2123-2135.

Shtepenko O.L., Hills C.D., Coleman N.J., Brough A., 2005. Characterization and preliminary assessment of a sorbent produced by accelerated mineral carbonation. Environmental Science and Technology 39, 345-354.

Siegmund B., Moser G., Neubauer C, et al., 2008. Aggregates case study – data gathering, final report, Umweltbundesamt.

Sipilä J., Teir S., Zevenhoven R., 2008. Carbon dioxide sequestration by mineral carbonation: literature review update 2005-2007. Report VT 2008-1, Åbo Akademi University, Faculty of Technology Heat Engineering Laboratory.

Stolaroff J.K., Lowry G.V., Keith D.W., 2005. Using CaO- and MgO-rich industrial waste streams for carbon sequestration. Energy Conversion and Management 46, 687-699.

Teir S., Eloneva S., Fogelholm C.J., Zevenhoven R., 2007b. Dissolution of steelmaking slags in acetic acid for precipitated calcium carbonate production. Energy 32, 528-539.

Teir S., Revitzer H., Eloneva S., Fogelholm C.J., Zevenhoven R., 2007a. Dissolution of natural serpentinite in mineral and organic acids. International Journal of Mineral Processing 83, 36–46.

Teir S., Eloneva S., Zevenhoven R., 2005. Production of precipitated calcium carbonate from calcium silicates and carbon dioxide. Energy Conversion and Management 46, 2954–2979.

Tippayawong N., Thanompongchart P., 2010. Biogas quality upgrade by simultaneous removal of CO_2 and H_2S in a packed column reactor. Energy 35, 4531–4535.

Van Essendelft D.T., Schobert H.H., 2009. Kinetics of the acid digestion of serpentine with concurrent grinding. 1. Initial investigations. Industrial & Engineering Chemistry Research 48, 2556-2565.

Van Gerven T., Van Keer E., Arickx S., Jaspers M., Wauters G., Vandecasteele C., 2005. Carbonation of MSWI-bottom ash to decrease heavy metal leaching, in view of recycling. Waste Management 25, 291–300

Verduyn M., Boerrigter H., Oudwater R., Mossel G.A.F.v., 2009. A novel process concept for CO_2 mineralization; technical opportunities and challenges, In: 5th Trondheim Conference on CO_2 Capture, Transport and Storage, Trondheim.

Wang X., Maroto-Valer MM, 2011. Dissolution of serpentine using recyclable ammonium salts for CO_2 mineral carbonation. Fuel 90, 1229-1237.

Werner M., Hariharan S., Zingaretti D., Baciocchi R., Mazzotti M., 2013b. Carbonation of activated serpentine using flue gas. In: Proceedings of Fourth International Conference on Accelerated Carbonation for Environmental and Materials Engineering (ACEME 2013), 9-12 April 2013 - Leuven, Belgium.

Werner M., Hariharan S.B., Bortolan A.V., Zingaretti D., Baciocchi R., Mazzotti M., 2013a. Carbonation of activated serpentine for direct flue gas mineralization. Energy Procedia (in press).

Werner M., Verduyn M., van Mossel G., Mazzotti M., 2011. Direct flue gas CO_2 mineralization using activated serpentine: Exploring the reaction kinetics by experiments and population balance modelling. Energy Procedia 4, 2043-2049;

World Coal Association. Coal and steel facts 2011.

Zevenhoven, R., Fagerlund, J., 2010 Fixation of carbon dioxide into inorganic carbonates: the natural and artificial "Weathering of Silicates", in carbon dioxide as chemical feedstock (ed M. Aresta), Wiley-VCH Verlag GmbH & Co. KGaA, Weinheim, Germany. doi: 10.1002/9783527629916.ch14.

Zhang H., He P.J., Shao L.M., Lee D.J., 2008. Temporary stabilization of air pollution control residues using carbonation. Waste Management 28, 509–517.

Zhang Z, Zheng Y, Ni Y, Liu Z, Chen J, Liang X., 2006. Temperature- and pH-dependent morphology and FT-IR analysis of magnesium carbonate hydrates. Journal of physical chemistry 110,12969–73.

Zhao L., Sang L., Chen J., Ji J., Teng H., 2010. Aqueous carbonation of natural brucite: Relevance to CO_2 sequestration. Environmental Science and Technology 44, 406-411

Zingaretti D., Costa G., Baciocchi R., 2013a. Assessment of the energy requirements for CO_2 storage by carbonation of industrial residues. Part 1: Definition of the process layout, Energy Procedia (in press).

Zingaretti D., Costa G., Baciocchi R., 2013b. Assessment of the energy requirements for CO_2 storage by carbonation of industrial residues: Mass and Energy balance (submitted to International Journal of Greenhouse Gas Control).

8 PUBLICATIONS

Baciocchi R., Carnevale E., Corti A., Costa G., Lombardi L., Olivieri T., Zanchi L., Zingaretti D., 2013a. Innovative process for biogas upgrading with CO_2 storage: results from pilot plant operation. Biomass & Bioenergy 53, 128-137.

Baciocchi R., Costa G., Gavasci R., Lombardi L., Zingaretti D., 2012. Regeneration of a spent alkaline solution from a biogas upgrading unit by carbonation of APC residues. Chemical Engineering Journal 179, 63-71.

Baciocchi R., Corti A., Costa G., Lombardi L., Zingaretti D., 2011. Storage of carbon dioxide captured in a pilot-scale biogas upgrading plant by accelerated carbonation of industrial residues. Energy Procedia 4, 4985-4992.

Lombardi L., Corti A., Carnevale E., Baciocchi R., Zingaretti D., 2011. Carbon dioxide removal and capture for landfill gas up-grading. Energy Procedia 4, 465-472.

Zingaretti D., Costa G., Baciocchi R., 2013a. Assessment of the energy requirements for CO_2 storage by carbonation of industrial residues. Part 1: Definition of the process layout, Energy Procedia (in press).

Baciocchi R., Carnevale E., Costa G., Lombardi L., Olivieri T., Paradisi A., Zanchi L., Zingaretti D., 2013b. Pilot-scale investigation of an innovative process for biogas upgrading with CO_2 capture and storage. Energy Procedia (in press).

Werner M., Hariharan S.B., Bortolan A.V., Zingaretti D., Baciocchi R., Mazzotti M., 2013. Carbonation of activated serpentine for direct flue gas mineralization. Energy Procedia (in press).

Hariharan S.B., Werner M., Zingaretti D., Baciocchi R., Mazzotti M., 2013a. Dissolution of activated serpentine for direct flue-gas mineralization. Energy Procedia (in press).

Zingaretti D., Costa G., Baciocchi R., 2013b. Assessment of the energy requirements for CO_2 storage by carbonation of industrial residues: Mass and Energy balance (submitted to International Journal of Greenhouse Gas Control).

Baciocchi R., Carnevale E., Costa G., Gavasci R., Lombardi L., Olivieri T., Zanchi L., Zingaretti D., 2013c. Performance of a biogas upgrading process based on alkali absorption with regeneration using APC residues (submitted to Waste Management).

9 CONFERENCE PROCEEDINGS

Baciocchi R., Costa G., Di Gianfilippo M., Polettini A., Pomi R., Stramazzo A., Zingaretti D., 2013. Influence of CO_2 partial pressure on direct accelerated carbonation of steel slag. In: Proceedings of Fourth International Conference on Accelerated Carbonation for Environmental and Materials Engineering (ACEME 2013), 9-12 April 2013 - Leuven, Belgium.

Baciocchi R., Costa G., Lombardi L., Olivieri T., Zanchi L., Zingaretti D., 2013. Pilot-scale carbonation of alkaline residues within an innovative biogas upgrading process. In: Proceedings of Fourth International Conference on Accelerated Carbonation for Environmental and Materials Engineering (ACEME 2013), 9-12 April 2013 - Leuven, Belgium.

Hariharan S., Werner M., Zingaretti D., Baciocchi R., Mazzotti M., 2013. Dissolution kinetics of thermally activated serpentine under flue gas atmosphere. In: Proceedings of Fourth International Conference on Accelerated Carbonation for Environmental and Materials Engineering (ACEME 2013), 9-12 April 2013 - Leuven, Belgium.

Werner M., Hariharan S., Zingaretti D., Baciocchi R., Mazzotti M., 2013. Carbonation of activated serpentine using flue gas. In: Proceedings of Fourth International Conference on Accelerated Carbonation for Environmental and Materials Engineering (ACEME 2013), 9-12 April 2013 - Leuven, Belgium.

Lombardi L., Baciocchi R., Carnevale E., Corti A., Costa G., Mostbauer P., Olivieri T., Paradisi A., Zingaretti D., Gabarrell X., Olivieri F., Starr K., Villalba G., Zanchi L., 2012. Investigation of innovative processes for biogas up-grading. Proceedings of International Solid Waste Association (ISWA) Conference, Florence 17-19 September 2012,
ISBN 978-88-907694-0-5.

Lombardi L., Baciocchi R., Carnevale E., Corti A., Costa G., Olivieri T., Paradisi A.,

Zingaretti D., 2012. Investigation of an innovative process for biogas up-grading. Proceedings of International Conference on Efficiency, Cost, Optimization, Simulation and Environmental Impact of Energy Systems (ECOS 2012), Perugia 26-29 June 2012.

Baciocchi R., Costa G., Lombardi L., Olivieri T., Capobianco O., Zingaretti D., 2012. CO_2 absorption integrated with carbonation of APC residues for alkali regeneration and CO_2 storage in a pilot-scale biogas upgrading plant. Proceedings of Simposio Internazionale di Ingegneria Sanitaria Ambientale (SIDISA 2012), Milan 26-29 June 2012
ISBN 978-88-9035-572-1.

Baciocchi R., Costa G., Faraoni G., Lombardi L., Olivieri T., Zingaretti D. 2011 Pilot-scale carbonation of APC residues for CO_2 storage and alkali regeneration downstream an absorption column for biogas upgrading. Proceedings of Sardinia 2011 Thirteenth International Waste Management and Landfill Symposium, 3 - 7 October 2011 S. Margherita di Pula (Cagliari). Sardinia. Italy,
ISBN 978-88-6265-000-7.

Lombardi L., Baciocchi R., Carnevale E., Corti A., Costa G., Gabarrell X., Mostbauer P., Olivieri F., Olivieri T., Paradisi A., Starr K., Villalba G., Zingaretti D., 2011. Innovative processes for biogas up-grading. Proceedings of Sardinia 2011 Thirteenth International Waste Management and Landfill Symposium, 3 - 7 October 2011 S. Margherita di Pula (Cagliari). Sardinia. Italy,
ISBN 978-88-6265-000-7.

Baciocchi R., Costa G., Lombardi L., Verginelli I., Zingaretti D., 2010. Storage of carbon dioxide captured in a pilot-scale biogas upgrading plant by accelerated carbonation of industrial residues. Proceedings of Third International Conference on Accelerated Carbonation for Environmental and Materials Engineering (ACEME 10), Turku (Finland), 29 November-01 December 2010
ISBN 978-952-12-2505-5;

Baciocchi R., Costa G., Lombardi L., Zingaretti D., 2010. Storage of carbon dioxide captured in a pilot-scale biogas upgrading plant by accelerated carbonation of industrial residues. Proceedings of Third International Symposium on Energy from Biomass and Waste (VENICE10) Venezia, 8-11 Novembre 2010,
ISBN 978-88-6265-008-3;